SLOVAK UNIVERSITY OF TECHNOLOGY IN BRATISLAVA
FACULTY OF CHEMICAL AND FOOD TECHNOLOGY

OPTIMAL CONTROL OF MEMBRANE PROCESSES IN THE PRESENCE OF FOULING

DISSERTATION THESIS

Bratislava, 2016   Ing. Martin Jelemenský

SLOVAK UNIVERSITY OF TECHNOLOGY IN BRATISLAVA
FACULTY OF CHEMICAL AND FOOD TECHNOLOGY

OPTIMAL CONTROL OF MEMBRANE PROCESSES IN THE PRESENCE OF MEMBRANE FOULING

DISSERTATION THESIS

FCHPT-19990-17457

Study program: Process Control
Study field number: 2621
Study field: 5.2.14 Automation
Workplace: Department of Information Engineering and Process Control
Supervisor: prof. Ing. Miroslav Fikar, DrSc.

Bratislava, 2016   **Ing. Martin Jelemenský**

STU
FCHPT

DISSERTATION THESIS TOPIC

Author of thesis: Ing. Martin Jelemenský
Study programme: Process Control
Study field: 5.2.14. Automation
Registration number: FCHPT-19990-17457
Student's ID: 17457

Thesis supervisor: prof. Ing. Miroslav Fikar, DrSc.

Title of the thesis: **Optimal Control of Membrane Processes in the
                              Presence of Fouling**

Date of entry: 02. 09. 2012
Date of submission: 27. 05. 2016

Ing. Martin Jelemenský
           Solver

prof. Ing. Miroslav Fikar, DrSc.   **prof. Ing. Miroslav Fikar, DrSc.**
        Head of department   Study programme supervisor

Acknowledgements

Abstract

This works deals with optimal control of membrane processes. More concretely, we focus our attention to optimal operation of batch membrane diafiltration processes in the presence of fouling. Diafiltration method is used for the separation of two or more solutes based on the molecular size difference from a solution. The goal is to increase the concentration of valuable components and simultaneously decrease the concentration of impurities. This goal is achieved by determination of the addition of a solute free solvent (diluant) into the feed tank to reach the final concentration in minimum time. We use Pontryagin's minimum principle to solve the time-optimal control problem analytically. By using the analytical approach we are able to determine the control structure as a sequence of arcs. In this work two cases are discussed. In the first we consider that the fouling decreases the membrane area. In this case we are able to obtain the control structure only but the individual time durations have to be determined numerically. In the second case we assume that fouling causes a gradual decrease of the permeate flux. The optimal control structure is fully analytical with prescribed control sequences and individual time intervals. We apply the theoretical results to demonstrate applications to different classes of fouling models. We also compare the derived time-optimal operation with traditional used operations to demonstrate the benefits of the proposed methodology.

Keywords: Dynamic Optimization, Pontryagin's Minimum Principle, Membrane Separation Processes, Membrane Fouling, Optimal Control

Abstrakt

Táto práca sa zaoberá optimálnym riadením membránových procesov. Konkrétne, zamerali sme sa na optimálnu prevádzku vsádzkových membránových diafiltračných procesov s uvažovaním zanášania membrány. Diafiltrácia je metóda na separáciu dvoch alebo viacerých zložiek na základe rozdielu veľkosti častíc z roztoku. Cieľom je zvýšenie koncentrácie cenných zložiek a zároveň zníženie koncentrácie nečistôt. Cieľom je zistiť režim pridávania rozpúšťadla do nádrže na dosiahnutie koncových koncentrácií v minimálnom čase. Použitím Pontrjaginovho princípu minima sme problém časovo optimálneho riadenia vyriešili analyticky. Použitím analytického prístupu sme schopní zistiť štruktúru optimálneho pridávania rozpúšťadla ako sekvenciu oblúkov. V práci sa diskutuje o dvoch prípadoch. V prvom prípade budeme uvažovať, že počas zanášania dochádza k upchaniu póroch na membráne, a teda k zmenšovaniu jej plochy. V takomto prípade získame iba štruktúru riadenia, ale jednotlivé časové intervaly medzi sekvenciami je potrebné získať numericky ako riešenie jednoduchého optimalizačného problému. V druhom prípade uvažujeme, že zanášanie postupne znižuje prietok permeátu. Štruktúra optimálneho riadenia je exaktne (analyticky) určená s predpísanými časovými intervalmi a riadením na každom intervale. Teoretické výsledky je možné aplikovať na rôzne druhy zanášacích modelov. V prípadových štúdiách sme vykonali porovnanie medzi optimálnou a tradičnou prevádzkou na demonštráciu zlepšenia existujúceho stavu.

Kľúčové slová: Dynamická optimalizácia, Pontrjaginov princíp minima, membránové separačné procesy, zanášanie membrány, optimálne riadenie

Contents

List of Figures

List of Tables

15

List of Abbreviations

AV	Adjoint Variables
C	Concentration (mode)
CVD	Constant-Volume Diafiltration
CVP	Control Vector Parametrization
DF	Diafiltration
D	Dilution (mode)
DO	Dynamic Optimization
EKF	Extended Kalman Filter
FD	Finite Differences
MF	Microfiltration
NCO	Necessary Conditions for Optimality
NF	Nanofiltration
NLP	Non Linear Programming
ODE	Ordinary Differential Equation
OC	Orthogonal Collocation
OCP	Optimal Control Problem
PMP	Pontryagin's Minimum Principle

PWC   Piece-wise Constant
RO   Reverse Osmosis
SE   Sensitivity Equations
UF   Ultrafiltration
VVD   Variable-Volume Diafiltration

Nomenclature

$\mathcal{F}(\cdot)$ integral part of objective functional

$\mathcal{G}(\cdot)$ non-integral part of objective functional

$\mathcal{J}$ objective functional

$\mathcal{R}$ separation resistance

ϕ time dependent function in state approximation

θ time dependent function in control approximation

$\boldsymbol{u}(t)$ vector of control variables

$\boldsymbol{x}(t)$ vector of state variables

A membrane area

c concentration

J flux, flow through the unit of membrane

J_0	permeate flux of unfouled membrane
K	fouling rate constant
K_c	complete fouling constant
K_g	cake-layer formation constant
K_i	intermediate fouling constant
K_s	standard (internal) fouling constant
n	fouling model constant
n_c	number of constraints
n_u	dimension of the vector of state variables
n_x	dimension of the vector of state variables
R	rejection coefficient
S	singular state surface
s_i	sensitivity
t	independent time variable
u	flowrate of diluant into the feed tank
V	feed tank volume
V_ν	permeate volume per unit of effective membrane are
V_p	permeate volume

Greek Symbols

α	control variable of diafiltration process

$\boldsymbol{\lambda}$ vector of adjoint variables

$\boldsymbol{\nu}$ vector of Lagrange multiplicators

Mathematical Notation

$\mathbb{R}$ real-state vector

Subscripts

0   initial

1   macro-solute

2   micro-solute

f   final

max   maximum, upper bound

min   minimum, lower bound

p   permeate

Chapter 1

Introduction

Finding the optimal solution to a problem is an every day struggle in everyones life. The mankind has been in search of optimality to any problem in every aspect of life such as work. These optimization problems can differ in many aspects. In private we search for optimal solution sometimes even without noticing it. Morning travel to work is a perfect example for this kind of situation when we want to get into the work in minimum time and to avoid traffic jams. Immediately we notice that the objective is the minimum time problem and traffic jams are the constraints that we have to consider. Similar optimization problems are also solved every day in work were we want to maximize the profit and simultaneously minimize costs. Over the years, mainly industry has turned their attention to optimization and optimal control. In electrical sector the logistics of energy distribution is optimized to minimize the electrical network and satisfy all the clients. Same principles can be also applied by product delivery by different logistic companies by air, sea and, land to minimize the time and fuel.

The most rising segment which has turned to optimization and process control is the chemical industry. Optimization has provided minimization of production costs and simultaneously maximization of produced products.

One of the groups that has received a lot of attention in the past years are membrane separation processes that have replaced many conventional separation processes. This is mainly due to low energy footprint of membrane operations. Carrére and René (1996); Cheryan (1998); Choi et al. (2005) show different configurations of membrane separation processes as single-pass and feed-and-bleed configurations. They also discuss the extension of the classical configuration to a multi-stage system which can consist of several feed-and-bleed systems. The biggest advantage of the multi-stage configurations is that the individual stages do not require large membrane areas. On the other hand, with increased number of stages also the number of pumps and valves increases which leads to the increase of the costs.

In this work we consider a batch diafiltration (DF) process, which operates under constant pressure and temperature. Diafiltration processes use a solute-free solvent (diluant e.g. water) to control the process via influencing the concentrations of solutes. Ng et al. (1976) derived conditions of optimal switching concentration for a standard, yet simple, DF process. Foley (1999) proposed to optimize switching times in the arbitrarily chosen sequence of the traditional control modes such as concentration mode or constant-volume diafiltration. Therein it was also shown that different control strategies of diluant addition can result in time-optimal operation or minimal diluant consumption. Procedures based on numerical optimization have been investigated in Fikar et al. (2010); Takači et al. (2009), where numerical methods of control vector parametrization (CVP) and orthogonal collocation (OC) were used to compute the optimal solution through approximation of control and state trajectories. These methods can be applied for arbitrary optimal control problems. Another way to solve them is to employ analytical methods. The advantage of analytical methods compared to numerical is the exact solution without any approxima-

tion. A fully analytical solution for optimal membrane operation without fouling was derived in Paulen et al. (2012) for arbitrarily initial and final conditions (e.g. concentrations).

However, one of main issues in membrane separation is membrane fouling. It causes a decrease in effective membrane area due to the deposit of the solutes in or on the membrane pores. This results in an increase of the processing time to reach the desired purification goal. Moreover, the fouled membrane needs to be cleaned or replaced (Luján-Facundo et al., 2015) which further increases the operational costs. For these reasons modeling of the fouling behavior has gained importance. The pioneering work of Hermia (1982) presented a unified fouling model describing this behavior from which four standard fouling models can be derived. These express the decrease in effective membrane area (Bolton et al., 2006) or the permeate flux (Vela et al., 2008). The main motivation of this work was the possibility of running the batch plant time-optimally in the presence of fouling and thus achieving minimum fouling operation of the batch. For this reason several studies dealt with optimal operation of diafiltration process in the presence in membrane fouling. In Jelemenský et al. (2014) preliminary results on time-optimal operation in the presence of membrane fouling have been published. A combination of numerical and analytical methods was used to compute the optimal control profiles. A fully analytical optimal operation was derived in Jelemenský et al. (2016b) where Pontryagin's minimum principle (PMP) was used. The authors in both works concluded that the time-optimal operation is a three step strategy with conventional control in first and last step and advanced control in middle.

However, optimal model-based control of membrane processes requires a knowledge of process model and its parameters where the use of inaccurate values of the parameters could lead to significantly suboptimal performance. Estimation of unknown parameters can be done using various methods. Common practice is to employ a least-squares method and to estimate multiple fouling models in parallel off-line (Charfi et al., 2012). Advanced method based on

on-line parameter estimation of the membrane fouling using extended Kalman filter (EKF) was proposed in Jelemenský et al. (2016a).

The thesis is organized as follows. We briefly explain the general description of dynamic optimization (Section 2) and analytical and numerical methods for solving a general dynamic optimization problem (Section 3). Section 4 provides introduction into membrane separation processes. In Section. 5 a detailed discussion about modeling and optimization is presented. Section 6 introduces the definition of the classical fouling models and also discusses the cleaning methods. In Section 7 we define the optimal control problem, and we provide the definition of the optimal operation in the presence of the fouling. We apply the results on two case studies from open literature and we compare the obtained results with traditionally used control approaches. In Section 8 we show the procedure for estimation of the fouling behavior. Section 9 concludes the work and discusses the future research.

The most important results of the author on optimal operation of membrane separation processes without fouling effects were published in:

- R. Paulen, M. Jelemenský, M. Fikar, and Z. Kovacs. Optimal balancing of temporal and buffer costs for ultrafiltration/diafiltration processes under limiting flux conditions. *Journal of Membrane Science*, vol. 444, pp. 87–95, 2013.

- R. Paulen, M. Jelemenský, Z. Kovacs, and M. Fikar. Optimal balancing of temporal and buffer costs for ultrafiltration/diafiltration processes under limiting flux conditions. *Journal of Process Control*, vol. 28, pp. 73–82, 2015.

- M. Jelemenský, R. Paulen, M. Fikar, and Z. Kovacs. Time-Optimal Operation of Multi-Component Batch Diafiltration. *Computers & Chemical Engineering*, 83, 131–138, 2015.

We have built on the theoretical basis from the previous studies and have de-

fined the optimal operation in the presence of membrane fouling. Multiple studies show great improvement in the performance of the membrane processes. Finally, we discuss advantages and disadvantages of the new developed optimal operation.

Optimal operation in the presence of membrane fouling was published in:

- M. Jelemenský, R. Paulen, M. Fikar, and Z. Kovacs. Time-optimal Diafiltration in the Presence of Membrane Fouling. In *Preprints of the 19th IFAC World Congress*, Cape Town, South Africa, pp. 4897–4902, 2014.

- A. Sharma, M. Jelemenský, R. Paulen, and M. Fikar. Estimation of membrane fouling parameters for concentrating lactose using nanofiltration. In *26th European Symposium on Computer Aided Process Engineering*, Portoroz, Slovenia, 2016.

- M. Jelemenský, M. Klaučo, R. Paulen, J. Lauwers, F. Logist, J. Van Impe, and M. Fikar. Time-optimal control and parameter estimation of diafiltration processes in the presence of membrane fouling. In *11th IFAC Symposium on Dynamics and Control of Process Systems*, Trondheim, Norway, 2016.

- M. Jelemenský, A. Sharma, R. Paulen, and M. Fikar. Time-optimal control of diafiltration processes in the presence of membrane fouling. *Computers & Chemical Engineering*, 2016, (accepted).

Goals of the Thesis

The aim of this thesis is to study optimal control of batch diafiltration processes in the presence of membrane fouling. The optimal control is explored through the methods of dynamic optimization and provides improvement compared to traditional operations.

The main objectives can be summarized as follows:

- Study of optimal operation of membrane processes in the presence of membrane fouling.

- Derivation of fully analytical optimal operation in the presence of membrane fouling.

- Implementation and verification of the proposed optimal operation in case studies and comparison of the results with traditional control approaches.

Part I

Theoretical Basis

Chapter 2

Dynamic Optimization

Dynamic optimization stands for a group of methods which seek state and control trajectories to ensure optimal behavior of embedded dynamic system. The optimal solution defines the best element from a set of available choises (e.g. satisfaction of constraints and minimal value of objective function). For solving a general dynamic optimization problem we need to define three important parts which all together formulate a general dynamic optimization problem. The three parts are as follows :

1. objective functional

2. mathematical description (model) of the controlled plant

3. constraints definition

In the rest of the chapter we discuss the three individual parts closer and show some classical optimal control problems.

2.1   Objective Functional

The first part of the each optimization problem is the objective functional. The objective functional represents losses or expenses which we want to reach or avoid. The objective functional can be expressed in three different forms which are equivalent and can be converted to each other. The individual objective functionals are

- Lagrange form

$$\mathcal{J} = \int\limits_{t_0}^{t_\mathrm{f}} \mathcal{F}(t, \boldsymbol{x}(t), \boldsymbol{u}(t)) \, \mathrm{d}t \tag{2.1a}$$

- Mayer form

$$\mathcal{J} = \mathcal{G}(t_\mathrm{f}, \boldsymbol{x}(t_\mathrm{f})) \tag{2.1b}$$

- Bolza form

$$\mathcal{J} = \mathcal{G}(t_\mathrm{f}, \boldsymbol{x}(t_\mathrm{f})) + \int\limits_{t_0}^{t_\mathrm{f}} \mathcal{F}(t, \boldsymbol{x}(t), \boldsymbol{u}(t)) \, \mathrm{d}t \tag{2.1c}$$

where $\boldsymbol{x}(t) \in \mathbb{R}^{n_x}$ is a vector of state variables, $\boldsymbol{u}(t) \in \mathbb{R}^{n_u}$ is vector of control variables, t is independent time variable, t_0 and t_f represent the initial and final time, respectively. Variables n_x, n_u denote the dimensions of the state and control vectors, respectively.

$\mathcal{J}$ represents the objective functional, $\mathcal{G} : \mathbb{R}^{n_x} \to \mathbb{R}$ and $\mathcal{F} : [t_0,\, t_\mathrm{f}] \times \mathbb{R}^{n_x} \times \mathbb{R}^{n_u} \to \mathbb{R}$ are differentiable scalar functions. However, in the rest of the thesis, for simplicity, we will omit the time-dependency of the state and control variables. Therefore, we consider that $\boldsymbol{x}(t) = \boldsymbol{x}$ and $\boldsymbol{u}(t) = \boldsymbol{u}$.

2.2   Process Model

Mathematical representation of a real process can be obtained by formulating a mathematical model. The process model is usually in form of differential and algebraic equations. We can also view the process model as additional equality constraint which has to be satisfied over time. We will focus on continuous time-dependent representation of the model, however, each continuous model can also be easily discretized. We consider the process described by a set of ordinary differential equations

$$\dot{\boldsymbol{x}} = \boldsymbol{f}(t, \boldsymbol{x}, \boldsymbol{u}), \qquad \forall t \in [t_0, t_{\mathrm{f}}], \qquad\qquad (2.2\text{a})$$

where $\boldsymbol{f}(.)$ is the vector function defined such that $\boldsymbol{f} : [t_0, t_{\mathrm{f}}] \times \mathbb{R}^{n_x} \times \mathbb{R}^{n_u} \to \mathbb{R}^{n_x}$ with the initial conditions

$$\boldsymbol{x}(t_0) = \boldsymbol{x}_0, \qquad\qquad (2.2\text{b})$$

and $\boldsymbol{x}(t_0)$ is a vector of initial conditions such that $\boldsymbol{x}_0 : \mathbb{R}^{n_x} \to \mathbb{R}^{n_x}$.

However, in some cases the process model can take a special form. In this work we will consider that the differential equations are affine in control. Then the mathematical representation of the model can be written as following

$$\dot{\boldsymbol{x}} = \tilde{\boldsymbol{f}}(t, \boldsymbol{x}) + \tilde{\boldsymbol{g}}(t, \boldsymbol{x})\boldsymbol{u}, \qquad \boldsymbol{x}(t_0) = \boldsymbol{x}_0, \qquad\qquad (2.2\text{c})$$

where $\tilde{\boldsymbol{f}}(.)$ and $\tilde{\boldsymbol{g}}(.)$ are non-linear functions such that $\tilde{\boldsymbol{f}} : [t_0, t_{\mathrm{f}}] \times \mathbb{R}^{n_x} \to \mathbb{R}^{n_x}$ and $\tilde{\boldsymbol{g}} : [t_0, t_{\mathrm{f}}] \times \mathbb{R}^{n_x} \to \mathbb{R}^{n_x \times n_u}$. In both cases we can observe that the dynamics of the system is not only influenced by the states and control but also explicitly by time.

2.3   Constraints

In addition to process model, which represents equality constraints as stated above, we also have to consider additional constraints. These constraints can

represent boundaries on control or state variables but also physical constraints
on the real process for safety (e.g. diameter of pipes, maximum/minimum flow,
maximum temperature). In the following we introduce general representation
of such constraints for the optimal control problem:

- Interior equality constraints

$$\boldsymbol{h}(t, \boldsymbol{x}, \boldsymbol{u}) = \boldsymbol{0}, \quad t \in [t_0, t_{\mathrm{f}}], \tag{2.3a}$$

  these constraints can be found in chemical processes. This type of con-
  straints can be used for example when we require that sum of mole frac-
  tions of individual components must be equal to one in each time.

- Interior inequality constraints

$$\boldsymbol{g}(t, \boldsymbol{x}, \boldsymbol{u}) \leq \boldsymbol{0} \quad t \in [t_0, t_{\mathrm{f}}], \tag{2.3b}$$

  are mainly used when we require that states or parameters have to be less
  than a maximum value in each time. This can be illustrated on for example
  when temperature or pressure inside of a system must be maintained under
  a certain value.

- Terminal equality constraints

$$\boldsymbol{h}(t_{\mathrm{f}}, \boldsymbol{x}, \boldsymbol{u}) = \boldsymbol{0} \tag{2.3c}$$

  are typical when we deal with fixed terminal point and states must reach a
  specific value at the end. These can represent that a desired concentration
  of product must be satisfied.

- Terminal inequality constraints

$$\boldsymbol{g}(t_{\mathrm{f}}, \boldsymbol{x}, \boldsymbol{u}) \leq \boldsymbol{0} \tag{2.3d}$$

  can represent such constraints when we need to ensure that specific states
  or decision variables will not exceed specific limits. For example, when a
  desired final purity of a product must be satisfied.

It is worth of mention that each of the discussed constraints can be written in canonical form which is equivalent to the objective function form (2.1)

$$\mathcal{J}_c = \mathcal{G}_c\left(t_c, \boldsymbol{x}(t_c)\right) + \int_{t_{c,0}}^{t_{c,\mathrm{f}}} \mathcal{F}_c\left(t, \boldsymbol{x}, \boldsymbol{u}\right) \mathrm{d}t, \tag{2.4}$$

where $c = 1, \ldots, n_c$ and n_c represents the number of constraints. Then the constraints can be added to the objective functional by introducing Lagrange multiplicators $\nu \in \mathbb{R}^{n_c}$ and forming an augmented functional $\bar{\mathcal{J}}$

$$\bar{\mathcal{J}} = \mathcal{J} + \sum_{c=1}^{n_c} \nu_c \mathcal{J}_c \tag{2.5}$$

where $\mathcal{J}$ is the original objective functional and the term after the sum $\nu_c \mathcal{J}_c$ are added constraints. Then the new form of the objective functional (Bolza form) can be written as follows

$$\bar{\mathcal{J}} = \bar{\mathcal{G}} + \int_{t_0}^{t_{\mathrm{f}}} \bar{\mathcal{F}} \mathrm{d}t \tag{2.6}$$

where

$$\bar{\mathcal{G}} = \mathcal{G} + \sum_{c=1}^{n_c} \nu_c \mathcal{G}_c \tag{2.7}$$

and

$$\bar{\mathcal{F}} = \mathcal{F} + \sum_{c=1}^{n_c} \nu_c \mathcal{F}_c. \tag{2.8}$$

2.4 Optimal Control Problems

Previously we have formulated the three most important parts of a general optimal control problem (optimization problem). Moreover, we have shown that each problem consists of several constraints of different form. In this section we will discuss four basic optimal control problems shown in Fig. 2.1. The difference between the problems is if we consider fixed or free final state or fixed/free
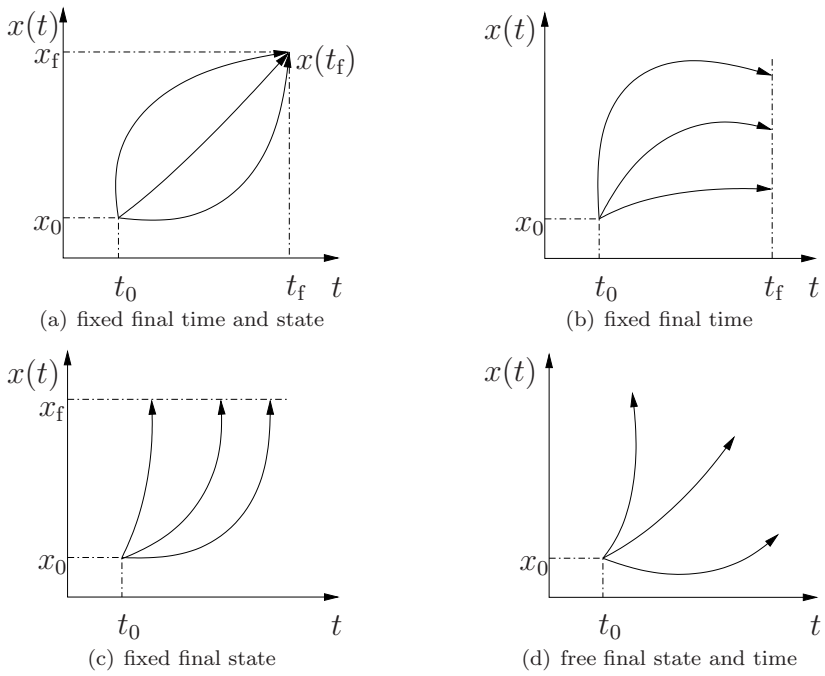
Figure 2.1: General description of optimal control problems.

final time. The main objective in each optimization problem is the minimization/maximization of the objective functional. Let us now in detail focus on the four basic optimal control problems. The first case shown in Fig. 2.1(a) is if we consider fixed final time and fixed final conditions for the state variables. In this case we need to find such optimal control trajectory which will steer the states from an initial point to final in a specific time (e.g. energy minimization). The second case (shown in Fig. 2.1(b)) considers that only the final time is fixed and we have no terminal conditions on states. In this case we want to for example maximize the amount of a substance that we need to produce over a fixed time. The third case illustrated by Fig. 2.1(c) shows an example when terminal conditions on states are specified and the final time is free. This case shows a typical minimum time problem, where we want to reach a desired value of states in minimum time (e.g. final concentrations). The last case (shown in Fig. 2.1(d)) represents the least restrictive case because the final time and states are not specified. An example to illustrate this case is when we want to find out in which time can we produce a maximal amount of substance.

2.5 Problem Definition

In the above sections we have introduced the three important parts of the optimization problem (process model, constraints, and objective function). Based on this we can formulate a general optimal control problem which reads as

$$\min_{\boldsymbol{u}} \left\{ \mathcal{G}(t_{\mathrm{f}}, \boldsymbol{x}(t_{\mathrm{f}})) + \int_{t_0}^{t_{\mathrm{f}}} \mathcal{F}(t, \boldsymbol{x}, \boldsymbol{u}) \, \mathrm{d}t \right\},$$

$$\text{s.t.} \quad \dot{\boldsymbol{x}} = \boldsymbol{f}(t, \boldsymbol{x}, \boldsymbol{u}), \quad \forall t \in [t_0, t_{\mathrm{f}}],$$

$$\boldsymbol{x}(t_0) = \boldsymbol{x}_0,$$

$$\boldsymbol{h}(t, \boldsymbol{x}, \boldsymbol{u}) = \boldsymbol{0}, \quad \forall t \in [t_0, t_{\mathrm{f}}], \tag{2.9}$$

$$\boldsymbol{g}(t, \boldsymbol{x}, \boldsymbol{u}) \leq \boldsymbol{0}, \quad \forall t \in [t_0, t_{\mathrm{f}}],$$

$$\boldsymbol{u} \in [\boldsymbol{u}_{\min}, \boldsymbol{u}_{\max}],$$

We can observe that the optimal control problem consists of objective functional where we want to find such control which will minimize the objective functional. Moreover, we have the process model equations with initial conditions and constraints in form of inequalities and equalities. Further, if a specific optimal control problem is defined constraints in final time can be added into the optimization it. At last, constraints on control and parameters are also added into the problem. For finding the solution to the problem (2.9) we can use several methods. These methods can be divided into two major groups: analytical or numerical methods. In the next chapter we will focus on these methods for solving a general optimal control problem.

Solution to Dynamic Optimization Problems

Previously we have formulated a classical optimal control problem. This chapter will be devoted to methods for solving such optimal control problems. There exists several often used methods which can be split into two major groups (analytical and numerical methods).

3.1 Necessary Conditions of Optimality

Throughout this section we will show the complete derivation of the necessary conditions of optimality (Bryson, Jr. and Ho, 1975; Hull, 2003), which can also provide information for the derivation of gradients for the objective function. We will consider an unconstrained case where the final conditions as well final time are free. However, if final conditions exists we have shown (in Section 2.3) that the constraints can be added into the objective functional. Further, the minimized function can be joined with process model (2.2a) by introducing

adjoint variables $\boldsymbol{\lambda}(t) \in \mathbb{R}^{n_x}$ and to obtain the functional in the following form

$$\mathcal{J} = \mathcal{G} + \int_{t_0}^{t_f} \left[\mathcal{F} + \boldsymbol{\lambda}^T (\boldsymbol{f} - \dot{\boldsymbol{x}})\right] \mathrm{d}t. \tag{3.1}$$

In the next step we define the Hamiltonian function as

$$H(t, \boldsymbol{x}, \boldsymbol{\lambda}, \boldsymbol{u}) = \mathcal{F}(t, \boldsymbol{x}, \boldsymbol{u}) + \boldsymbol{\lambda}^T \boldsymbol{f}(t, \boldsymbol{x}, \boldsymbol{u}). \tag{3.2}$$

New form of augmented functional can be written as follows

$$\mathcal{J}(\boldsymbol{u}) = \mathcal{G}(\boldsymbol{x}(t_f), \boldsymbol{x}(t_i), t_f, t_i) + \int_{t_0}^{t_f} \left[H(t, \boldsymbol{x}, \boldsymbol{\lambda}, \boldsymbol{u}) - \boldsymbol{\lambda}^T \dot{\boldsymbol{x}}\right] \mathrm{d}t \tag{3.3}$$

where $t_i \in [t_0,\, t_f]$ represent interior time points. We will consider the optimal control problem with free final state and time (Fig. 2.1(d)).

The differential of functional (3.3) can be expressed in the following form

$$\mathrm{d}\mathcal{J} = \mathrm{d}\mathcal{G} + \int_{t_0}^{t_f} \delta H \,\mathrm{d}t - \int_{t_0}^{t_f} \delta(\boldsymbol{\lambda}^T \dot{\boldsymbol{x}}) \,\mathrm{d}t + (H - \boldsymbol{\lambda}^T \dot{\boldsymbol{x}})|_{t_f} \,\mathrm{d}t_f + \sum_{i=1}^{n_i} [H - \boldsymbol{\lambda}^T \dot{\boldsymbol{x}}]_{t_i^+}^{t_i^-} \,\mathrm{d}t_i. \tag{3.4}$$

By applying the integration method *by parts* we can transform $\int_{t_0}^{t_f} \delta(\boldsymbol{\lambda}^T \dot{\boldsymbol{x}}) \mathrm{d}t$ into

$$-\int_{t_0}^{t_f} \delta(\boldsymbol{\lambda}^T \dot{\boldsymbol{x}}) \,\mathrm{d}t = -\int_{t_0}^{t_f} (\delta\boldsymbol{\lambda}^T \dot{\boldsymbol{x}} + \boldsymbol{\lambda}^T \delta\dot{\boldsymbol{x}}) \,\mathrm{d}t, \tag{3.5}$$

$$= \int_{t_0}^{t_f} (\dot{\boldsymbol{\lambda}}^T \delta\boldsymbol{x} - \delta\boldsymbol{\lambda}^T \dot{\boldsymbol{x}}) \,\mathrm{d}t - [\boldsymbol{\lambda}^T \delta\boldsymbol{x}]_{t_0}^{t_f} - \sum_{i=1}^{n_i} [\boldsymbol{\lambda}^T \delta\boldsymbol{x}]_{t_i^+}^{t_i^-}.$$

The differentials and variations can be expressed by equation (3.4) where equa-

tion (3.5) must be considered and we obtain the following form

$$
\begin{aligned}
\mathrm{d}\mathcal{J} =& \frac{\partial \mathcal{G}}{\partial \boldsymbol{x}^T}\bigg|_{t=t_\mathrm{f}} \mathrm{d}\boldsymbol{x}_{t_\mathrm{f}} + \sum_{i=1}^{n_i} \frac{\partial \mathcal{G}}{\partial \boldsymbol{x}^T}\bigg|_{t=t_i} \mathrm{d}\boldsymbol{x}_{t_i} + \frac{\partial \mathcal{G}}{\partial t_\mathrm{f}}\mathrm{d}t_\mathrm{f} + \sum_{i=1}^{n_i} \frac{\partial \mathcal{G}}{\partial t_i}\mathrm{d}t_i \\
&+ \int_{t_0}^{t_\mathrm{f}} \left(\frac{\partial H}{\partial \boldsymbol{x}^T}\delta \boldsymbol{x} + \frac{\partial H}{\partial \boldsymbol{\lambda}^T}\delta \boldsymbol{\lambda} + \frac{\partial H}{\partial \boldsymbol{u}^T}\delta \boldsymbol{u} + \dot{\boldsymbol{\lambda}}^T \delta \boldsymbol{x} - \delta \boldsymbol{\lambda}^T \dot{\boldsymbol{x}} \right) \mathrm{d}t \quad (3.6) \\
&- \boldsymbol{\lambda}_{t_\mathrm{f}}^T \delta \boldsymbol{x}_{t_\mathrm{f}} + \boldsymbol{\lambda}_{t_0}^T \delta \boldsymbol{x}_{t_0} + \sum_{i=1}^{n_i} (\boldsymbol{\lambda}_{t_i^+}^T \delta \boldsymbol{x}_{t_i^+} - \boldsymbol{\lambda}_{t_i^-}^T \delta \boldsymbol{x}_{t_i^-}) + H_{t_\mathrm{f}}\mathrm{d}t_\mathrm{f} - \boldsymbol{\lambda}_{t_\mathrm{f}}^T \dot{\boldsymbol{x}}_{t_\mathrm{f}}\mathrm{d}t_\mathrm{f} \\
&+ \sum_{i=1}^{n_i} (H_{t_i^-} - H_{t_i^+})\,\mathrm{d}t_i + \sum_{i=1}^{n_i} (\boldsymbol{\lambda}_{t_i^+}^T \dot{\boldsymbol{x}}_{t_i^+} - \boldsymbol{\lambda}_{t_i^-}^T \dot{\boldsymbol{x}}_{t_i^-})\,\mathrm{d}t_i.
\end{aligned}
$$

In the last step we regroup the differential and variational terms together. Note that $\mathrm{d}\boldsymbol{x}_{t_i} = \delta \boldsymbol{x}_{t_i^\pm} + \dot{\boldsymbol{x}}_{t_i^\pm}\mathrm{d}t_i$ and $\delta \boldsymbol{x}_{t_0} = \boldsymbol{0}$ since $\boldsymbol{x}_0$ is fixed, hence

$$
\begin{aligned}
\mathrm{d}\mathcal{J} =& \left(\frac{\partial \mathcal{G}}{\partial \boldsymbol{x}^T}\bigg|_{t_\mathrm{f}} - \boldsymbol{\lambda}_{t_\mathrm{f}}^T \right) \mathrm{d}\boldsymbol{x}_{t_\mathrm{f}} + \left(\frac{\partial \mathcal{G}}{\partial t_\mathrm{f}} + H_{t_\mathrm{f}} \right) \mathrm{d}t_\mathrm{f} + \\
&+ \sum_{i=1}^{n_i} \left(\frac{\partial \mathcal{G}}{\partial t_i} + H_{t_i^-} - H_{t_i^+} \right) \mathrm{d}t_i + \sum_{i=1}^{n_i} \left(\frac{\partial \mathcal{G}}{\partial \boldsymbol{x}^T}\bigg|_{t=t_i} + \boldsymbol{\lambda}_{t_i^+}^T - \boldsymbol{\lambda}_{t_i^-}^T \right) \mathrm{d}\boldsymbol{x}_{t_i} + \\
&+ \int_{t_0}^{t_\mathrm{f}} \left[\left(\frac{\partial H}{\partial \boldsymbol{x}^T} + \dot{\boldsymbol{\lambda}}^T \right) \delta \boldsymbol{x} + \left(\frac{\partial H}{\partial \boldsymbol{\lambda}^T} - \dot{\boldsymbol{x}}^T \right) \delta \boldsymbol{\lambda} + \frac{\partial H}{\partial \boldsymbol{u}^T}\delta \boldsymbol{u} \right] \mathrm{d}t. \quad (3.7)
\end{aligned}
$$

Conditions of optimality follow from the equation (3.7) where the differential of the functional $\mathcal{J}$ must be equal to zero at optimum. This is when all terms in brackets in equation (3.7) are equal to zero. Then the necessary conditions of optimality are as follows

- optimality condition for

  control variables
  $$
  \frac{\partial H}{\partial \boldsymbol{u}} = \boldsymbol{0} \tag{3.8a}
  $$

  final time
  $$
  \frac{\partial \mathcal{G}}{\partial t_\mathrm{f}} + H_{t_\mathrm{f}} = 0 \tag{3.8b}
  $$

state variables

$$\dot{\boldsymbol{x}} = \frac{\partial H}{\partial \boldsymbol{\lambda}} \quad \forall t \in [t_0, t_\mathrm{f}] \tag{3.8c}$$

- optimal switching conditions for

  times

$$\frac{\partial \mathcal{G}}{\partial t_i} + H_{t_i^-} - H_{t_i^+} = 0 \quad \forall i \in \{1, \ldots, n_i\} \tag{3.8d}$$

  adjoint variables

$$\left.\frac{\partial \mathcal{G}}{\partial \boldsymbol{x}}\right|_{t=t_i} + \boldsymbol{\lambda}_{t_i^-} - \boldsymbol{\lambda}_{t_i^+} = \boldsymbol{0} \quad \forall i \in \{1, \ldots, n_i\} \tag{3.8e}$$

- adjoint variables

  definition

$$\dot{\boldsymbol{\lambda}} = -\frac{\partial H}{\partial \boldsymbol{x}} \quad \forall t \in [t_0, t_\mathrm{f}] \tag{3.8f}$$

  boundary conditions

$$\boldsymbol{\lambda}_{t_\mathrm{f}} = \left.\frac{\partial \mathcal{G}}{\partial \boldsymbol{x}}\right|_{t=t_\mathrm{f}} \tag{3.8g}$$

3.2 Analytical Methods

The first group of methods used to solve optimal control problems are the analytical methods. These methods represent a framework for obtaining optimal trajectories for states and control for a non-linear optimization problem analytically. These methods are dynamic programming, variational calculus and Pontryagin's minimum principle. In the rest of this section we discuss all these mentioned methods.

3.2.1 Dynamic Programming

Dynamic programming method is based on Bellman's principle of optimality (Bellman, 1957). The method builds on the fact that the optimal control

depends only on the initial and final state. The overall optimal trajectory is piece-wise optimal. The function that has to be minimized reads as

$$\mathcal{J}(t, \boldsymbol{x}) = \min_{\boldsymbol{u}} \left\{ \mathcal{G}(t_{\mathrm{f}}, \boldsymbol{x}(t_{\mathrm{f}})) + \int_t^{t_{\mathrm{f}}} \mathcal{F}(\tau, \boldsymbol{x}, \boldsymbol{u}) \mathrm{d}\tau \right\}. \tag{3.9}$$

The optimal control can be found by solving the Hamilton-Jacobi-Bellman equation

$$-\frac{\mathcal{J}(t, \boldsymbol{x})}{\partial t} = \min_{\boldsymbol{u}} \left\{ \mathcal{F}(t, \boldsymbol{x}, \boldsymbol{u}) + \frac{\partial \mathcal{J}(t, x)}{\partial \boldsymbol{x}^T} \boldsymbol{f}(\boldsymbol{x}, \boldsymbol{u}) \right\}, \tag{3.10}$$

which provides sufficient conditions of optimality.

3.2.2   Calculus of Variations

The variational calculus relations can be obtained from Bellman's partial differential equations. Result of the variational calculus is the Euler-Lagrange function of the form

$$\frac{\partial \mathcal{F}}{\partial \boldsymbol{x}} - \frac{\mathrm{d}}{\mathrm{d}t} \frac{\partial \mathcal{F}}{\partial \dot{\boldsymbol{x}}} = 0, \tag{3.11}$$

where $\mathcal{F}$ is the Lagrange function

$$\mathcal{F}(t, \dot{\boldsymbol{x}}, \boldsymbol{x}, \boldsymbol{u}, \boldsymbol{\lambda}) = \mathcal{F}(t, \dot{\boldsymbol{x}}, \boldsymbol{x}, \boldsymbol{u}) + \boldsymbol{\lambda}^T [\boldsymbol{f}(t, \boldsymbol{x}, \boldsymbol{u}) - \dot{\boldsymbol{x}}]. \tag{3.12}$$

This method gives the equivalent necessary conditions of optimality as shown previously. However, the biggest disadvantage of this method is the inability to solve optimization problems with constrained control.

3.2.3   Pontryagin's Minimum Principle

An extension to the previous analytical methods in the Pontryagin's minimum principle (PMP) formulated by Pontryagin et al. (1962). The advantage of this method lies in the fact that we can solve dynamic optimal control problems

where constraints on control and parameters take place. The general definition
is as follows

$$\min_{\boldsymbol{u}\in[\boldsymbol{u}_{\min},\boldsymbol{u}_{\max}]} H(t,\boldsymbol{x},\boldsymbol{\lambda},\boldsymbol{u}) \tag{3.13}$$

$$\text{s.t.} \quad \dot{\boldsymbol{x}} = \boldsymbol{f}(t,\boldsymbol{x},\boldsymbol{u}), \qquad \boldsymbol{x}(t_0) = \boldsymbol{x}_0, \tag{3.14}$$

$$\dot{\boldsymbol{\lambda}} = -\frac{\partial H}{\partial \boldsymbol{x}}, \qquad \boldsymbol{\lambda}(t_{\mathrm{f}}) = \left.\frac{\partial \mathcal{G}}{\partial \boldsymbol{x}}\right|_{t_{\mathrm{f}}}. \tag{3.15}$$

The conditions for Pontryagin's minimum principle were derived from the nec-
essary conditions of optimality.

We will distinguish two types of problem formulations. The first is for au-
tonomous systems (implicit function of time) and the second for non-autonomous
systems (explicit function of time). Further, we will assume in the derivation of
the optimal operation that the system equations are affine in control (2.2c) and
that the final time is free. Moreover, we also assume that the Lagrange type
objective function is affine in control and reads as

$$\mathcal{J} = \int_{t_0}^{t_{\mathrm{f}}} \mathcal{F}(t,\boldsymbol{x},\boldsymbol{u})\mathrm{d}t = \int_{t_0}^{t_{\mathrm{f}}} [\mathcal{F}_0(t,\boldsymbol{x}) + \mathcal{F}_u(t,\boldsymbol{x})\boldsymbol{u}]\,\mathrm{d}t. \tag{3.16}$$

PMP for Autonomous Systems

In the first case we consider that the system equations and objective function
are an inplict function of time. Then the general formulation for PMP in case
of autonomous systems is as follows

$$\boldsymbol{u}^* = \arg\min_{\boldsymbol{u}\in[\boldsymbol{u}_{\min},\boldsymbol{u}_{\max}]} H(\boldsymbol{x},\boldsymbol{\lambda},\boldsymbol{u}) \equiv H_0(\boldsymbol{x},\boldsymbol{\lambda}) + H_u(\boldsymbol{x},\boldsymbol{\lambda})\boldsymbol{u} \tag{3.17a}$$

$$\dot{\boldsymbol{x}} = \tilde{\boldsymbol{f}}(\boldsymbol{x}) + \tilde{\boldsymbol{g}}(\boldsymbol{x})\boldsymbol{u}, \quad \boldsymbol{x}(t_0) = \boldsymbol{x}_0, \quad \boldsymbol{x}(t_{\mathrm{f}}) = \boldsymbol{x}_{\mathrm{f}}, \tag{3.17b}$$

$$\dot{\boldsymbol{\lambda}} = -\frac{\partial H}{\partial \boldsymbol{x}} \tag{3.17c}$$

$$H = 0, \qquad \forall t \in [t_0,\,t_{\mathrm{f}}] \tag{3.17d}$$

Since the Hamiltonian function, system equations, and objective function are
implicit functions of time the Hamiltonian function will be zero over the entire

time horizon. And since the final time is free the Hamiltonian is zero at the final time. Moreover, since the Hamiltonian function is affine in control $\boldsymbol{u}$ the minimum will be attained with control on its boundaries or when it is singular

$$
\boldsymbol{u}^* = \begin{cases} \boldsymbol{u}_{\min} & \text{if } H_u > 0, \\ \boldsymbol{u}_{\max} & \text{if } H_u < 0, \\ \boldsymbol{u}_{\text{sing}} & \text{if } H_u = 0 \end{cases} \tag{3.18}
$$

In case that the Hamiltonian is singular ($H_u = 0$) the Hamiltonian function does not depend on control. In this case it is possible to obtain the so-called singular surface $S(\boldsymbol{x}) = 0$ and singular control $\boldsymbol{u}_{\text{sing}}(\boldsymbol{x})$ which both depend only on the state variables. This is caused by the fact that the Hamiltonian function is zero over the entire time horizon and $H_u = 0$ that implies that also $H_0 = 0$ and the time derivatives of both parts will be equal to zero. We can then generate the set of following equations

$$
H_0(\boldsymbol{x}, \boldsymbol{\lambda}) = 0, \tag{3.19a}
$$

$$
H_u(\boldsymbol{x}, \boldsymbol{\lambda}) = 0, \tag{3.19b}
$$

$$
\frac{\mathrm{d}^i H_0}{\mathrm{d}t^i}(\boldsymbol{x}, \boldsymbol{\lambda}, \boldsymbol{u}) = 0, \tag{3.19c}
$$

$$
\frac{\mathrm{d}^i H_u}{\mathrm{d}t^i}(\boldsymbol{x}, \boldsymbol{\lambda}, \boldsymbol{u}) = 0, \tag{3.19d}
$$

where i represents the order of time derivative. We can eliminate the adjoint variables $\boldsymbol{\lambda}$ and obtain the singular surface $S(\boldsymbol{x}) = 0$ which depends only on the state variables. To obtain the singular control $\boldsymbol{u}(\boldsymbol{x})$ we differentiate the singular surface w.r.t. time. It is worth of mention that the singular surface can be only derived for second order system (two state variables). Once a higher order system is considered the singular surface cannot be derived, however it is still possible to obtain the singular control.

PMP for Non-Autonomous Systems

In this case we will consider that the system equations are an explicit function of time. Then the general formulation for PMP can be written as follows

$$u^* = \arg \min_{\boldsymbol{u} \in [\boldsymbol{u}_{\min}, \boldsymbol{u}_{\max}]} H(t, \boldsymbol{x}, \boldsymbol{\lambda}, \boldsymbol{u}) \equiv H_0(t, \boldsymbol{x}, \boldsymbol{\lambda}) + H_u(t, \boldsymbol{x}, \boldsymbol{\lambda})\boldsymbol{u} \qquad (3.20a)$$

$$\dot{\boldsymbol{x}} = \tilde{\boldsymbol{f}}(t, \boldsymbol{x}) + \tilde{\boldsymbol{g}}(t, \boldsymbol{x})\boldsymbol{u}, \quad \boldsymbol{x}(t_0) = \boldsymbol{x}_0, \quad \boldsymbol{x}(t_{\mathrm{f}}) = \boldsymbol{x}_{\mathrm{f}}, \qquad (3.20b)$$

$$\dot{\boldsymbol{\lambda}} = -\frac{\partial H}{\partial \boldsymbol{x}} \qquad (3.20c)$$

$$H(t_{\mathrm{f}}) = 0. \qquad (3.20d)$$

Since Hamiltonian is an explicit function of time it is not equal to zero over the whole time horizon as in the previous case. Therefore, unlike in the previous case we cannot consider that both parts of the Hamiltonian function will be equal to zero (Chachuat, 2009). Moreover, also the the derivative of Hamiltonian w.r.t. time is not constant and it is defined as follows

$$\dot{H}(t, \boldsymbol{x}, \boldsymbol{\lambda}, \boldsymbol{u}) = \frac{\partial}{\partial t} \left[\mathcal{F}_0(t, \boldsymbol{x}) + \mathcal{F}_u(t, \boldsymbol{x})\boldsymbol{u} \right] + \qquad (3.21)$$

$$+ \frac{\partial \boldsymbol{\lambda}^T}{\partial t} \left[\tilde{\boldsymbol{f}}(t, \boldsymbol{x}) + \tilde{\boldsymbol{g}}(t, \boldsymbol{x})\boldsymbol{u} \right] +$$

$$+ \boldsymbol{\lambda}^T \left[\frac{\partial}{\partial t} \left(\tilde{\boldsymbol{f}}(t, \boldsymbol{x}) + \tilde{\boldsymbol{g}}(t, \boldsymbol{x})\boldsymbol{u} \right) \right] \neq 0.$$

As in the previous case the Hamiltonian is affine in control and therefore, also in this case the minimum will be attained with control on its boundaries. For the derivation of the optimal operation we can use the same procedure as described in the previous subsection with the exception that it is not longer possible to set $H_0(t, \boldsymbol{x}, \boldsymbol{\lambda}) = 0$ since the Hamiltonian is an explicit function of time. The only possibility is only to set $H_u(t, \boldsymbol{x}, \boldsymbol{\lambda}) = 0$ and the respective time derivatives defined as follows

$$H_u(t, \boldsymbol{x}, \boldsymbol{\lambda}) = 0, \qquad (3.22a)$$

$$\frac{\mathrm{d}^i H_u}{\mathrm{d}t^i}(t, \boldsymbol{x}, \boldsymbol{\lambda}, \boldsymbol{u}) = 0, \qquad (3.22b)$$

where i represent the order of time derivative. The expression for singular surface $S(t, \boldsymbol{x}) = 0$ which is a fuction of states and time can be derived by elimination of the adjoint variables. And if the singular surface is differentiated w.r.t. time we obtain the singular control $\boldsymbol{u}(t, \boldsymbol{x})$. Moreover, also in this case like in the previous one the singular surface can only be derived for the second order systems.

3.3 Numerical Methods

The second group of methods which we will focus on by solving optimal control problems are the numerical methods. In general many optimization problems are very difficult (maybe impossible) to solve analytically. Therefore, it is necessary to use different approaches compared to analytical methods. We will focus on two methods which are the most used when dealing with non-linear optimization problems. These methods belong into the group of direct methods. The mentioned methods are the following

- complete discretization,

- control vector parametrization,

and these methods differ in the way if only the control or both control and state trajectories are discretized. The reason why the discretization is needed is that in case of continuous trajectories (state, control) one has to compute the optimal value in each time. Since there are infinite number of times the problem is intractable. Therefore by discretization with finite numbers of intervals we reduce the infinite number of optimized variables to finite.

3.3.1 Complete Discretization

The first numerical method for solving dynamic optimization methods is complete discretization. The main idea is that the state and control trajectories
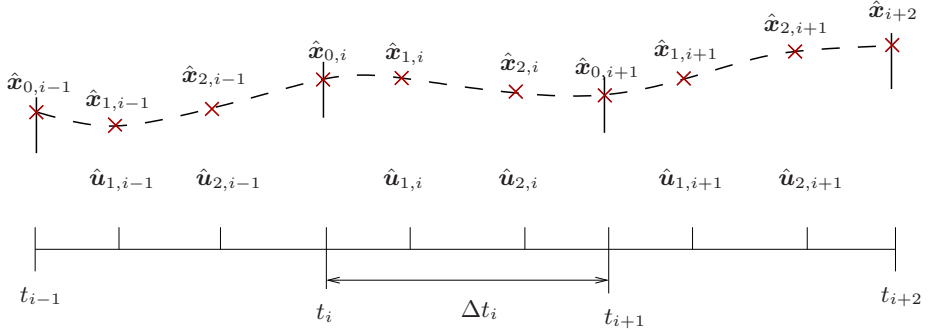
Figure 3.1: Distribution of time intervals and collocation points for state and control variables for $K_x = K_u = 2$

are simultaneously discretized with piece-wise Lagrange polynomial functions on some chosen number of intervals (finite number of elements). The approximation is exact at the collocation points. The roots of Legendre polynomials determine the distribution of these collocation points (Biegler, 1984; Čižniar et al., 2005).

Consider that the system is described by a set of ordinary differential equations (2.2a) and we consider the discretization on finite number of elements N_I. Then we approximate the state and control trajectories with Lagrange polynomial functions which are defined as follows

$$\hat{\boldsymbol{x}}_i(t) = \sum_{k=0}^{K_x} \hat{\boldsymbol{x}}_{k,i} \phi_k(t) \qquad \phi_k(t) = \prod_{r=0, r\neq k}^{K_x} \frac{t - t_{r,i}}{t_{k,i} - t_{r,i}}, \qquad (3.23a)$$

$$\hat{\boldsymbol{u}}_i(t) = \sum_{j=1}^{K_u} \hat{\boldsymbol{u}}_{j,i} \theta_j(t) \qquad \theta_j(t) = \prod_{r=1, r\neq j}^{K_u} \frac{t - t_{r,i}}{t_{k,i} - t_{r,i}}, \qquad (3.23b)$$

$$\text{for } i = 1, \dots, N_I, \qquad\qquad\qquad\qquad\qquad (3.23c)$$

where K_x and K_u denote the number of collocation points on states and control, respectively. Moreover, $\hat{\boldsymbol{x}}$ and $\hat{\boldsymbol{u}}$ denote the vectors of approximated state and control variables, respectively. The vector of optimized variables ($\boldsymbol{y}$) consists of

the collocation points for states and control and the time intervals.

$$\boldsymbol{y} = [\hat{\boldsymbol{x}}_{k,i}^T, \hat{\boldsymbol{u}}_{j,i}^T, \Delta t_i^T]^T, \tag{3.24}$$
$$k = 0, \ldots, K_x, \quad j = 1, \ldots, K_u, \quad i = 1, \ldots, N_I$$

In Fig. 3.1 we show approximation of state and control trajectories were we consider that number of collocation points on states are equal number of collocation points on control. Then the system equations (2.2a) can be approximated over the collocation points into the following form

$$\sum \hat{\boldsymbol{x}}_{k,i} \dot{\phi}_k(\tau_k) - \Delta t_i \boldsymbol{f}(t_{k,i}, \hat{\boldsymbol{x}}_{k,i}, \hat{\boldsymbol{u}}_{j,i}) = \boldsymbol{0}, \tag{3.25}$$
$$k = 0, \ldots, K_x, \quad j = 1, \ldots, K_u, \quad i = 1, \ldots, N_I,$$

were the finite elements are normalized on interval $\tau \in [0, 1]$. The overall optimization problem that needs to be solved is then of the following form

$$\min_{\hat{\boldsymbol{x}}_{k,i}, \hat{\boldsymbol{u}}_{j,i}, \Delta t_i} \left\{ G(\hat{\boldsymbol{x}}_{t_f, N_I}) + \sum_{i=1}^{N_I} \int_{t_{i,0}}^{t_{i,f}} F(\hat{\boldsymbol{x}}_{k,i}, \hat{\boldsymbol{u}}_{j,i}, t) \, \mathrm{d}t \right\}, \tag{3.26}$$

s.t.

$$\sum \hat{\boldsymbol{x}}_{k,i} \dot{\phi}_k(\tau_k) = \Delta t_i \boldsymbol{f}(t_{k,i}, \hat{\boldsymbol{x}}_{k,i}, \hat{\boldsymbol{u}}_{j,i}), \tag{3.27}$$
$$\hat{\boldsymbol{x}}_{0,1}(t_{1,0}) = \boldsymbol{x}_0, \qquad \hat{\boldsymbol{x}}_{K_x, N_I}(t_{N_I, f}) = \boldsymbol{x}_f, \tag{3.28}$$
$$\hat{\boldsymbol{x}}_i(t_{i,0}) = \hat{\boldsymbol{x}}_{i-1}(t_{i-1,f}), \tag{3.29}$$
$$\hat{\boldsymbol{u}}_{j,i} \in [\hat{\boldsymbol{u}}_{\min}, \hat{\boldsymbol{u}}_{\max}], \tag{3.30}$$

where $k = 0, \ldots, K_x$, $j = 1, \ldots, K_u$, $i = 1, \ldots, N_I$. The advantage of this approach lies in the transformation of the ODE equations into algebraic ones. Therefore, by this approach we can avoid any numerical integration of the differential equations. On the other hand, if high precision of the approximation is required the number of collocation points (states and control) must be increased as well. This means that even a simple non-linear problem (NLP) can generate many optimized variables.

(a) Continuous control trajectory   (b) Discretized control trajectory
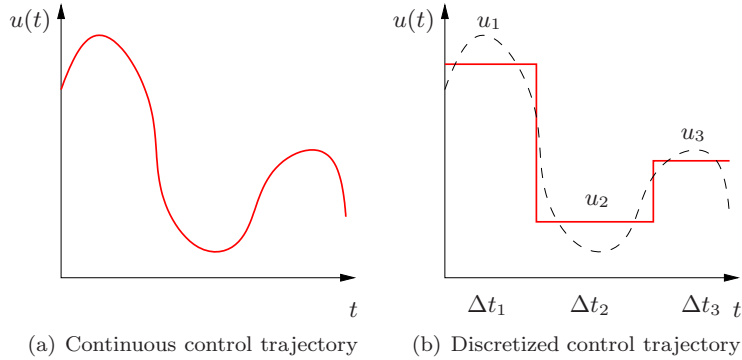
Figure 3.2: Graphical representation of the control vector parametrization method.

3.3.2   Control Vector Parametrization

Control vector parametrization (CVP) is one of the most used methods from numerical methods because of the simple implementation. The main idea behind this method is that only the original control trajectory (shown in Fig. 3.2(a)) is discretized with finite number of constant (shown in Fig. 3.2(b)) or linear controls over the time intervals (Fikar et al., 1998; Teo et al., 1991). The difference between CVP and the previous method lies in the fact that in complete discretization method also the states were approximated with polynomial functions compared to CVP where we only discretize the control trajectory.

As mentioned before the discretization can be of piece-wise constant or piece-wise linear nature. The individual formulas for the discretization are as follows

- piece-wise constant discretization

$$
\hat{\boldsymbol{u}}(t) = \sum_{i=1}^{N_I} \hat{\boldsymbol{u}}_i \varphi_i(t) \qquad \varphi_{[t_{i-1},t_i)} := \begin{cases} 1, & \text{if } t \in [t_{i-1}, t_i), \\ 0, & \text{if } t \notin [t_{i-1}, t_i). \end{cases} \tag{3.31}
$$

where i denotes the corresponding time interval.

- piece-wise linear discretization

$$\hat{\boldsymbol{u}}(t) = \hat{\boldsymbol{u}}_{i-1} + \frac{\hat{\boldsymbol{u}}_i - \hat{\boldsymbol{u}}_{i-1}}{t_i - t_{i-1}}(t - t_{i-1}), \qquad \forall i \in 1, \ldots, N_I. \tag{3.32}$$

Throughout this work we will consider piece-wise constant approximation of the control trajectory. The vector of optimized variables consists of controls (constant) and delta intervals which is as follows

$$\boldsymbol{y} = (\hat{\boldsymbol{u}}_1^T, \ldots, \hat{\boldsymbol{u}}_{N_I}^T, \Delta t_1, \ldots, \Delta t_{N_I})^T \tag{3.33}$$

The overall optimization problem that needs to be solved is of the following structure

$$\min_{\boldsymbol{y}} \left\{ \mathcal{G}(\boldsymbol{x}(t_f^{N_I})) + \sum_{i=1}^{N_I} \int_{t_{i,0}}^{t_{i,f}} \mathcal{F}(t, \boldsymbol{x}, \hat{\boldsymbol{u}}_i) \, \mathrm{d}t \right\},$$

$$\text{s.t. } \dot{\boldsymbol{x}} = \boldsymbol{f}(t, \boldsymbol{x}, \hat{\boldsymbol{u}}_i), \quad \forall t \in [t_{i,0}, t_{i_f}], \, \forall i \in \overline{1, N_I},$$

$$\boldsymbol{x}(t_{1,0}) = \boldsymbol{x}_0,$$

$$\boldsymbol{h}(t, \boldsymbol{x}, \hat{\boldsymbol{u}}_i) = 0, \quad \forall t \in [t_0, t_f], \, \forall i \in \overline{1, N_I}, \tag{3.34}$$

$$\boldsymbol{g}(t, \boldsymbol{x}, \hat{\boldsymbol{u}}_i) \leq 0, \quad \forall t \in [t_{i,0}, t_{i,f}], \, \forall i \in \overline{1, N_I},$$

$$\hat{\boldsymbol{u}}_i \in [\hat{\boldsymbol{u}}_{i,\min}, \hat{\boldsymbol{u}}_{i,\max}], \quad \forall i \in \overline{1, N_I},$$

This problem can be solved by using efficient NLP solvers and numerical solvers for the differential equations. However, for better computational performance and also to achieve better convergence gradients w.r.t. to objective function and constraints need to be provided. There exist three approaches for the computation of gradients: (i) finite differences, (ii) sensitivity equations, and (iii) adjoint variables. In the rest of this chapter we will discuss them individually and show the differences between the approaches.

Finite Differences (FD)

Using the finite differences approach to calculate gradients (objective function and constraints) we need to integrate the system as many times as we have

optimized variables. Then, in each step we perturb the optimized variables by
a small value $(y_i + \Delta y)$. Then the gradients can be calculated as follows

$$\nabla_{y_i} \mathcal{J} = \frac{\mathcal{J}(y_1, \ldots, y_i + \Delta y_i, \ldots, y_n) - \mathcal{J}(\boldsymbol{y})}{\Delta y_i}. \tag{3.35}$$

The advantage is that this method does not generate any additional differential
equations. On the other hand, the integration of the ODE must be performed as
many times as is the number of optimized variables. Also, the finite difference
method is the most inaccurate methods from all but compared to other methods
it is very easy to implement.

Sensitivity Equations (SE)

Sensitivity equations method (Caracotsios and Stewart, 1985) is used when we
have large number of constraints but small number of optimized variables. The
gradients can be calculated as follows

$$\frac{\partial \mathcal{J}}{\partial y_i} = \frac{\partial \mathcal{G}}{\partial \boldsymbol{x}}\bigg|_{t_f} \frac{\partial \boldsymbol{x}}{\partial y_i} + \int_{t_0}^{t_f} \frac{\partial \mathcal{F}}{\partial \boldsymbol{x}} \frac{\partial \boldsymbol{x}}{\partial y_i} + \frac{\partial \mathcal{F}}{\partial \boldsymbol{u}} \frac{\partial \boldsymbol{u}}{\partial y_i} \mathrm{d}t, \tag{3.36}$$

where

$$\frac{\partial \boldsymbol{x}}{\partial y_i} = \boldsymbol{s}_i, \qquad i = 1 \ldots n_y, \tag{3.37}$$

are the sensitivities w.r.t. to the optimized variables and n_y denote the dimen-
sion of the vector of optimized variables. The sensitivities can be calculated as
follows

$$\dot{\boldsymbol{s}}_i = \frac{\partial \dot{\boldsymbol{x}}}{\partial y_i} = \frac{\partial \boldsymbol{f}}{\partial \boldsymbol{x}} \frac{\partial \boldsymbol{x}}{\partial y_i} + \frac{\partial \boldsymbol{f}}{\partial \boldsymbol{u}} \frac{\partial \boldsymbol{u}}{\partial y_i} \qquad \boldsymbol{s}_i(0) = \boldsymbol{0}, \qquad i = 1 \ldots n_y. \tag{3.38}$$

We can observe that the each optimized variable generates a system of sensitivity
equations that needs to be integrated forward. The integration of the sensitivity
system is done with the system equations.

Adjoint Variables (AV)

Based on the necessary conditions of optimality and the adjoint variables we can express the gradients w.r.t. to final time, times, parameters and control. The gradients can be calculated as follows

$$\frac{\partial \mathcal{J}}{\partial t_{\mathrm{f}}} = H(t_{\mathrm{f}}) + \frac{\partial \mathcal{G}}{\partial t_{\mathrm{f}}} \tag{3.39a}$$

$$\frac{\partial \mathcal{J}}{\partial t_j} = H(t_j^-) - H(t_j^+) \qquad j = 1, \ldots, N_I - 1 \tag{3.39b}$$

$$\frac{\partial \mathcal{J}}{\partial u_j} = \mathcal{J}_u(t_{j-1}) - \mathcal{J}_u(t_j) \qquad j = 1, \ldots, N_I - 1 \tag{3.39c}$$

where

$$\dot{\mathcal{J}}_u = \frac{\partial H}{\partial \boldsymbol{u}^T} \qquad \mathcal{J}_u(t_{\mathrm{f}}) = \mathbf{0}, \tag{3.39d}$$

However, we need to realize that the optimization variables are not times (t_j) but the time increments (delta intervals Δt_j). Therefore, we need to express the gradients w.r.t. to delta intervals. The gradients are calculated as

$$\frac{\partial \mathcal{J}_i}{\partial \Delta t_j} = \sum_{k=1}^{N_I} \frac{\partial \mathcal{J}_i}{\partial t_k}, \tag{3.40}$$

where we can observe that the gradients w.r.t. delta intervals are the sum of the individual times (3.39b).

This method is mainly used in case we have few constraints and large number of optimized variables. Because each constraint generates a new adjoint system which needs to be integrated backwards. The adjoint system (3.8f) is integrated backwards in time since we have only the knowledge about the values of the adjoint variables in final time.

The general algorithm for solving a optimal control problem with the control vector parametrization is shown in Fig. 3.3. In the first step we discretize the continuous control trajectory with piece-wise constant (or linear) control to
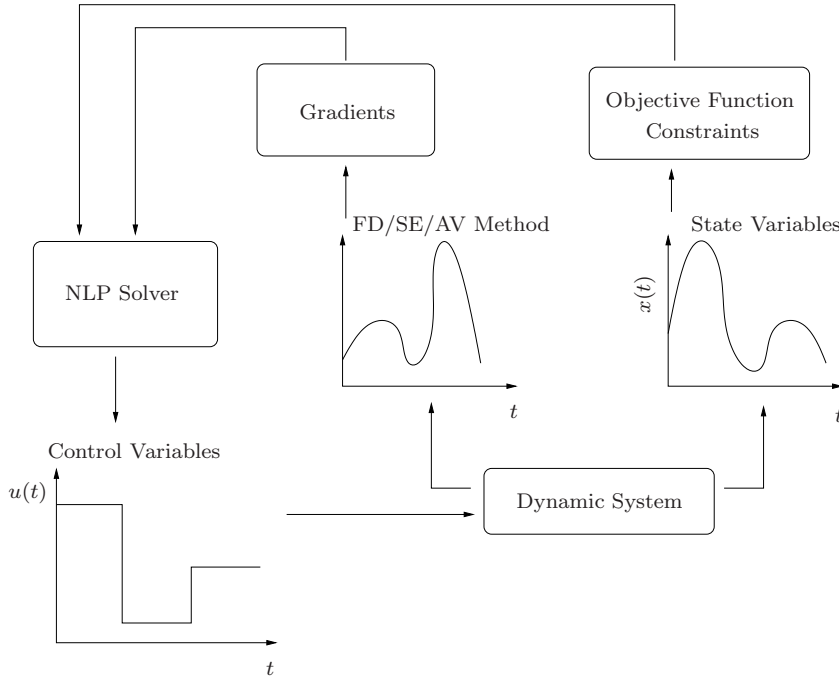
Figure 3.3: General procedure for solving problems using control vector parametrization method

make an initial guess for the optimized variables. In the second step we calculate the state trajectories and evaluate the objective function and constraints. Simultaneously we calculate the gradients w.r.t. to objective function and constraints. If the optimality conditions are satisfied then we obtained the optimal control, else we use non-linear programming solver (NLP) to obtain a new initial guess for the optimized variables.

Part II

Membrane Processes

Chapter 4

Process Description

Throughout this chapter we will discuss several types of membrane filtration techniques and configurations used in the industry (Cheryan, 1998; Jönsson and Trägårdh, 1990). Membrane filtration stands for the separation of two and more solutes in a solution. The separation of the solutes is based on the molecular size difference of the individual solutes. The process configuration can be of batch or continuous setup. Moreover, different types of membranes based on the pore size are also discussed in this chapter. Finally we show a classical representation of a diafiltration process and also discuss several operation modes which are used in the industry.

4.1   Membrane Filtration

Membrane filtration processes can be separated into two main classes according to filtration principles: dead-end and cross-flow filtration shown in Fig. 4.1. These two principles differ in a way how the feed is brought to the membrane. Dead-end filtration shown in Fig. 4.1(a) considers the feed brought directly to the membrane (McAdam and Judd, 2008). The filtration pressure is applied for

(a) dead-end filtration   (b) cross-flow filtration
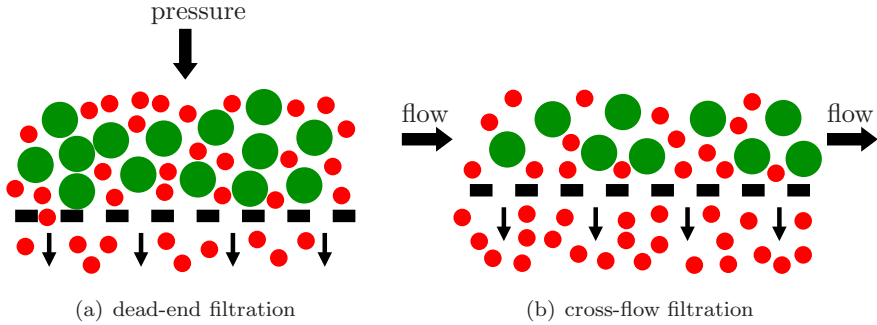
Figure 4.1: Dead-end and cross-flow membrane filtration.

the filtration. This is performed until the desired concentrations of macro and micro-solute are reached. This type of application is mainly performed for batch operations. The biggest disadvantage of this operation is that the membrane has to be changed or cleaned after every batch because of the high fouling.

The second and the most used operation is cross-flow (Hwang and Sz, 2011) operation illustrated in Fig. 4.1(b). In this case the feed is continuously brought to the membrane. The membrane is usually of a cylindrical construction with many cylindrically shaped pores inside. The feed is pumped into the membranes and the pressure forces the separation. The feed flows tangentially to the surface of the membrane. The biggest advantage of cross-flow filtration is that the fouling is reduced. This is due to fact that the feed is pumped into the membrane continuously unlike in the dead-end filtration. The cross-flow filtration has found its use in all fields of industrial applications. Its main use is in chemical and biochemical industries and for protein purification in pharmaceutical production.
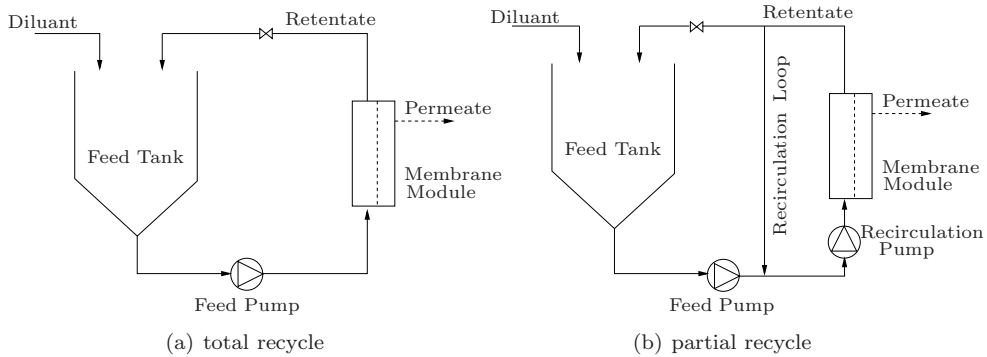
Figure 4.2: Batch membrane system with total and partial recycle.

4.2 Process Configurations

Membrane separation systems can operate either in a batch or in a continuous manner. Batch systems consider discontinuous inflow of the feed into the system. It means that the feed is put directly into the feed tank before the separation starts. In the rest of the section we will show the common process configurations and discuss the advantages and disadvantages of the mentioned processes.

At first, batch membrane process is shown in Fig. 4.2 with two different configurations. In addition a possible extension is considered with diluant addition. Diluant causes decrease of the concentrations of the individual solutes. The first configuration, shown in Fig. 4.2(a) is a general batch membrane process. In this case the total recycle brings the retentate back into the feed tank, where one of the solutes is concentrated. The feed pump then transports the solution to the membrane unit. Usually the separation is performed under constant temperature and pressure. Therefore, heat-exchanger and retentate valve are required. Advantage of this setup is a small membrane area. On the other hand, due to the increased concentration of one of the solutes the separation time can increase due to the fouling phenomena.
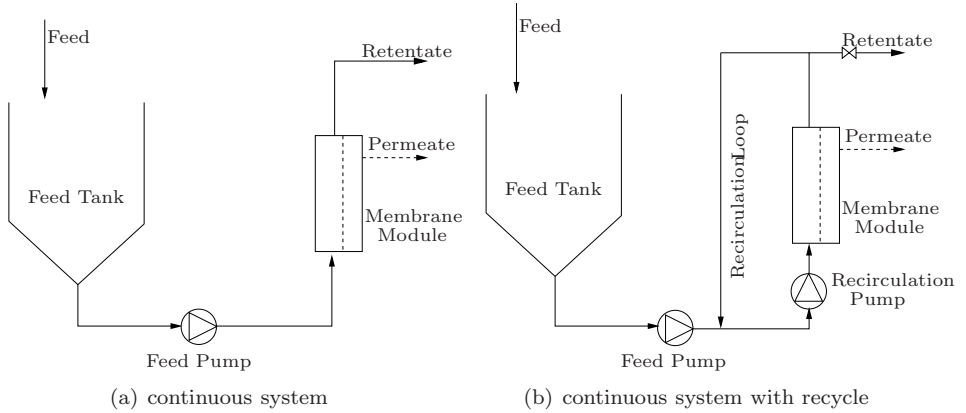
Figure 4.3: Continuous membrane system with total and partial recycle.

An extension to the general batch membrane process is the addition of the recycle loop as shown in Fig. 4.2(b). In this configuration the retentate is introduced back into the feed tank, however some portion of it is directed back through the recirculation loop (Sharma et al., 2015). The main usage of this configuration is mostly the same as in the general batch membrane process, however there are some advantages compared to the previous setup: higher cross-flow velocity because of the additional recirculation pump, smaller pipe diameters, smaller feed tank because the solution is in the recirculation loop and reduction of foaming. However, the main disadvantage is the increase in the investments costs due to the recirculation pump. Further, this setup is also mainly used in case of large systems with remote tanks where the costs are decreased thanks to smaller pipes which also reduce the amount of needed energy.

Compared to batch systems, continuous systems consider the feed continuously added into the feed tank. Fig. 4.3 shows two types of configurations of continuous separation system. In the single-pass configuration (Fig. 4.3(a))

the feed is brought to the membrane with feed pump. The leaving streams of retentate and permeate can then be collected in different tanks. The disadvantage of this configuration is the very low volume of permeate unless a very large membrane is used. The single-pass configuration is mostly used when concentration polarization effects are negligible and we do not require high flow rates. This configuration is mostly used for water treatment or removal of pyrogens (Cheryan, 1998).

In the second configuration (Fig. 4.3(b)) a recirculation loop is used. This configuration is mostly applied in continuous full-scale operations. The continuous system with recycle configuration is a merge of a standard batch and single-pass configuration. In this case we require two pumps (Choi et al., 2005). The first pump is required for providing transmembrane pressure or system pressure. The transmembrane pressure is forcing the feed to the membrane. The second pump maintains the cross-flow. The feed pump is only required at the startup to fill the recirculation loop, then the recirculation pump starts. The feed will flow into the recirculation loop at the same rate as the permeate flow rate plus retentate flow rate. The biggest advantage of this setup is the high selectivity of the processed feed. The disadvantage is that the loop is operating continuously at a concentration factor which is equivalent to a concentration factor of a batch system. Therefore, the flux is lower as the average flux in the batch mode. Moreover the membrane area is required to be large.

In case of long term operations are required at high cross-flow velocities for the reduction of the concentration layer as discussed in (Mannapperuma, 1997) and low transmembrane pressure. In this case due to the fouling phenomena the pressure increases and the permeate flux decreases. The cocurrent permeate flow systems shown in Fig. 4.4 consist of permeate pump parallel to the retentate pump. This is done so that the pressure profile in the permeate is identical to the pressure profile in the retentate loop (Bhave, 1991). This results in uniform pressure drop along the membrane. Moreover, by pumping the permeate backwards to the membrane the particles (solutes) which cause the
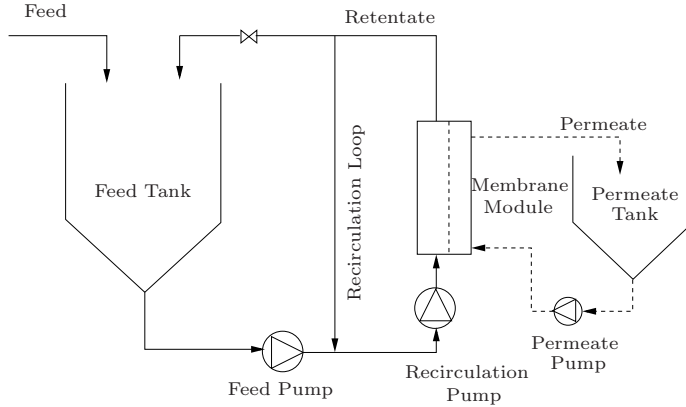
Figure 4.4: Continuous cocurrent permeate flow system.

fouling by deposing on/in the membrane surface are released and the permeate flow increases.

An extension to classical single membrane system, we also consider the multi membrane systems which can be either of batch or continuous configuration. One of the possible multi membrane configuration is shown in Fig. 4.5. The multi membrane systems are mainly used in food and pharmaceutical industry, for purification or removal of impurities in the solution. The solution circulates in the loop until the desired purity is reached. The advantage of this setup is that we do not require membranes with large area, but instead several smaller membranes can be used. However, the additional recirculation pumps increase the investments costs.

A multi-membrane system shown in Fig. 4.6 can be constructed to resolve the problems with low flux as it was observed in the partial recycle configuration (Carrére and René, 1996). The multi-membrane system consists of several continuous systems. This configuration is mainly used for large-scale systems. The individual stages are classical continuous systems that operate in series. Here, retentate flow is in serial and permeate flow in parallel configuration. The
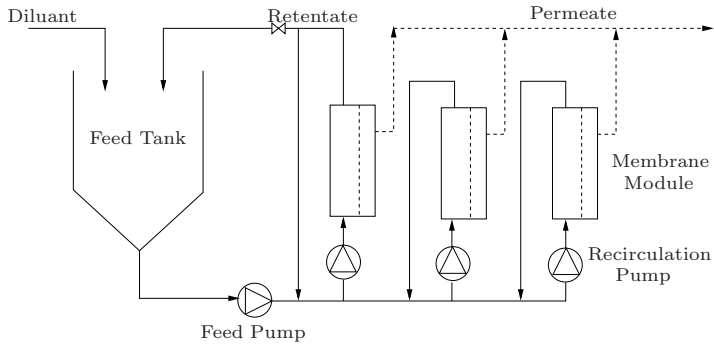
Figure 4.5: Mutli membrane system with recirculation.
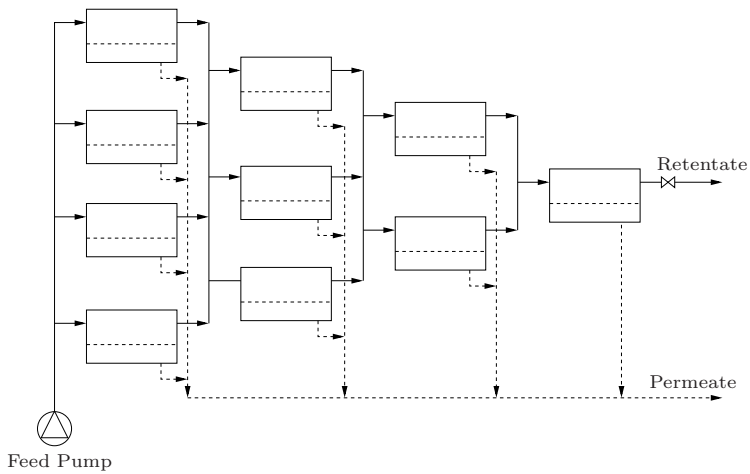
Figure 4.6: Single pass multi–membrane system.
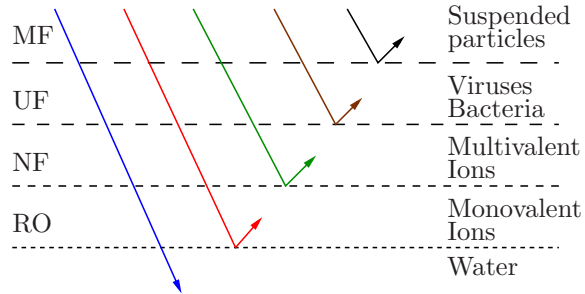
Figure 4.7: Classification of membranes with regard to pore size and filterable/retained components.

final stage operates with high concentrations and low flux. On the other hand the rest of the stages operates with low concentration and high flux. Further, the total membrane area should be less than by single-pass and partial recycle operation and should be approximately equal to the area for a batch process. From the economical point of view it is recommended to use from 3 to 7 stages while every stage increases the price of valves or pumps and controllers. This configuration is mainly used for desalination of sea water, where the salt water is pumped directly from sea and proceeds through the membranes where the permeate then represents only purified water and retentate the highly concentrated salt solution.

4.3   Membrane Characteristic

A membrane is in classical terms a very thin porous sheet which is made to separate components (solutes) in fluid. By the separation processes we distinguish four mostly used types of membranes. The difference in these membranes is based on the pore size and the applied pressure needed for the separation.

Fig. 4.7 shows the classical membrane types which are distinguished by the

pore size of the membrane and usage for the separation.

Microfiltration

Microfiltration (MF) is usually used as pre-treatment for other separation processes. It is mainly used for water treatment, sterilization, and dairy processing. Typical application for microfiltration is filtration of microorganisms. From all membranes, microfiltration has the larges pore size. The macro-solute are usually suspended particles and bacterias (Zhang et al., 2013).

Ultrafiltration

Ultrafiltration (UF) is the most used in chemical and pharmaceutical industries. The most common application for ultrafiltration is for waste-water treatment, food and beverage processing or fruit-juice clarification (Xiao et al., 2013). The macro-solute are represented by proteins and species (large particle size).

Nanofiltration

Nanofiltration (NF) is a recent technology compared to the others membrane technologies. Originally nanofiltration was used for waste water treatment and water softening. In the recent years, nanofiltration has found many new applications such as milk and juice production. Further, nanofiltration starts to find also application in pharmaceutical and chemical industries. The macro-solute are mainly dissociated acids, divalent salts, sugars and species with larger particle sizes. The micro-solute is represented by undissociated acids and monovalent salts (Boussu et al., 2008).

Reverse Osmosis

The Reverse Osmosis (RO) membrane has the smallest pores of all membranes. Because of the small pore size only water can pass through. This is the reason why RO membranes are mainly used for water treatment. Therefore, all species

Table 4.1: Typically applied pressures and pore sizes for different types of pressure-driven membrane processes.

	Applied pressure [bar]	Pore size [μm]
Microfiltration	$0.1 - 2$	$10 - 0.05$
Ultrafiltration	$1 - 10$	$0.05 - 0.002$
Nanofiltration	$5 - 20$	$0.002 - 0.001$
Reverse Osmosis	$10 - 100$	< 0.001

like viruses, proteins and others are retained and pure water is obtained from separation. RO membranes are also often used in households where they serve for cleaning water which is obtained from rain or from polluted piping. Further, RO technology has found also his use in cosmetic, pharmaceutical, medical, and semiconductor productions. Main applications of RO membranes are de-salination of seawater and purification of liquids where the water is unwanted impurity (Lee et al., 2011).

Tab. 4.1 shows individual types of the most common membranes and compares them according to the pore size and pressure under which they operate. Therefore, we can choose a corresponding membrane type based on a suitable pore size.

4.4   Membrane Modules

A membrane module represents a housing were the membrane is placed (Baker, 2012). These are mainly chosen in terms of the membrane area and the costs for the housing (cartridge) for the membrane. The common and most used types of membrane modules are (i) hollow fiber membranes, (ii) spiral wound membranes and (iii) flat plate membranes. Each membrane module will be described below.
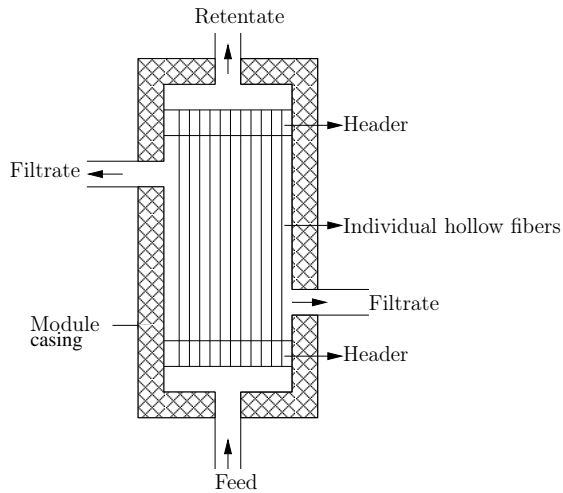
Figure 4.8: Hollow fiber membrane.

Hollow Fiber Membrane

Hollow fiber membranes were developed in the 1960's mainly for reverse osmosis applications. The hollow fiber membranes contain a high number of flexible fibers. All fibers are packed inside a tube. The feed is introduced into the outer side of the fibers and the pressure forces the smaller molecules to pass through the fiber pores (Mat et al., 2014). In other words, the permeate (filtrate) pass through the membrane pores and the retentate is on the outer side of the fibers as shown in Fig. 4.8. Hollow fiber membranes are most used in the pharmaceutical industry, treatment of drinking and industrial waste water.

Spiral Wound Membrane

Spiral wound membranes consist of flat-sheet membranes, permeate spacer, and a permeate tube. The flat-sheet membranes are wrapped around the permeate tube, where the permeate spacer is placed between the individual layers. The
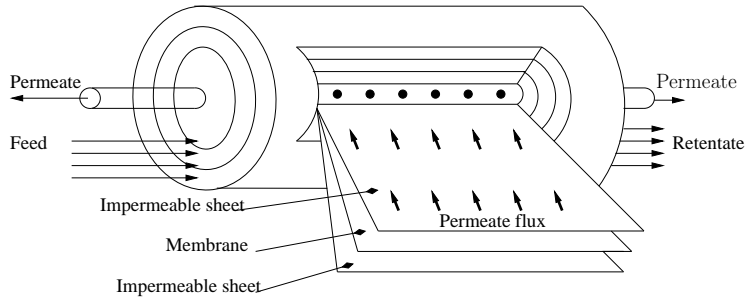
Figure 4.9: Spiral wound membrane.

purpose of the permeate spacer is to provide space between the layers of the membrane for the water (solution) to flow through (Shi et al., 2015). The permeate is then collected in the permeate tube shown in Fig. 4.9. The spiral wound membranes are one of the most used membranes. The easy constructions of the membranes allows for different configurations in terms of length, diameter and material. Moreover, the biggest advantage of the spiral wound membrane is that a large membrane area is wrapped into small membrane therefore, the cost for the housing is also small. The common applications for spiral wound membranes are seawater desalination, dairy processing, protein separation, and whey protein concentration.

Flat Plate Membrane

Flat plate membranes belong to the earliest membranes. The individual layers of membranes are placed on each other with very thin separator. The feed is then separated between filtrate (permeate) and the rejected flow (retentate). The basic representation of a flat plate membrane is shown in Fig. 4.10. Nowadays the flat plate membranes are only in electro-dialysis and pervaporation systems. Mostly in case of reverse osmosis or ultrafiltration applications (Arunkumar et al., 2016) where high fouling occurs.
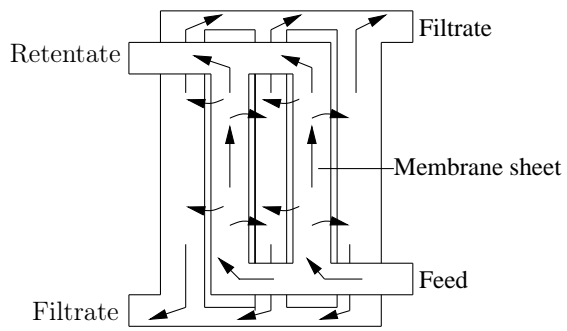
Figure 4.10: Flat plate membrane.

Modeling and Optimization of Diafiltration Processes

In the previous section we have described several configurations of membrane processes. Next, we will focus on the general batch diafiltration membrane process. Modeling, control, and several types of optimization objectives will be discussed here. Based on this theory, general optimization problem will be formulated.

5.1 Modeling of a Diafiltration Process

We consider the batch diafiltration process shown in Fig. 5.1. The process operates under constant pressure and temperature. The batch diafiltration process consists of a feed tank and a membrane. The process solution containing a solvent and two solutes (macro- and micro-solute) is brought from the feed tank to the membrane. The stream which is rejected by the membrane (retentate) is taken back into the feed tank. The rejection coefficient is a dimensionless
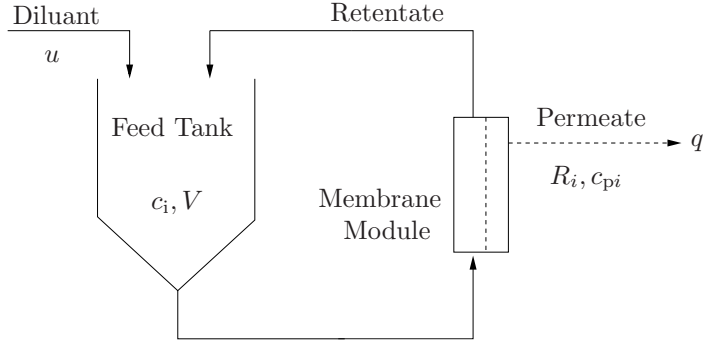
Figure 5.1: Schematic representation of a generalized UF/DF process.

number between 0 and 1 that measures the ability of the membrane to retain the ith species. It is defined as

$$R_i = 1 - \frac{c_{p,i}}{c_i}, \quad i = 1, 2, \tag{5.1}$$

where $c_{p,i}$ stands for the concentration of the ith species in the permeate and $i = 1, 2$ denotes the macro-solute and micro-solute, respectively. The rejection coefficients for the individual solutes can be constants or functions of the concentrations $R_i(c_1, c_2)$. The permeate stream that leaves the system at a given flow-rate $q = AJ$, where A represents the membrane area and J is the permeate flux subjected to unit membrane area. The permeate stream is often a function of both concentrations. In addition, it is also a function of time as it decreases when fouling occurs. The total mass balance for each solute can be written of the following form

$$\frac{\mathrm{d}(c_i V)}{\mathrm{d}t} = -c_{\mathrm{p}i} q = -c_{\mathrm{p}i} AJ. \tag{5.2}$$

Let us define a dimensionless variable $\alpha(t)$ as the ratio between the inflow into the process $u(t)$ and the outflow $q(t)$

$$\alpha(t) = \frac{u(t)}{q(t)}. \tag{5.3}$$

The total mass balance can then be written as

$$\frac{\mathrm{d}V}{\mathrm{d}t} = u - q = (\alpha - 1)AJ, \quad V(0) = V_0, \tag{5.4}$$

with V is the feed tank volume at time t, V_0 being the initial volume of the processed solution. Using (5.1) and (5.4) we can rewrite the balance of each solute as (Kovács et al., 2009)

$$\frac{\mathrm{d}c_i}{\mathrm{d}t} = \frac{c_i AJ}{V}(R_i - \alpha), \quad c_i(0) = c_{i,0}. \tag{5.5}$$

The permeate flux, rejection coefficients are in general functions of concentrations. However, let us assume that the rejection coefficient for the macro-solute is $R_1 = 1$, which is industrially a relevant case and the micro-solute rejection is a functions of concentrations $R_2 = R_2(c_1, c_2)$. This means that the membrane is absolutely impermeable for the macro-solute and permeability of micro-solute is a function of both concentrations. Therefore, the macro-solute will be completely rejected by the membrane and concentrated in the feed tank. As the rejection of the macro-solute is perfect, its total mass in the system is constant

$$c_1(t)V(t) = c_{1,0}V_0 \tag{5.6}$$

and thus the differential equation (5.4) can be omitted because the volume in each time can be directly calculated from the previous equation. Based on these assumptions the process model is of the following form

$$\dot{c}_1 = \frac{c_1^2 AJ}{c_{1,0}V_0}(1 - \alpha), \qquad\qquad c_1(0) = c_{1,0}, \tag{5.7a}$$

$$\dot{c}_2 = \frac{c_1 c_2 AJ}{c_{1,0}V_0}(R_2 - \alpha), \qquad\qquad c_2(0) = c_{2,0}. \tag{5.7b}$$

Multi-Component Separation

Consider now the case that the solution consists of several solutes. We will study the process evolution by considering the concentrations of kth and lth

solute and the volume (Jelemenský et al., 2015). We can rewrite the process model described by equations (5.4) and (5.5) as

$$\frac{\mathrm{d}c_k}{\mathrm{d}V} = \frac{c_k}{V}\frac{R_k - \alpha}{\alpha - 1}, \qquad \frac{\mathrm{d}c_l}{\mathrm{d}V} = \frac{c_l}{V}\frac{R_l - \alpha}{\alpha - 1}, \qquad \frac{\mathrm{d}c_k}{\mathrm{d}c_l} = \frac{c_k}{c_l}\frac{R_k - \alpha}{R_l - \alpha}. \tag{5.8}$$

From the above equations, control variable α can be eliminated in order to obtain the quantitative behavior of the system. When other two solutes (m and n) are considered, we can arrive at the control-invariant expression

$$\frac{R_l - 1}{R_k - R_l}\frac{\mathrm{d}c_k}{c_k} - \frac{R_k - 1}{R_k - R_l}\frac{\mathrm{d}c_l}{c_l} = \frac{R_n - 1}{R_m - R_n}\frac{\mathrm{d}c_m}{c_m} - \frac{R_m - 1}{R_m - R_n}\frac{\mathrm{d}c_n}{c_n}. \tag{5.9}$$

Several conclusions can be drawn at this point.

1. When rejection coefficients are constant the expression (5.9) can be integrated until the final time of operation yielding

$$\left(\frac{c_{k,\mathrm{f}}}{c_{k,0}}\right)^{\frac{R_l - 1}{R_k - R_l}} \left(\frac{c_{l,\mathrm{f}}}{c_{l,0}}\right)^{\frac{R_k - 1}{R_l - R_k}} = \left(\frac{c_{m,\mathrm{f}}}{c_{m,0}}\right)^{\frac{R_n - 1}{R_m - R_n}} \left(\frac{c_{n,\mathrm{f}}}{c_{n,0}}\right)^{\frac{R_m - 1}{R_n - R_m}}. \tag{5.10}$$

   Hence, when the final concentrations of two solutes are specified, the reachable concentrations of the rest of the solutes are fixed. This result states that, in general, it is not possible to reach the separation goal exactly but the over-concentration or over-purification of the process liquor will take place. In this respect, the design of optimal operation of DF process can be simplified to specification of final concentrations of two (decisive) solutes whose increase/decrease stands for a limit factor.

2. For non-constant solute rejections, it might be possible to reach the desired process end-point although this operation could result in increased processing time in comparison with situation when over-concentration or over-purification of some solutes is allowed. This situation requires thorough investigation. A possible workaround is to consider constant average rejection coefficients in the operational range to approximately de-

termine decisive final concentrations and to leave the remaining solutes over-purified.

In the rest of the thesis we will focus only on the general batch membrane process with two solutes in a solution. It is possible to generalise the proposed solutions to multi-component solution using the facts stated above.

5.2 Optimization of Diafiltration Process

One of the requirements of the applications of the membrane processes is to minimize the operational costs of the separation. The minimization is achieved through optimization, where a detailed description of the process model and constraints are needed, discussed in the previous chapters. Three types of objectives are defined: the processing time, the diluant consumption, or the combination of the previous two objectives is minimized.

In the thesis we will focus only on minimum time problem. The reason for this is mainly in the fact that with the minimum time strategy we are able to increase production due to the shorter batches. For these reasons the minimum time strategy has gained great attention in the industry.

Minimum-Time Problem

Minimum-time problem belongs to one of the most considered objectives for the membrane separation processes. Since batch process is considered the objective is to process as much solution as possible. Therefore, the separation time has to be minimized. The formulation for the minimum time problem, which drives

the system from initial to final concentrations in minimum time is as follows

$$\mathcal{J}_1 = \min_{\alpha(t)} \int_{t_0}^{t_f} 1 \, \mathrm{d}t. \tag{5.11a}$$

s.t.

$$\dot{c}_1 = \frac{c_1^2 AJ}{c_{1,0} V_0}(1 - \alpha), \qquad c_1(t_0) = c_{1,0}, \qquad c_1(t_f) = c_{1,f}, \tag{5.11b}$$

$$\dot{c}_2 = \frac{c_1 c_2 AJ}{c_{1,0} V_0}(R_2 - \alpha), \qquad c_2(t_0) = c_{2,0}, \qquad c_2(t_f) = c_{2,f}, \tag{5.11c}$$

$$\alpha \in [\alpha_{\min}, \alpha_{\max}], \tag{5.11d}$$

where, $\alpha_{\min}, \alpha_{\max}$ represent the lower and upper bound for the control variable, respectively.

Minimum Diluant Problem

In the case the diluant represents a valuable substance, it is necessary to formulate such optimization problem that will minimize the amount of diluant added during the separation. To construct the optimization problem, we use the same process differential equations (5.11) and replace the objective function with the following

$$\mathcal{J}_2 = \min_{\alpha(t)} \int_{t_0}^{t_f} \alpha(t) AJ(t, c_1, c_2) \, \mathrm{d}t. \tag{5.12}$$

Multi-Objective Problem

The last presented case is called the multi-objective optimization problem. It is a combination of the two common optimization problems combined in one (Paulen et al., 2015). The multi-objective formulation is a weighted linear combination of final time and diluant consumption. The objective function of such problem can be formulated as follows

$$\mathcal{J}_3 = \min_{\alpha(t)} \int_{t_0}^{t_f} (w_T + w_D \alpha AJ) \, \mathrm{d}t, \tag{5.13}$$

where $w_T \geq 0$ and $w_D \geq 0$ are weighting coefficients for the final processing time and total diluant consumption, respectively. The weighting coefficients can be interpreted as the prices of the unit of processing time (attributed to e.g. energy costs) and of the utilized diluant. As in the previous cases the mathematical formulation of the optimization problem described by equations (5.11) is unchanged except the objective function is replaced.

All considered optimization problems are affine in control variable $\alpha(t)$ which means that the problem may exhibit singular solutions (Bryson, Jr. and Ho, 1975; Srinivasan et al., 2003) treated in the previous chapters.

5.3   Control of a Diafiltration Process

There exist several different ways how to control a batch diafiltration process. These strategies differ in the way how to diluant is added into the process. Moreover, we can distinguish between two approaches. The first is the traditional approach how to control the diafiltration process and the second is the optimal approach which can guarantee one of the objectives from the previous section.

Traditional Control

In the industry there are several commonly used control modes such as

- concentration (C) mode when $\alpha = 0$,

- variable-volume diafiltration (VVD) when $\alpha \in (0, 1)$,

- constant-volume diafiltration (CVD) when $\alpha = 1$,

- instantaneous pure dilution (D) when $\alpha \to \infty$.

The dilution mode is characterized by a certain amount of diluant added instantaneously into the feed tank. Traditional operation strategies used in the industry then consist of sequences of the individual control modes (e.g. C-CVD)
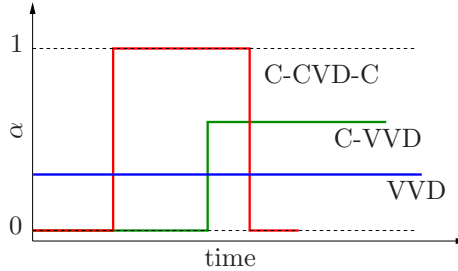
Figure 5.2: Representation of traditional control strategies in terms of the α
         function.

as it is shown in Fig. 5.2. Another traditional diluant utilization approach,
variable-volume diafiltration (VVD) possesses only 2 degrees of freedom (con-
stant α value and process duration) and thus is very unlikely to achieve an
optimal operation.

Optimal Control

Optimal operation of a diafiltration process can be computed using numerical
or analytical methods of dynamic optimization. In the work of Paulen et al.
(2011) the authors have used the numerical method control vector parametriza-
tion to compute the optimal diluant addition. Even more effective approach
was published in Paulen et al. (2013, 2015) where a complete analytical opti-
mal operation was derived using Pontryagin's minimum principle. The optimal
operation is three step strategy and is defined as follows

1. In the initial step we use the control on the boundaries $\alpha = 0$ or $\alpha = \infty$
   depending on the initial concentrations until the singular surface is met.
   The singular surface is defined as

$$S(c_1, c_2) = (R_2 - 1)\left(J + c_1\frac{\partial J}{\partial c_1} + c_2\frac{\partial J}{\partial c_2}\right) + J\left(c_1\frac{\partial R_2}{\partial c_1} + c_2\frac{\partial R_2}{\partial c_2}\right) = 0.$$

$$(5.14)$$

2. During the second step we stay on the singular surface and apply the singular control which reads as

$$\alpha(c_1, c_2) = \frac{\dfrac{\partial S}{\partial c_1} c_1 + \dfrac{\partial S}{\partial c_2} c_2 R_2}{\dfrac{\partial S}{\partial c_1} c_1 + \dfrac{\partial S}{\partial c_2} c_2}. \tag{5.15}$$

3. In the last step we use either $\alpha = 0$ or $\alpha = \infty$ until the final concentrations are reached.

However, the biggest disadvantage of the proposed strategy is the absence of any information about the fouling behavior which in membrane separation process poses the biggest obstacle.

Chapter 6

Membrane Fouling

Membrane fouling belongs to one of the main obstacles in the membrane separation processes. The main cause of the membrane fouling is the deposit of the solutes in/on the membrane pores. As a consequence, a decrease of the effective membrane area occurs. The membrane fouling depends on several factors. It is more pronounced when strong concentration (gel) polarization effects occur. During filtration, retained macro-solutes form a so-called gel layer over the surface of the membrane (Baker, 2012). This increases the likeliness of the macro-solute particles to interact with the surface of the membrane and to block its pores. The precise mechanisms of such interactions are not known but there are several models describing these effects. Additionally, the factors that influence the membrane fouling, both quantitatively and qualitatively, are represented by feed properties, membrane material, temperature, and pressure (Zhao et al., 2000).

Hence, the inevitable phenomenon of membrane fouling results in the decrease of permeate flow. As the consequence the overall processing time increases. Moreover, once the membrane becomes significantly fouled cleaning has to be performed. If the cleaning is insufficient the membrane has to be

replaced. All this leads to an increase of operational costs.

Modeling of fouling became highly important in the past years. In Hermia (1982) a unified fouling model for dead-end filtration systems was derived in terms of total permeate flux and time and reads as

$$\frac{\mathrm{d}^2 t}{\mathrm{d}V_{\mathrm{p}}^2} = K \left(\frac{\mathrm{d}t}{\mathrm{d}V_{\mathrm{p}}} \right)^n, \tag{6.1}$$

where

$$\frac{\mathrm{d}t}{\mathrm{d}V_{\mathrm{p}}} = \frac{1}{A J_{\mathrm{p}}}, \tag{6.2}$$

$$\frac{\mathrm{d}^2 t}{\mathrm{d}V_{\mathrm{p}}^2} = \frac{\mathrm{d}}{\mathrm{d}V_{\mathrm{p}}} \left(\frac{1}{A J_{\mathrm{p}}} \right) = -\frac{1}{A J_{\mathrm{p}}^2} \frac{\mathrm{d}J_{\mathrm{p}}}{\mathrm{d}t} \frac{\mathrm{d}t}{\mathrm{d}V_{\mathrm{p}}} = -\frac{1}{A^2 J_{\mathrm{p}}^3} \frac{\mathrm{d}J_{\mathrm{p}}}{\mathrm{d}t}, \tag{6.3}$$

and V_{p} represents the permeate volume, t is time, and K is the fouling rate constant. Four classical fouling models are characterized by different values of n. We recognize cake ($n = 0$), intermediate ($n = 1$), standard (internal) ($n = 3/2$), and complete fouling ($n = 2$) models. The corresponding differential equation for permeate flux can then be derived as (Bolton et al., 2006; Vela et al., 2008)

$$\frac{\mathrm{d}J}{\mathrm{d}t} = -K A^{2-n} J^{3-n}. \tag{6.4}$$

If n, K, A are considered constant, this differential equation can be solved to give an explicit solution

$$J(t, n, K, A, J_0) = J_0 \left(1 + K(2-n)(A J_0)^{2-n} t \right)^{(1/(n-2))} \tag{6.5}$$

where J_0 represents initial flux at time $t = 0$. However, the equation is only valid for the case where $n = [0, 2)$. For the complete fouling ($n = 2$) different explicit solution must be considered of the form

$$J(t, K, J_0) = J_0 \mathrm{e}^{-Kt}. \tag{6.6}$$

It can happen that the fouling parameters are not constant or that different fouling phenomena occurs in parallel or in series. For this reason, it is crucial to

determine on-line or off-line both the fouling rate and the fouling model. In our recent study (Sharma et al., 2016) we assumed constant area and estimated the fouling model and the fouling rate constants. Different approach was studied using on-line estimation of the fouling parameters (Jelemenský et al., 2016a) using extended Kalman filter. Another approach was studied in Jelemenský et al. (2014), where the fouling considered effective membrane area decrease in time due to deposit of the solutes.

To apply this model to cross-flow systems considered in this study, we propose to substitute the initial flux $J_0(t = 0)$ by the unfouled flux $J_0(c_1, c_2)$ that depends on actual concentrations. This change will make possible to unify procedures and results for systems with and without fouling.

6.1 Description and Derivation of Fouling Models

Fig. 6.1 shows graphical representation of the individual fouling mechanisms. These models differ in the way the molecules deposit in/on the membrane. In the next subsections we will describe the individual fouling models in detail and explain the differences in the individual models. Moreover, we explain in detail the procedure how to derive the fouling models from the unified model described by (6.1) which were verified with the models derived in Charfi et al. (2012) and Vela et al. (2008). Finally, we summarize the Hermia's fouling models in tabular form.

6.1.1 Complete Pore Blocking Model

Complete pore blocking model considers that solutes which are brought to the membrane surface will seal the membrane pores (Fig. 6.1(a)). Flow through such pores is no longer possible. The molecules which deposit on the membrane surface are larger then the membrane pores. The model can be derived

(a) Complete blocking model

(b) Intermediate blocking model

(c) Cake filtration model

(d) Internal blocking model
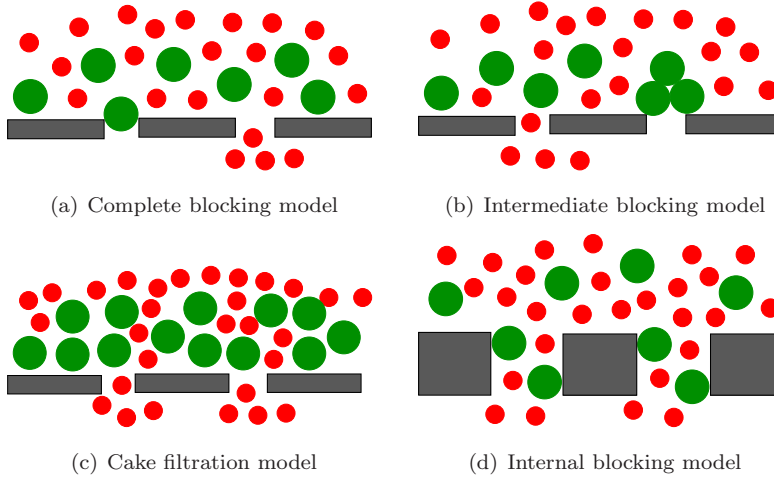
Figure 6.1: Graphical representation of the four classical fouling models developed by Hermia.

from (6.1) after setting the parameter n equal to 2. The model is expressed in terms of permeate flux versus time and is of the form

$$\ln J = \ln J_0 - K_c t, \tag{6.7}$$

where J is the permeate flux in [m/s], J_0 is the permeate flux of unfouled membrane and K_c represents the fouling rate constant in [1/s].

Derivation of the Model

The complete pore blocking model can be derived from (6.1), substituting the individual parts by (6.2), (6.3) and setting n equal to 2. The detailed derivation

is then as follows

$$-\frac{1}{J_{\mathrm{p}}^3 A^2}\frac{\mathrm{d}J_{\mathrm{p}}}{\mathrm{d}t} = K\left(\frac{1}{AJ_{\mathrm{p}}}\right)^2 \tag{6.8}$$

$$-\int_{J_0}^{J}\frac{\mathrm{d}J_{\mathrm{p}}}{J_{\mathrm{p}}} = K\int_0^t \mathrm{d}t \tag{6.9}$$

$$\ln J = \ln J_0 - Kt \tag{6.10}$$

with the final equation (6.7) where $K_{\mathrm{c}} = K$.

6.1.2 Intermediate Blocking Model

The intermediate pore blocking model again assumes that all solutes brought to the membrane surface will block the membrane pores. However, in this case the solutes can deposit on each others as illustrated in Fig. 6.1(b). The parameter n is equal to 1 and the permeate flux is of the form

$$\frac{1}{J} = \frac{1}{J_0} + K_{\mathrm{i}}t, \tag{6.11}$$

with K_{i} being the fouling rate constant in $[1/\mathrm{m}]$.

Derivation of the Model

We use the same procedure as previously, however in this case we set n equal to 1 and the derivation is as follows

$$-\frac{1}{J_{\mathrm{p}}^3 A^2}\frac{\mathrm{d}J_{\mathrm{p}}}{\mathrm{d}t} = K\left(\frac{1}{AJ_{\mathrm{p}}}\right)^1 \tag{6.12}$$

$$-\int_{J_0}^{J}\frac{\mathrm{d}J_{\mathrm{p}}}{J_{\mathrm{p}}^2} = KA\int_0^t \mathrm{d}t \tag{6.13}$$

$$\frac{1}{J} = \frac{1}{J_0} + KAt \tag{6.14}$$

with final equation (6.11) where $K_{\mathrm{i}} = KA$.

6.1.3   Cake Filtration Model

The fouling according to this model is caused by deposition of solutes on the surface of membrane. The process repeats itself, that is with each cycle the solutes keep depositing over the previously deposited solutes and this results in forming of a multi-layered cake of solutes, as it is shown in Fig. 6.1(c). The parameter n in this case is equal to 0 and the permeate flux is of the form

$$\frac{1}{J^2} = \frac{1}{J_0^2} + K_g t, \tag{6.15}$$

where K_g is the fouling constant with the following unit in $[s/m^2]$.

Derivation of the Model

The cake filtration model can be derived by substituting n equal to 0 and the derivation is as follows

$$-\frac{1}{J_p^3 A^2}\frac{dJ_p}{dt} = K\left(\frac{1}{J_p A}\right)^0 \tag{6.16}$$

$$-\int_{J_0}^{J}\frac{dJ_p}{J_p^3} = KA^2\int_0^t dt \tag{6.17}$$

$$\frac{1}{J^2} = \frac{1}{J_0^2} + 2KA^2 t \tag{6.18}$$

with the final equation (6.15) where $K_g = 2KA^2$.

6.1.4   Internal Blocking Model

On the contrary to previous fouling models discussed, this model defines fouling internally. The model describes that the solutes instead of depositing on the surface of the membrane, are small enough to clog the pores of the membrane illustrated in Fig. 6.1(d). The phenomenon results in the reduction of pore diameter and hence in decrease of the permeate flux. The parameter n is equal

to 3/2 and the flux is of the form

$$\frac{1}{\sqrt{J}} = \frac{1}{\sqrt{J_0}} + K_s t \tag{6.19}$$

where K_s is the fouling rate constant in $[1/\mathrm{m}^{1/2}/\mathrm{s}^{1/2}]$.

Derivation of the Model

The internal blocking model can be derived by using n equal to 3/2

$$-\frac{1}{J_\mathrm{p}^3 A^2}\frac{\mathrm{d}J_\mathrm{p}}{\mathrm{d}t} = K\left(\frac{1}{AJ_\mathrm{p}}\right)^{3/2} \tag{6.20}$$

$$-\int_{J_0}^{J}\frac{\mathrm{d}J_\mathrm{p}}{J_\mathrm{p}^{3/2}} = KA^{1/2}\int_0^t \mathrm{d}t \tag{6.21}$$

$$\frac{2}{J^{1/2}} - \frac{2}{J_0^{1/2}} = KA^{1/2}t \tag{6.22}$$

$$\frac{1}{J^{1/2}} = \frac{1}{J_0^{1/2}} + \frac{A^{1/2}}{2}Kt \tag{6.23}$$

with the final equation (6.19) where $K_\mathrm{s} = \frac{1}{2}A^{1/2}K$.

To summarize the derived Hermia models we provide a detailed overview in Tab. 6.1 where the individual fouling are described and we also show the functionality of the fouling rates in terms of fouling rate K and membrane area A. In all fouling models we can observe that the model is an explicit function of time. Moreover, since $J_0(c_1, c_2)$ is a function of concentrations the final resulting fouling model is a function of time and concentrations. This means that the fouling is increasing not only due to the increase of the concentrations of the solute but also due to the increase of the processing time.

6.1.5 Membrane Area Fouling Models

In this section we will investigate the case where the fouling of the membrane occurs due to the blockage of the membrane pores. The blockage of the membrane

Table 6.1: Hermia's fouling models in terms of total permeate flux and time.

fouling model	n	Hermia's model	flux expression	fouling rate
cake filtration	0	$\dfrac{1}{J^2} = \dfrac{1}{J_0^2} + K_{\mathrm{g}}t$	$J = \dfrac{J_0}{J_0^2 K_{\mathrm{g}}t + 1}$	$K_{\mathrm{g}} = 2KA^2$
intermediate	1	$\dfrac{1}{J} = \dfrac{1}{J_0} + K_{\mathrm{i}}t$	$J = \dfrac{J_0}{J_0 K_{\mathrm{i}}t + 1}$	$K_{\mathrm{i}} = KA$
internal	3/2	$\dfrac{1}{\sqrt{J}} = \dfrac{1}{\sqrt{J_0}} + K_{\mathrm{s}}t$	$J = \dfrac{J_0}{\left(\sqrt{J_0}K_{\mathrm{s}}t + 1\right)^2}$	$K_{\mathrm{s}} = \dfrac{1}{2}KA^{1/2}$
complete	2	$\ln J = \ln J_0 - K_{\mathrm{c}}t$	$J = J_0 \mathrm{e}^{-K_{\mathrm{c}}t}$	$K_{\mathrm{c}} = K$

effects the effective membrane area. From the following derivation we obtain
the differential equations which will characterize the decrease in the effective
membrane area in time. In Bolton et al. (2006); Iritani and Katagiri (2016)
the authors reported that only the complete and intermediate fouling models
contribute in the decrease of the effective membrane area. However in this case
it is important to mention that J_0 will represent the initial flux when initial
effective membrane area A_0 is available. Moreover, this approach considers the
permeate flux as a function permeate volume per unit of effective membrane
area. After this considerations we define the unified fouling model as follows

$$\frac{\mathrm{d}^2 t}{\mathrm{d}V_\nu^2} = K \left(\frac{\mathrm{d}t}{\mathrm{d}V_\nu} \right)^n, \tag{6.24}$$

where

$$\frac{\mathrm{d}t}{\mathrm{d}V_\nu} = \frac{1}{J_{\mathrm{p}}}, \tag{6.25}$$

$$\frac{\mathrm{d}^2 t}{\mathrm{d}V_\nu^2} = \frac{\mathrm{d}}{\mathrm{d}V_\nu}\left(\frac{1}{J_{\mathrm{p}}} \right) = -\frac{1}{J_{\mathrm{p}}^2}\frac{\mathrm{d}J_{\mathrm{p}}}{\mathrm{d}V_\nu} = -\frac{1}{J_{\mathrm{p}}^2}\frac{\mathrm{d}J_{\mathrm{p}}}{\mathrm{d}V_\nu}, \tag{6.26}$$

and V_ν represents the permeate volume per unit of effective membrane area $[\mathrm{m}^3/\mathrm{m}^2]$.
Derivation of the four fouling models from (6.25) and (6.26) is exactly the same

as stated in the previous sections. Therefore, we will only derive the complete fouling model with $n = 2$ to show the detailed procedure. The procedure is the following. We insert the equations (6.25) and (6.26) into (6.24) and obtain

$$-\frac{1}{J_\mathrm{p}^2}\frac{\mathrm{d}J_\mathrm{p}}{\mathrm{d}V_\nu} = K\left(\frac{1}{J_\mathrm{p}}\right)^2 \tag{6.27}$$

after some manipulations we get

$$\mathrm{d}J_\mathrm{p} = -K\mathrm{d}V_\nu, \tag{6.28}$$

as the last step we integrate the equation (6.28) to obtain

$$\int_{J_0}^{J} \mathrm{d}J_\mathrm{p} = -K\int_0^{V_\nu} \mathrm{d}V_\nu, \tag{6.29}$$

$$J - J_0 = -K_\mathrm{c}V_\nu, \tag{6.30}$$

where the final permeate flux equation is as follows

$$J = J_0 - K_\mathrm{c}V_\nu, \tag{6.31}$$

where

$$K_\mathrm{c} = K, \tag{6.32}$$

and J and J_0 is the permeate flux and the initial flux [m/s], respectively and K_c is the complete pore blocking constant [1/s]. Applying the same procedure for different n we obtain the four standard fouling models. In Tab. 6.2 we show all fouling models in terms of permeate flux per unit of effective membrane area. We can observe that in this case, compared to the previous one, the functionality of the fouling rates does not depend on the membrane area.

Based on the presented fouling models we are now ready to derive the differential equation for the decrease in the effective membrane area. According to Darcy's law the flow rate q through the membrane area can be defined as a function of resistance $\mathcal{R}$ and effective membrane area A and reads as

$$q = \frac{\mathcal{R}}{A}\frac{P}{\mu}, \tag{6.33}$$

Table 6.2: Hermia's fouling models in terms of permeate flux per unit of effective
            membrane area.

fouling model	n	Hermia's model	flux expression	fouling rate
cake filtration	0	$\dfrac{1}{J} - \dfrac{1}{J_0} = K_{\mathrm{g}} V_\nu$	$J = \dfrac{J_0}{1 + J_0 K_{\mathrm{g}} V_\nu}$	$K_{\mathrm{g}} = K$
intermediate	1	$\ln J - \ln J_0 = -K_{\mathrm{i}} V_\nu$	$J = J_0 \mathrm{e}^{-K_{\mathrm{i}} V_\nu}$	$K_{\mathrm{i}} = K$
internal	3/2	$\sqrt{J} - \sqrt{J_0} = -K_{\mathrm{s}} V_\nu$	$J = J_0 \left(1 - \dfrac{K_{\mathrm{s}}}{2} V_\nu\right)^2$	$K_{\mathrm{s}} = K$
complete	2	$J - J_0 = K_{\mathrm{c}} V_\nu$	$J = J_0 - K_{\mathrm{c}} V_\nu$	$K_{\mathrm{c}} = K$

where P is the trans-membrane pressure and μ is the viscosity of the solution (Ir-
itani and Katagiri, 2016). Since the membrane area is constant throughout the
separation the permeate flux is proportional to the flow rate

$$\frac{J}{J_0} = \frac{q}{q_0},$$
(6.34)

where q_0 represents the initial flow rate $q_0 = A_0 J_0$. By substituting equa-
tion (6.33) into (6.34) we obtain

$$\frac{J}{J_0} = \frac{\mathcal{R}_0 A}{\mathcal{R} A_0}.$$
(6.35)

This model represents a combined model to account for the effects for losses in
effective membrane area with the increased resistance caused by cake formation
on the membrane surface (Bolton et al., 2006). The model assumes that two
fouling mechanisms occur simultaneously during the separation (e.g. complete
blocking and cake formation mechanism). However, in this derivation we only
investigate the influence of the complete pore blocking mechanism on the de-
crease of effective membrane area. Therefore we do not assume any resistance
caused by cake formation. Based on these assumptions we can set $\mathcal{R} = \mathcal{R}_0$ and

the reduced equation has the following form

$$\frac{A}{A_0} = \frac{J}{J_0}.$$ (6.36)

By inserting the final equations of permeate flux for complete and intermediate fouling models into (6.36) we obtain the final equations in terms of variations in the effective membrane area for complete and intermediate fouling mechanisms, respectively, which reads as

$$\frac{A}{A_0} = 1 - \frac{K_c}{J_0} V_\nu,$$ (6.37a)

$$\frac{A}{A_0} = e^{-K_i V_\nu}.$$ (6.37b)

By differentiating the equations (6.37a) w.r.t. to time we obtain the final differential equations which are as follows

$$\frac{dA}{dt} = -A_0 \frac{K_c}{J_0} \frac{dV_\nu}{dt} = -A_0 \frac{K_c}{J_0} J, \qquad A(0) = A_0,$$ (6.38a)

$$\frac{dA}{dt} = -A_0 K_i e^{-K_i V_\nu} \frac{dV_\nu}{dt} = -A_0 K_i e^{-K_i V_\nu} J, \quad A(0) = A_0.$$ (6.38b)

The derived differential equations describe the decrease in the effective membrane area in time depending on the fouling constant and the permeate flux.

6.2 Factors Affecting Membrane Fouling

The main factors which affect the fouling of the membrane can be divided in several groups (Zhao et al., 2000)

- effect of the feed properties,

- effect of the membrane material and its properties,

- effect of the processing variables (environment variables) – temperature and pressure.

Each of these factors plays a major role in the membrane fouling (Al-Amoudi et al., 2007). It is because the feed can contain large molecules which can block the pores on the membrane. Further, properties such as pore size, porosity or pore size distribution can influence membrane fouling. If most of the pores on the membrane are blocked the flux is decreased. Also, the temperature or the pressure influences the process. As the pressure increases the molecules are pushed to the membrane by greater force which can lead to a cake layer or to internal blockage of the pores.

6.2.1   Feed Properties

The first major effect is the concentration of the feed. It has been shown that the permeate flux is decreasing with the increase of the feed concentration. If internal fouling is considered, increased concentration highly contributes to the membrane fouling. If the concentrations of the solutes are high, one can expect cake or complete fouling of the membrane.

The second major effect is the pH of the solution. Muller et al. (1973) presented that for example proteins are complex molecules whose interactions with the membrane surface highly depend on the pH of the solution. They also stated that this behavior is not clearly understood and described three possible explanations for it:

1. Changes in protein conformation affect the deposit of the proteins' molecules on the surface of the membrane.

2. The changes of the proteins effects the porosity of the dynamic membrane which is formed on top of the original membrane.

3. The different charge of the proteins molecules and membrane surface affects the adsorption and deposition of the protein molecules.

The third major effect is the component interaction of the solutes which are present in the solution. As it has been stated, the solution consists of macro

and micro-molecules. The macro-molecules are much more larger than micro-molecules. It may occur that the larger molecules form a dynamic membrane on top the original membrane. This dynamic membrane has than smaller porosity compared to the original membrane. This can cause that the smaller molecules cannot pass through the membrane (Blatt et al., 1970).

The last effect is prefiltration and removal of the aggregates. It has been shown that the prefiltration of the solution can in many ways improve the permeate flux and decrease the fouling. It is mainly because the larger molecules would deposit on the surface of the membrane and block all pores in the membrane. Therefore, the removal of these molecules is crucial to minimize the presence of the fouling during the process.

6.2.2   Membrane Material and its Properties

Pore Size

It has been shown that with increased pore size the fouling is also increasing. It is mainly because many molecules are deposited inside the membrane (internal fouling) and in time can form cake layer on the surface of the membrane. Gatenholm et al. (1988) discussed an optimal pore size. If the pore size is less than the optimal one the membrane resistance restricts permeate flow. On the other hand if the diameter of the pore size is greater than the optimal pore size the increased fouling of the membrane causes decrease in flux.

Porosity and Pore Size Distribution

In many UF and MF membranes there exists a wide pore size distribution. This means that the pores with different diameters are present on the membrane. The dominant permeate flow is provided by the largest pores. The main issue occurs when the largest pores on the membrane become fouled, for example by proteins. Then the fouling changes the pore size distribution, because the

larger pores became fouled or their diameter is decreased. As a consequence the permeate flow and membrane retention are changing in time.

Physico-Chemical Properties

It has been shown that many molecules such as proteins can interact with membrane surface through electrostatic interaction, hydrophobic effects and charge transfer (Hofstee, 1982).

- charge effect – the charge on the membrane depends mainly on membrane material and the pH of the feed solution. If the charge of the membrane is the same as of the molecules then the permeate flux is enhanced.

- Hydrophobility – a series of experiments by Fane et al. (1985) shows that larger molecules (proteins) adsorbed less when dealing with hydrophilic membranes than by hydrophobic membranes. Therefore, it can be concluded that hydrophobic membranes improve the permeate flux.

6.2.3   Processing Variables

Transmembrane Pressure

Transmembrane pressure is the pressure which is forcing the feed to the membrane and can be calculated as

$$\text{TMP} = \frac{P_F + P_R}{2} + P_P \tag{6.39}$$

where P_F is the pressure of the feed, P_R represents the pressure on the retentate site and P_P is the permeate pressure. The main indicator is the pressure difference which is the difference of pressure on the membrane and beyond the membrane (Forman et al., 1990). It has been shown that an increase of transmembrane pressure results in an increase of the permeate flux and fouling rate. Fig. 6.2 shows the graphical representation of the transmembrane pressure. The
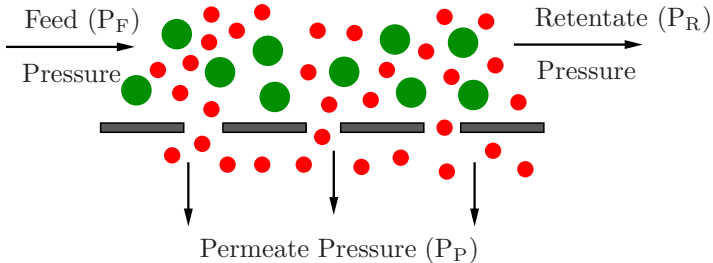
Figure 6.2: Graphical representation of the transmembrane pressure.

feed is brought to membrane and the transmembrane pressure is forcing the molecules of the feed solution to pass through the membrane.

Temperature

Temperature significantly impacts the performance of the membrane. The temperature impacts the density and viscosity of water. When viscosity and density increases the transmembrane pressure which is required for water to pass through the membrane increases (Attia et al., 1991). Moreover by increasing the temperature the permeate flux is also increased because the permeate viscosity is decreased and improves the flow rate.

6.3   Membrane Cleaning

The cleaning of a fouled membrane became a highly discussed topic in the recent years. In the work of See et al. (1999) they discuss that little attention has been paid to study the importance of scheduling the regeneration and cleaning of the membranes. They also show that by optimized scheduling of cleaning the membrane operating costs can be significantly reduced. Further, in the work of Williams et al. (2012) it has been shown that one of the most important parts by desalination of the seawater is the membrane cleaning. It is mainly because

that by desalination of seawater the major issue is the fouling which is caused by blockage of the pores by salts molecules. The development of new methods and procedures is manly because to extend the lifetime of membrane and to lower production costs Zhao et al. (2000). The main methods discussed in this work can be divided into three major groups: physical, chemical, and biological methods.

6.3.1   Physical Methods

The physical methods depend on the physical removal of the solids (material) on or inside the membrane. One of the most used physical methods is back-flushing (Galaj et al., 1984). In this method the water which is the primary cleaning agent is pushed onto the membrane from the permeate side, thus the solids which are trapped in the membrane are pushed back into the system by pressure. It has been shown that this cleaning procedure highly depends on the type of the fouling and on the suspension. Still many works have shown that this procedure is one of the most used procedures to clean fouled membranes (Psoch and Schiewer, 2006). In the work of (Kim et al., 2007) the authors have optimized the back-flushing periods to obtain a stable permeate flux during the whole experiment.

A different method which is used is air sparge (flush) method (Takizawa et al., 1988). In this method air (with water) is injected into the forward permeate flush. The mixture forms bubbles which cause the high turbulence to be formed. Because of this behavior the fouling on the surface of the membrane is removed. In some papers (Kim et al., 2007; Van Geluwe et al., 2011) authors perform cleaning with ozone gas. Further, it has been also shown (Ziylan and Ince, 2013) that with pre-ozonation of raw water it has the same effect as with flushing the membrane with ozone gas. Moreover a mixture of ozone and chlorine gas can unblock the membrane pores more efficiently. Therefore better permeate flux recovery is achieved.

6.3.2 Chemical Methods

Chemical cleaning of a membrane is widely used for its cleaning and also for regeneration. Chemical agents are mostly used to dissolve solids which are trapped inside the pores or on the surface of the membrane. As it has been mentioned before chemical agents are also used for regeneration of the membrane. It means that after cleaning procedure the membrane can be damaged through aggressive cleaning agents. Therefore several-step procedure can be used, where in the first step we perform the cleaning and in the second step regeneration of the membrane is carried out. Chemical agents are used for dissolving the fouling on the membrane, to keep the loosen foulant in solution and at last to avoid new fouling (Bird and Bartlett, 1995). Typical chemical agents are: alkalies, hydroxides, carbonates, phosphates, acids, nitric and phosphoric, ethylenediaminetetraacetic acid (EDTA). Most of the todays chemical agents consist of a mixture of the mentioned cleaning agents for improving the cleaning of the membrane and also to improve the regeneration. In work of Bird and Bartlett (1995) it is shown that cleaning of MF membrane fouled by whey protein the flux recovery was 97 % by using sodium hydroxide. In case of UF membrane, which was used to prepare chymosin the flux recovery was 100 % by using dilute NaOCl (Crawford and Stober, 1995).

6.3.3 Biological Methods

In biological methods the cleaning mixture contains bioactive agents, such as micro-organisms and enzymes, to remove the foulant from a membrane. The environmental friendliness of the biological agents has lead to increase in the usage of such agents not only for household usage but also for industrial usage (Chen et al., 1992). However, these agents have not yet been used for a large scale membrane cleaning. The main advantage of biological agents is that they act under soft conditions such as pH and temperature. Therefore the, membrane surface is not damaged as by physical or chemical cleaning. Moreover, there is no

use for further regeneration of the membrane. Nevertheless, Razavi et al. (1996) showed that the flux recovery was not full as by using physical and chemical agents.

Part III

Optimal Operation

Chapter 7

Optimal Operation in the Presence of Membrane Fouling

In the previous chapters we discussed theoretical foundations of membrane separation processes. We showed that the main objective is to drive the concentrations from the initial to a final point. Further, in Chapter 5 we showed that there exist several traditional operations which are in use in the industry (e.g. C-CVD, VVD). In our previous research (Jelemenský et al., 2015; Paulen et al., 2013, 2015) we derived time-optimal operation of diafiltration process, however without considering the fouling phenomena. This chapter will show a detailed derivation of time-optimal operation of diafiltration processes in the presence of membrane fouling. The derivation of the new time-optimal operation is based on Pontryagin's minimum principle.

We will consider two approaches how to derive the time-optimal operation. In both approaches the permeate flow ($q = JA$) will decrease due to the membrane fouling. In the first approach we will investigate the case where fouling affects membrane area (Jelemenský et al., 2014). The second approach accounts

for membrane fouling due to the decrease of the permeate flux with time (Jelemenský et al., 2016b). We will consider perfect rejection of the macro-solute ($R_1 = 1$) and process model described by equations (5.7).

7.1   Membrane Area Fouling

The first discussed approach considers that the effective membrane area decreases due to the blockage of the membrane pores (Jelemenský et al., 2014).

7.1.1   Problem Definition

We assume a solution which consist of two solutes with concentrations c_1 and c_2. The system is well mixed and we operate under constant temperature and pressure. The balance of each solute can then be expressed by (5.7). We consider a general case when the membrane flux is a function of concentrations ($J = J(c_1, c_2)$). We use the complete pore blocking model (6.38a) derived in Sec. 6.1.5 to account for the membrane fouling.

The objective of the optimization is to find such time-dependent function $\alpha(t)$ which drives the process from initial to final concentrations in minimum time. The mathematical formulation of this dynamic optimization problem is as follows

$$\min_{\alpha(t)} \int_0^{t_\mathrm{f}} 1 \, \mathrm{d}t, \tag{7.1a}$$

s.t.

$$\dot{c}_1 = \frac{c_1^2 AJ}{c_{1,0} V_0}(1 - \alpha), \qquad c_1(0) = c_{1,0}, \qquad c_1(t_\mathrm{f}) = c_{1,\mathrm{f}}, \tag{7.1b}$$

$$\dot{c}_2 = -\frac{c_1 c_2 AJ}{c_{1,0} V_0}\alpha, \qquad c_2(0) = c_{2,0}, \qquad c_2(t_\mathrm{f}) = c_{2,\mathrm{f}}, \tag{7.1c}$$

$$\dot{A} = -A_0 \frac{K_\mathrm{c}}{J_0} J, \qquad A(0) = A_0, \tag{7.1d}$$

$$\alpha \in [0, \infty). \tag{7.1e}$$

where A is the effective membrane area and V_0 stands for initial volume of the processed solution.

7.1.2 Characterization of the Optimal Operation

To derive the time-optimal operation using PMP we define the Hamiltonian function

$$H = H(c_1, c_2, A, \lambda_1, \lambda_2, \lambda_3, \alpha), \tag{7.2}$$

and based on the optimization problem (7.1) it can be written as

$$H = 1 + \left[\frac{c_1^2 AJ}{c_{1,0}V_0}(\alpha - 1) \right]\lambda_1 + \left[-\frac{c_1 c_2 AJ}{c_{1,0}V_0}\alpha \right]\lambda_2 + \left[-\frac{A_0 K_c J}{J_0} \right]\lambda_3 \tag{7.3a}$$

$$= \left[1 + \frac{c_1^2 AJ}{c_{10}V_0}\lambda_1 - \frac{A_0 K_c J}{J_0}\lambda_3 \right] + \left[-\frac{c_1^2 AJ}{c_{10}V_0}\lambda_1 - \frac{c_1 c_2 AJ}{c_{10}V_0}\lambda_2 \right]\alpha \tag{7.3b}$$

$$= H_0 + H_\alpha \alpha \tag{7.3c}$$

where the adjoint variables are defined as

$$\dot{\lambda}_1 = \frac{c_1(\alpha - 1)}{c_{1,0}V_0}\left[A(2J + c_1 J_1)\lambda_1 + Ac_1 J_2 \lambda_2 + c_1 J \lambda_3 \right], \tag{7.4a}$$

$$\dot{\lambda}_2 = \frac{\alpha}{c_{1,0}V_0}\left[Ac_2(c_1 J_1 + J)\lambda_1 + Ac_1(c_2 J_2 + J)\lambda_2 + c_1 c_2 J \lambda_3 \right], \tag{7.4b}$$

$$\dot{\lambda}_3 = \frac{A_0 K_c}{J_0}\left[J_1 \lambda_1 + J_2 \lambda_3 \right]. \tag{7.4c}$$

and

$$J_i = \frac{\partial J}{\partial c_i}, \qquad i = 1, 2. \tag{7.5}$$

The optimality conditions (3.19) are as follows

$$H_\alpha = Ac_1 J(c_1 \lambda_1 + c_2 \lambda_2) = 0 \tag{7.6a}$$

$$\dot{H}_\alpha = c_1 J \left[c_1(A^2 J_0 c_2 J - A^2 J_0 c_1 c_2 J_2 - A_0 K_c V_0 c_{1,0} J)\lambda_1 + \right. \tag{7.6b}$$

$$+ c_2(A^2 J_0 c_1^2 J_1 - A_0 K_c V_0 c_{1,0} J)\lambda_2 +$$

$$\left. + AA_0 V_0 c_{1,0}(c_1 J_1 + c_2 J_2)\lambda_3 \right] = 0,$$

since we have three states we also require $\dddot{H}_\alpha = 0$ condition. However, this equations is too long and for simplicity we only define it as

$$\ddot{H}_\alpha = \ddot{H}_\alpha(c_1, c_2, A, \lambda_1, \lambda_2, \lambda_3, \alpha) = 0, \qquad (7.6c)$$

where we can notice that it also depends on the control variable (α) compared to H_α and $\dot{H}_\alpha$ which only depend on state and adjoint variables. As discussed in Section 3.2.3 we are not able to obtain the expression for singular surface, since we have three differential equations (third order system). However, we can derive the expression for singular control. We rewrite the equations (7.6) into the following form

$$\begin{pmatrix} H_\alpha \\ \dot{H}_\alpha \\ \ddot{H}_\alpha \end{pmatrix} = \begin{pmatrix} m_{11} & m_{12} & m_{13} \\ m_{21} & m_{22} & m_{23} \\ m_{31} & m_{32} & m_{33} \end{pmatrix} \begin{pmatrix} \lambda_1 \\ \lambda_2 \\ \lambda_3 \end{pmatrix} = \begin{pmatrix} 0 \\ 0 \\ 0 \end{pmatrix}, \qquad (7.7)$$

which in compact form can be written as

$$\boldsymbol{M}\boldsymbol{\lambda} = \mathbf{0}, \qquad (7.8)$$

we can observe that this is a homogeneous system which is linear in adjoint variables. We can obtain a nontrivial solution only if the determinant of $\boldsymbol{M}$ is equal to zero (Steiner, 2008). This is a nonlinear function of states c_1, c_2, A and control α

$$\det(\boldsymbol{M}(c_1, c_2, A, \alpha_{\text{sing}})) = 0, \qquad (7.9)$$

which after certain algebraic manipulations gives the expresssion for singular control

$$\alpha_{\text{sing}}(c_1, c_2, A) = \frac{L_1}{L_2} - \frac{L_3}{L_2} K_{\text{c}}, \qquad (7.10)$$

where

$$L_1 = 2c_1 c_2 J_1 J_2 - c_1 c_2 J_{21} J + 2c_1^2 J_1^2 - c_1^2 J_{11} J, \qquad (7.11)$$

$$L_2 = 2(c_1 J_1 + c_2 J_2)^2 - J(c_1^2 J_{11} + 2c_1 c_2 J_{21} + c_2^2 J_{22}), \qquad (7.12)$$

$$L_3 = \frac{A_0 V_0 c_{1,0} J}{A^2 c_1 J_0}(c_1 J_1 + c_2 J_2), \qquad (7.13)$$

and

$$J_{ij} = \frac{\partial^2 J}{\partial c_i \partial c_j}, \qquad i, j = 1, 2. \tag{7.14}$$

The optimal operation structure is a three step strategy with control on the boundaries in the first and the last step. In the middle step we apply the derived singular control. We have no information about the switching conditions between the individual modes, because it was not possible to obtain the equation for singular surface. Therefore, we propose to solve a small nonlinear programming (NLP) problem that will provide lengths of the intervals. Note that control on these intervals is completely characterized by PMP. Optimized time intervals can be initialized based on their counterparts if fouling is not assumed. Therefore, such NLP is very easily solvable with only a few iterations and converges without difficulties. This should be compared to application of a general NLP formulation for the optimization of the membrane process based on control vector parametrization (Goh and Teo, 1988) where both times and control need to be suitably parametrized and optimized.

7.1.3 Application of Optimal Operation

We apply the theoretical results derived in above section to study the optimal operation on a case study were we show the advantages of the time-optimal operation compared to traditional operation.

Case Study – Separation under Limiting Flux Conditions

We consider a membrane plant which operates under limiting flux conditions which is the common model in membrane separation (Aimar and Field, 1992). The permeate flux is given by

$$J(c_1) = k \ln \frac{c_{\lim}}{c_1} \tag{7.15}$$

where k is the mass transfer coefficient and c_{lim} represents the limiting concentration for of macro-product. This example was treated in Jelemenský et al. (2013) without the pore blocking model. In this example we demonstrate the time-optimal operation on the case when $c_{\text{lim}} = 55.96\,\text{g/dL}$, $k = 12.439\,\text{m/h}$ and the initial effective membrane area $A_0 = 1\,\text{m}^2$. The goal is to process $100\,\text{dL}$ of solution, to increase the concentration of proteins from $c_{1,0} = 3.3\,\text{g/dL}$ to $c_{1,\text{f}} = 9.04\,\text{g/dL}$, and simultaneously decrease the concentration of lactose from $c_{2,0} = 5.5\,\text{g/dL}$ to $c_{2,\text{f}} = 0.64\,\text{g/dL}$.

The initial and final concentrations determine the first and the third step of the optimal control. In the first step we use concentration mode ($\alpha = 0$). NLP problem will provide time interval length and optimal concentration of the macro-solute to switch to singular surface. As the last step is characterized by dilution mode ($\alpha = \infty$), the optimal concentration to switch from the singular arc is fully determined from the final concentrations. The ratio of the concentrations at time of the switch should be equal the ratio of their final values. The optimal control in the singular arc (7.10) is of the form

$$\alpha_s = 1 - \frac{c_{1,0} V_0 A_0}{A^2 c_1 J_0} \left(\frac{\ln \dfrac{c_{\text{lim}}}{c_1}}{\ln \dfrac{c_{\text{lim}}}{c_1} - 2} \right) K_{\text{c}}. \tag{7.16}$$

If there is no fouling ($K_{\text{c}} = 0\,\text{h}^{-1}$) then the singular control is equal to one.

In Fig. 7.1 we show the time-optimal operation for different values of fouling rate. The top figure plots state trajectories. We start at initial concentrations of both solutes (green circle) and finish at the red cross. The right figure shows the corresponding optimal control. We can observe that by increasing the value of fouling rate the processing time increases as well. This behavior was expected increased as fouling decreases the effective membrane. To illustrate the effect of the fouling constant K_b on the membrane area, one hour operation with $K_{\text{c}} = 0.05$ or $K_{\text{c}} = 0.15$ reduces the area to approximately 84% or 39% of its initial value, respectively.
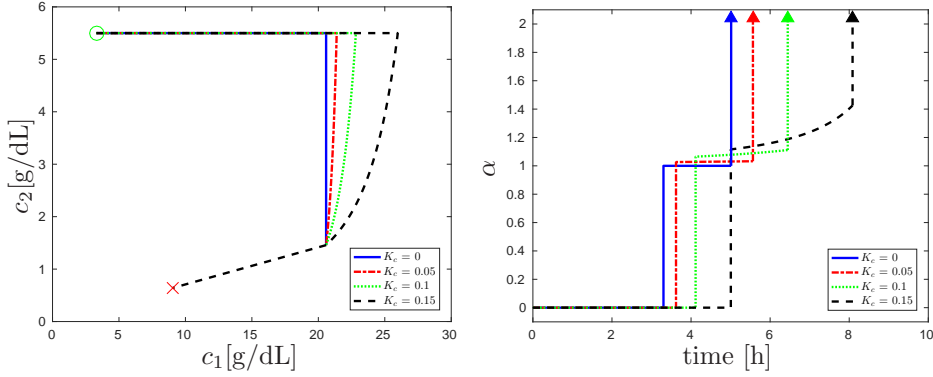
Figure 7.1: Concentration state diagram and optimal control profiles for DF at limiting flux conditions with different fouling rates.

Table 7.1: Time-optimal operation of diafiltration under limiting flux conditions compared with traditionally used operation with different values of fouling rate.

K_c [h^{-1}]	minimum time t_f [h]	C-CVD t_f [h]	%
0	5.01	5.61	11.97
0.05	5.57	6.39	14.72
0.1	6.45	7.99	23.88
0.15	8.08	14.31	77.11

Table 7.1 summarizes the comparison of final time in case of minimum time and traditionally used operation for different values of fouling rates. The traditionally used operation consists of concentration mode followed by constant-volume diafiltration mode (C-CVD). In the first case when $K_c = 0$ the fouling does not effect the separation. In this case the difference between the final processing times is more then 11%. However, once the membrane fouling becomes more pronounced the difference in the processing times increases as well. This behavior was expected since stronger fouling translates to higher processing time. Interesting observation can be made if we compare the time-optimal operation and traditional operation at the highest fouling rate ($K_c = 0.15\,\mathrm{h}^{-1}$). In this case the using the time-optimal operation we were able to reach the desired concentrations in approximately $t_f = 8\,\mathrm{h}$ and the difference between the optimal and traditional operation is more then 77%. Therefore, we can conclude that once high fouling is expected it is necessary to use the time-optimal operation to reduce the processing time and thereby we achieve the reduction in production costs as well.

We note that it was possible to derive the singular control for this specific fouling model only. It is because the rest of the models generate a more complex system of differential equations and it was no longer possible to derive the singular control. Such problems are only possible to solve by employing general numerical methods (e.g. CVP).

7.2   Permeate Flux Fouling

In this approach we will consider that the fouling of the permeate flow $q = JA$ is caused by changes in the permeate flux J. Therefore, we can model it as a function of concentrations and also of time ($J = J(t, c_1, c_2)$). The derivation of the of the analytical optimal operation is very similar to the previous approach. The biggest difference is that the derived time-optimal operation is completely analytical as shown in (Jelemenský et al., 2016b) and general for any fouling

model. Thus, it seems to be more appropriate to solve the optimal control problem.

7.2.1 Problem Definition

The optimization goal is to find such time-dependent function $\alpha(t)$ which guarantees the transition from given initial to final concentrations in minimum time. We assume that the membrane is absolutely impermeable to macro-solute ($R_1 = 1$), the permeability of micro-solute changes as a function of concentrations, and is expressed using rejection coefficient $R_2 = R_2(c_1, c_2)$. Finally, we assume that the unfouled flux is a known function of both concentrations $J_0(c_1, c_2)$ and the fouling model of the flux J is given. The optimization problem then reads as:

$$\mathcal{J}^* = \min_{\alpha(t)} \int_0^{t_f} 1 \, dt, \tag{7.17a}$$

s.t.

$$\dot{c}_1 = c_1^2 \frac{AJ}{c_{1,0} V_0} (1 - \alpha), \qquad c_1(0) = c_{1,0}, \quad c_1(t_f) = c_{1,f}, \tag{7.17b}$$

$$\dot{c}_2 = c_1 c_2 \frac{AJ}{c_{1,0} V_0} (R_2 - \alpha), \qquad c_2(0) = c_{2,0}, \quad c_2(t_f) = c_{2,f}, \tag{7.17c}$$

$$J = J(t, J_0(c_1, c_2), K, n), \tag{7.17d}$$

$$\alpha \in [0, \infty). \tag{7.17e}$$

We note that the optimization problem posses a similar structure as the one presented previously (7.1). The main difference lies in the fact that the model explicitly depends on time (non-autonomous system). However, in this case compared to the previous one, we only have a second order system, where according the theoretical results in Sec. 3.2.3 it is possible to derive the singular surface and singular control. The reduction of the original third order system described by (5.4) and (5.5) was possible due to the fact that $R_1 = 1$ as explained in Sec. 5.1.

7.2.2   Characterization of the Optimal Operation

There are two possible approaches to handle optimal control of non-autonomous systems. The first one considers time explicitly in the process model. Then, the optimal Hamiltonian function is zero only at final time. Therefore, there are two variables (concentrations) and PMP has to supply two equations for optimality. The second approach adds an additional state variable $\dot{x}_a = 1$ with initial condition $x_a(0) = 0$ and replaces t with x_a. Therefore, the new problem is autonomous with increased number of variables. In this case, Hamiltonian function is zero along the optimal trajectory and this fact can be used to provide additional conditions for finding an optimal solution.

Our derivation will use the first approach. The Hamiltonian function can be then defined as

$$H(t, c_1, c_2, \lambda_1, \lambda_2, \alpha) = 1 + \lambda_1 \frac{A c_1^2 J}{c_{1,0} V_0}(1 - \alpha) + \lambda_2 \frac{A c_1 c_2 J}{c_{1,0} V_0}(R_2 - \alpha) \quad (7.18a)$$

$$= \left[1 + \lambda_1 \frac{A c_1^2 J}{c_{1,0} V_0} + \lambda_2 \frac{A c_1 c_2 J R_2}{c_{1,0} V_0} \right] + \quad (7.18b)$$

$$+ \left[-\lambda_1 \frac{A c_1^2 J}{c_{1,0} V_0} - \lambda_2 \frac{A c_1 c_2 J}{c_{1,0} V_0} \right] \alpha$$

$$= H_0 + H_\alpha \alpha \quad (7.18c)$$

where adjoint variables λ_1, λ_2 are defined from differential equations (3.20c) and are as follows

$$\dot{\lambda}_1 = -\frac{A}{c_{1,0} V_0}[\lambda_1(2c_1 J + c_1^2 J)(1 - \alpha)+ \quad (7.19a)$$

$$+ \lambda_2((c_2 J + c_1 c_2 J_1)(R_2 - \alpha) + c_1 c_2 J R_{21})]$$

$$\dot{\lambda}_2 = -\frac{A}{c_{1,0} V_0}[\lambda_1(c_1^2 J_2)(\alpha - 1) \quad (7.19b)$$

$$+ \lambda_2((c_1 J + c_1 c_2 J_2)(R_2 - \alpha) + c_1 c_2 J R_{22})]$$

where

$$J_i = \frac{\partial J}{\partial c_i}, \quad R_{2i} = \frac{\partial R_2}{\partial c_i}, \quad i = 1, 2. \tag{7.20}$$

Based on the optimality conditions (3.22) we can define $H_\alpha = 0$ and the derivative w.r.t. time ($\dot{H}_\alpha = 0$) which are as follows

$$H_\alpha = c_1^2 J \lambda_1 - c_1 c_2 J \lambda_2 = 0, \tag{7.21}$$

the derivative of H_α w.r.t. time is as follows

$$\dot{H}_\alpha = \left[c_{1,0} V_0 c_1^2 J_t - A c_1^3 c_2 J_2 J + A c_1^3 c_2 R_2 J_2 J \right] \lambda_1 + \tag{7.22}$$
$$+ \left[A c_1^2 J \left(c_1 J + c_1 c_2 J + c_1 c_2 J_1 - c_2 R_2 J - c_2^2 R_{22} J - c_1 c_2 R_{21} J - c_1 c_2 R_2 J_1 \right) + \right.$$
$$\left. + c_{1,0} V_0 c_1 c_2 J_t \right] \lambda_2 = 0,$$

where

$$J_t = \frac{\partial J}{\partial t}. \tag{7.23}$$

We can rewrite the above equations for H_α and $\dot{H}_\alpha$ in to the following form

$$\begin{pmatrix} H_\alpha \\ \dot{H}_\alpha \end{pmatrix} = \begin{pmatrix} z_{11} & z_{12} \\ z_{21} & z_{22} \end{pmatrix} \begin{pmatrix} \lambda_1 \\ \lambda_2 \end{pmatrix} = \begin{pmatrix} 0 \\ 0 \end{pmatrix}, \tag{7.24}$$

which can be written in compact form as

$$\mathbf{Z}\boldsymbol{\lambda} = \mathbf{0}, \tag{7.25}$$

where

$$z_{11} = c_1^2 J, \tag{7.26a}$$
$$z_{12} = c_1 c_2 J, \tag{7.26b}$$
$$z_{21} = c_{1,0} V_0 c_1^2 J_t + A c_1^3 c_2 J_2 J (R_2 - 1), \tag{7.26c}$$
$$z_{22} = A c_1^2 J \left[c_1 J + c_1 c_2 J + c_1 c_2 J_1 - c_2 R_2 J - c_2^2 R_{22} J - c_1 c_2 R_{21} J - \right. \tag{7.26d}$$
$$\left. - c_1 c_2 R_2 J_1 \right] + c_{1,0} V_0 c_1 c_2 J_t.$$

Elimination of adjoint variables (λ_1, λ_2) and solving the determinant $(\det(\mathbf{Z}) = 0)$ leads to the expression for singular surface which reads as

$$S(t, c_1, c_2) = (R_2 - 1)\left(J + c_1\frac{\partial J}{\partial c_1} + c_2\frac{\partial J}{\partial c_2}\right) + J\left(c_1\frac{\partial R_2}{\partial c_1} + c_2\frac{\partial R_2}{\partial c_2}\right) = 0.$$
(7.27)

It is interesting to note that the expression (7.27) is formally identical to the one without fouling (5.14), as derived in Paulen et al. (2012). The only difference lies in the fact that J (and thus S) is not only a function of concentrations but also of time. For example, an expression for the singular surface in case of $R_2 = 0$ and the intermediate blocking model boils down to

$$S(t, c_1, c_2) = J_0 + c_1\frac{\partial J_0}{\partial c_1} + c_2\frac{\partial J_0}{\partial c_2} + K_{\mathrm{i}}J_0^2 t = 0.$$
(7.28)

The above relation clearly shows the shift in the optimal operation with fouling $(K_i \neq 0)$ and without fouling $(K_i = 0)$ as reported by Paulen et al. (2012).

To obtain the control which keeps the states on the singular surface, we differentiate the singular surface described by equation (7.27) w.r.t. time. The obtained singular control is:

$$\alpha(t, c_1, c_2) = \frac{\frac{\partial S}{\partial c_1}c_1 + \frac{\partial S}{\partial c_2}c_2 R_2}{\frac{\partial S}{\partial c_1}c_1 + \frac{\partial S}{\partial c_2}c_2} + \frac{\frac{\partial S}{\partial t}}{\frac{c_1 J A}{c_{1,0}V_0}\left(\frac{\partial S}{\partial c_1}c_1 + \frac{\partial S}{\partial c_2}c_2\right)}.$$
(7.29)

This can be again formally separated into two parts: the first one corresponding to the unfouled singular control (5.15) and the second one handling the influence of fouling on the optimal operation.

Based on the obtained results we can now define the optimal operation which is a simple feed-back control law. For both cases the optimal operation shown in Fig. 7.2 consists of three three arcs and it is defined by

1. The control in first step is found from

$$\alpha = \begin{cases} 0\,(\text{green line}) & \text{if } S(t,\, c_1,\, c_2) > 0, \\ \infty\,(\text{red line}) & \text{if } S(t,\, c_1,\, c_2) < 0. \end{cases}$$
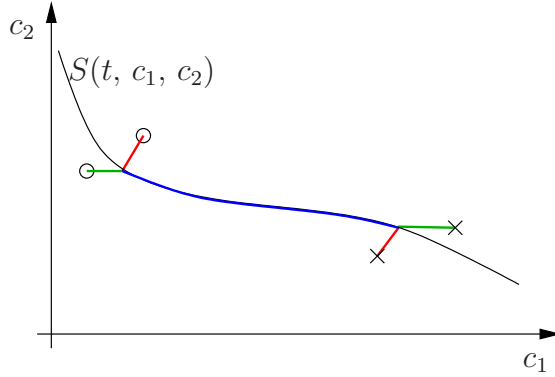(7.30)

Figure 7.2: Graphical representation of optimal operation in concentration diagram.

It is applied until the condition $S(t, c_1, c_2) = 0$ (blue line) is met.

2. In the second step, the states reside on the singular surface with singular control (7.29).

3. The last step uses again either $\alpha = 0$ (green line) or $\alpha = \infty$ (red line) until the final concentrations are reached.

Note that the optimal control does not depend on the fouling model and the fouling constant in the first and the last step. This property is used in the proposed methodology as it helps to retain optimality even if the process model is initially not known perfectly. The optimal sequence of operations depends on the initial and final states. Therefore, any of the steps can be missing from the optimal control structure. For example, the singular step can be skipped and the optimal control will be saturated on constraints for a particular set of initial and final conditions. Further, some applications constrain the maximum value of α to 1. In this the overall optimal operation stays the same, however, in the first and the last section instead of using $\alpha = \infty$ we would use $\alpha = 1$. Moreover, the exact optimal operation also holds for the case without membrane fouling.

7.2.3   Application of Optimal Operation

In the previous sections we derived the optimal operation for the membrane batch processes. In this section applications of such optimal operation will be shown. We will discuss three case studies with different scenarios are considered. In the first and second we show the differences when perfect and imperfect rejections on micro-solute are considered. The third case study is devoted for the comparison of analytical and numerical results for imperfect macro-solute rejection.

Case Study 1 – Diafiltration at Limiting Flux Conditions

In this case study we use a classical setup of the separation of two solutes by diafiltration with constant rejection coefficients ($R_1 = 1$ and $R_2 = 0$). The model of the unfouled flux J_0 we use the limiting flux model as in the previous study described by equation (7.15).

The goal is to drive the concentrations from the initial point $[c_{1,0}, c_{2,0}] = [3.3\,\mathrm{g/dL}, 5.5\,\mathrm{g/dL}]$ to the final point $[c_{1,\mathrm{f}}, c_{2,\mathrm{f}}] = [9.04\,\mathrm{g/dL}, s0.64\,\mathrm{g/dL}]$ for $100\,\mathrm{dL}$ of solution and for the employed membrane area of $1\,\mathrm{m}^2$. The limiting concentration of the product is $56\,\mathrm{g/dL}$ and the mass transfer coefficient is $k = 12.439\,\mathrm{m/h}$. The singular surface can be derived from (7.27) and is of the form

$$S(t,\,c_1) = \left(\ln \frac{c_{\lim}}{c_1} - 1 \right) + 2tkK_i \ln \frac{c_{\lim}}{c_1} = 0. \qquad (7.31)$$

If we differentiate the singular surface with respect to time we obtain the singular control

$$\alpha(t, c_1) = 1 + \frac{K_i c_{1,0} V_0 (K_i J_0 t + 1) \left[\ln \left(\frac{c_{\lim}}{c_1} \right) (K_i J_0 t + 1) - 2 \right]}{A c_1 (K_i t(2k + J_0) + 1)}, \qquad (7.32)$$

where V_0 stands for the initial volume. We can observe that, besides concentrations, singular surface and control also depend on fouling rate and time. Note
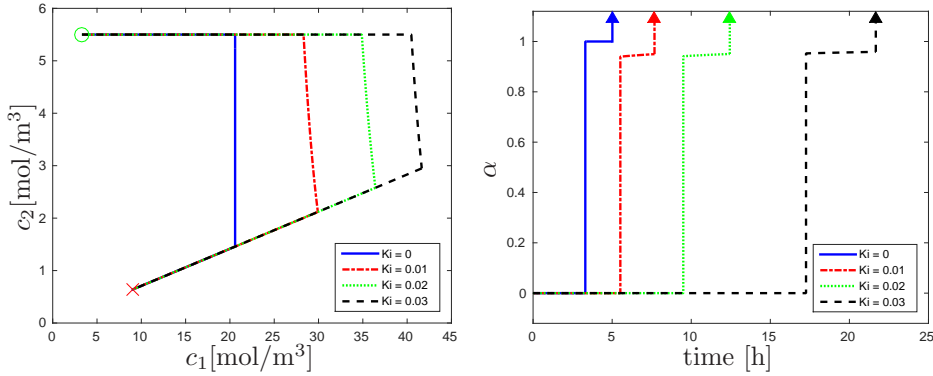
Figure 7.3: Comparison of different control strategies (left – state space, right – control profiles).

that when no fouling is present, the optimal operation boils down to the classical result, i.e. the CVD step should be commenced when $c_1 = c_{\lim}/e$.

Using the presented theoretical results and knowledge on initial and final conditions, the time-optimal operation in the presence of fouling comprises a sequence of following three steps:

1. The first step is the concentration mode $\alpha = 0$ till the singular surface (7.31) is reached.

2. Then, in the second step, the states reside on the singular surface with the singular control (7.32). This step is performed until the condition $c_1(t)/c_2(t) = c_{1,f}/c_{2,f}$ is satisfied.

3. In the last step we perform pure dilution mode with $\alpha = \infty$ to reach the final concentrations.

In Fig. 7.3 we depicts the optimal control strategy (states and control) for the minimum-time operation for different fouling rates. The control structure in all the cases is the three-step strategy described above. The circle in the state diagram represents the initial concentrations and the cross depicts the final

Table 7.2: Time-optimal operation compared to traditional operation for different fouling rates.

K_i $[10^{-3}\,\mathrm{m}^{-1}]$	minimum time t_f [h]	switching time t_s [h]	C-CVD t_f [h]	$\Delta[\%]$
0	5.01	3.31	5.61	11.97
10	7.68	5.52	11.70	52.34
20	12.44	9.49	28.37	128.05
30	21.67	17.26	78.02	260.04

ones. We can observe that the switching concentration to singular surface (7.31) changes with different fouling rates K_i. Furthermore we can observe that the increase of these values translates to longer processing time, as expected.

Table 7.2 presents a comparison of the final processing times in case of the proposed minimum-time operation and the traditionally used operation (C-CVD). Moreover, we also report the corresponding switching time (t_s) when the time-optimal operation switches from concentration mode to singular mode. The traditional mode of operation consists of two steps. It starts with the same concentration mode as the proposed approach. However, its second step is constant volume diafiltration ($\alpha = 1$) and it is switched on at $c_1 = c_{1,f}$. Clearly, as fouling pronounces, this diafiltration step is suboptimal causing overall increase of processing time. Further, we can also observe that by the increase of the fouling rate the switching times increase. This is mainly caused by the the decrease in the permeate flow and slower reduction of the feed volume, which eventually results in longer time to reach the optimal switching concentration. For the highest rate of fouling considered here, the savings in terms of processing time are almost threefold.

A care must be taken when applying this optimal operation on a real process. The traditional C-CVD operation and model (7.15) operate with concentration

$c_1 < 10\,\mathrm{g/dL}$. The proposed optimal operation uses much higher concentrations of macro-solute up to $40\,\mathrm{g/dL}$. Therefore, a new model has to be estimated that also covers this area. Such high concentration can cause strong polarization effects and necessity to move the operation in lower-concentration region. In that case, the singular surface would not be attained and constraint-based operation would be applied as shown in Jelemenský et al. (2014). Moreover, if the rejection coefficient for macro-solute (with concentration c_1) would be less than one, the switching time t_s would be reached later compared to the case when $R_1 = 1$. This is caused by the outflow of the macro-solute from the system, which results in longer time to reach the desired switching concentration. However, in this case numerical optimization would be needed to compute the optimal switching concentration. This is because the time-optimal operation can be derived analytically only in the case when $R_1 = 1$.

Case Study 2 – Separation of Lactose from Proteins

We study separation of lactose (with concentration c_2) from proteins (with concentration c_1). The separation problem was originally formulated in Rajagopalan and Cheryan (1991) and its optimal unfouled control was derived in Paulen et al. (2012). The experimentally verified model for the permeate flux is given as

$$J_0(c_1, c_2) = b_0 + b_1 \ln c_1 + b_2 \ln c_2 = 63.42 - 12.439 \ln c_1 - 7.836 \ln c_2. \quad (7.33)$$

The permeate flux model can be alternatively rewritten into the form

$$J_0(c_1, c_2) = -b_1 \left(\ln \mathrm{e}^{-\frac{b_0}{b_1}} - \ln c_1 + \ln c_2^{-\frac{b_2}{b_1}} \right) = -b_1 \ln \frac{\mathrm{e}^{-\frac{b_0}{b_1}} c_2^{-\frac{b_2}{b_1}}}{c_1}, \quad (7.34)$$

which resembles the expression for limiting flux (equation (7.15)). However, compared to the previous case study, in this case the limiting macro-solute concentration depends on the concentration of c_2. We will consider the same

initial and final concentrations, the membrane area, rejection coefficients and the initial volume as in the previous case study.

The singular surface is of the following form

$$S(t, c_1, c_2) = b_0 + b_1(\ln c_1 + 1) + b_2(\ln c_2 + 1) + K_i t J_0^2 t = 0, \qquad (7.35)$$

and singular control is as follows

$$\alpha(t, c_1, c_2) = \frac{b_1}{b_1 + b_2} + \frac{K_i c_{1,0} V_0 (K_i J_0 t + 1)(2b_1 + 2b_2 + J_0(K_i J_0 t + 1))}{K_i t A c_1 (b_1 + b_2)(2b_1 + 2b_2 - J_0 - 1)}.$$

$$(7.36)$$

Here we can easily distinguish the contribution of the fouling to the optimal operation of unfouled membrane system.

The time-optimal operation in the presence of membrane fouling consists of the same three steps as presented in the previous case study. As explained in the previous case study, when different rejection for macro-solute would be considered the switching time would be reached in higher time. In addition, the optimal switching time and the singular control would need to be computed by numerical optimization.

In Fig. 7.4 we show the optimal control strategy (states and control) for the minimum-time operation for different fouling rates. Compared to the previous case study, the unfouled singular control mode is variable volume diafiltration ($\alpha \approx 0.61$) which changes slightly with increased fouling rate. As in the previous case study, the macro-solute concentration that switches to singular mode increases with the fouling rate and the total processing time increases as well.

Table 7.3 presents a comparison of the final processing time in case of proposed minimum-time operation and the traditionally used operation (C-CVD). In the table we also show the switching time (t_s) where in the case of time-optimal operation we switch from concentration mode to singular control mode. The differences in the duration of the respective operations get more significant as the fouling rate increases. For the highest rate of fouling considered here, the savings in terms of processing time are almost threefold.
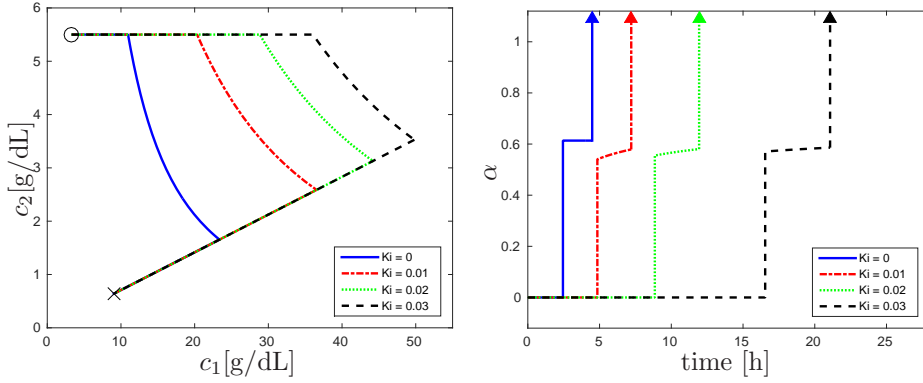
Figure 7.4: Comparison of different control strategies (left – state space, right – control profiles).

Table 7.3: Time-optimal operation compared to traditional operation for different fouling rates.

K_i $[10^{-3}\,\mathrm{m}^{-1}]$	minimum time t_f [h]	switching time t_s [h]	C-CVD t_f [h]	$\Delta[\%]$
0	4.49	2.45	4.74	5.57
10	7.24	4.85	10.52	45.30
20	12.02	8.85	26.70	122.13
30	21.27	16.54	75.57	255.29

When we compare the two case studies, we can observe different processing times and also different switching times. These differences also result in different savings for the same fouling rates. This is caused mainly due to the fact that in the second case study the limiting concentration for the macro-solute was a function of concentration c_2. We can also observe that this difference in the model of the permeate flux resulted in different expression for singular surface and thus to different singular control.

Case Study 3 – Imperfect Macro-Solute Rejection

The purpose of this study is to show the properties of the proposed approach if some of the assumptions are not satisfied. Namely, we will study a membrane separation process where the rejection of the macro-solute by the membrane is not complete, and varies according to the concentrations of both solutes. As it was pointed out in Paulen et al. (2015), analytical expressions of singular surface are no longer possible for such a case and the resulting optimal control problem needs to be solved numerically.

The considered process model is taken from Fikar et al. (2010). The original experiment (Kovács et al., 2009) providing the models of permeate flux and rejection coefficients, dealt with separation of technical grade sucrose and sodium chloride in aqueous solvent. Sucrose being the macro-solute (product), and sodium chloride the micro-solute (impurity). The purpose of the experiment was to find the relation between permeate flux, rejection coefficient, and the concentrations. The separation was achieved using cross-flow nanofiltration ($A = 0.45\text{m}^2$), as it has the appropriate pore size and structure, applicable for demineralization of saccharides. The experiment was carried out at constant temperature and pressure. The empirical relations for J_0, R_1 and R_2 as

Table 7.4: Experimentally obtained coefficient values for R_1, R_2, and J_0.

i	s_i	w_i	z_i
1	68.1250×10^{-9}	7.8407×10^{-6}	-0.0769×10^{-6}
2	-56.4512×10^{-6}	-4.0507×10^{-3}	-0.0035×10^{-3}
3	32.5553×10^{-3}	1.0585	0.0349×10^{-3}
4	-4.3529×10^{-9}	1.2318×10^{-9}	0.9961
5	3.3216×10^{-6}	-9.7660×10^{-6}	
6	-2.7141×10^{-3}	-1.1677×10^{-3}	

functions of component concentrations are as follows:

$$J_0 = S_1\,(c_2)\,\mathrm{e}^{S_2\,(c_2)\,c_1}, \tag{7.37a}$$

$$R_1 = (z_1\,c_2 + z_2)c_1 + (z_3\,c_2 + z_4), \tag{7.37b}$$

$$R_2 = W_1\,(c_2)\,\mathrm{e}^{W_2\,(c_2)\,c_1}, \tag{7.37c}$$

where S_1, S_2, W_1, W_2 are

$$S_1 = s_1\,c_2^2 + s_2\,c_2 + s_3, \tag{7.38a}$$

$$S_2 = s_4\,c_2^2 + s_5\,c_2 + s_6, \tag{7.38b}$$

$$W_1 = w_1\,c_2^2 + w_2\,c_2 + w_3, \tag{7.38c}$$

$$W_2 = w_4\,c_2^2 + w_5\,c_2 + w_6, \tag{7.38d}$$

and s_{1-6}, z_{1-4} and w_{1-6} are experimentally evaluated coefficients with the process solution (see Table. 7.4). The intermediate fouling model is considered with values of K_i up to $5\,\mathrm{m}^{-1}$. The maximum value of α is constrained by 1.

Numerical method of orthogonal collocation was used to compute the optimal control and state trajectories. In our case we chose 3–7 time intervals, 5 collocation points on states and 3 collocation points on control to find the optimal separation strategy. Differences in final processing times between 3 and 7 time intervals were not significant.
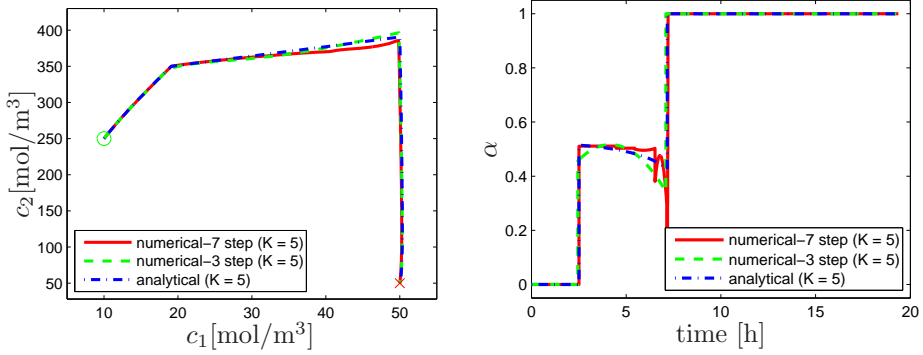
Figure 7.5: Comparison of different control strategies (top – state space, bottom
– control profiles).

Fig. 7.5 depicts the optimal trajectory of concentration of sucrose and sodium
chloride to drive from initial states (circle) to final states (cross). It compares op-
timal trajectories of sucrose and sodium chloride for both analytical and numer-
ical control approaches with maximum membrane fouling studied ($K_i = 5 \, \text{m}^{-1}$).
The state trajectory consists of three steps, i.e. concentration mode, diafiltra-
tion with time-varying profile of α, and constant volume diafiltration mode.
Therefore, the control variable α is equal to 0 in the first step to increase the
concentration of both product and impurity. In the second part the control
varies in a mid range, and that highly contributes to the concentration increase
in our product. The final step is constant volume diafiltration mode with $\alpha = 1$
and directly translates to reduction in impurity to achieve the final product and
impurity concentration.

The optimal control trajectory obtained numerically shows some typical os-
cillations in singular mode due to a low sensitivity of the cost function to this
part of the control trajectory. The magnitude and frequency of the oscilla-
tions increase as the number of time intervals increase and hence we can see
comparatively more oscillations in the seven-step strategy, than three-step or

analytical strategy. This is mainly caused due to more optimization variables and numerical insensitivity. In fact, the second step could be replaced, for practical purposes, with a constant α (variable volume diafiltration mode) without a major change in the duration of the operation.

Simulations with other values of the fouling parameter K_i showed the similar behavior, although processing time for lower values of K_i was shorter. Even if the assumptions for the proposed method are not valid, the resulting state and control trajectories are almost optimal and the final processing times are practically the same as those obtained with numerical optimization. This is due to the fact that the rejection coefficient is close to 1 for the entire operation. Note that the analytical approach is not able to reach final concentrations perfectly due to mismatch between assumed ($R_1 = 1$) and real rejection of the macro-solute, but the differences are negligible (less than $1\,\%_{oo}$).

7.3 Summary and Discussion

In this part of the work we have proposed optimal control of batch diafiltration processes in the presence of membrane fouling. We have shown two types of problems which deal with membrane fouling. These types (approaches) differ in a way how the fouling of the membrane was described. In the first approach the fouling was described by the decrease in the effective membrane area. In the second approach we assumed that the permeate flux can be modelled as an explicit function of time and also of concentrations. In both approaches optimal operation was derived to drive the system from initial to final concentrations in minimum time.

In the first case the optimal operation was a combination of analytical and numerical solutions. The number of intervals and the control was fully determined by the PMP and the lengths of individual time intervals had to be determined by solving a NLP problem. The drawback of this approach was that the optimal operation was only possible to obtain for one of the standard

Table 7.5: Comparison of the final processing time and permeate flow for chosen fouling constants.

	$K_c = 0.15$	$K_i = 0.01$
t_f	8.08	7.68
$q(t_f)$	4.89	4.87

fouling models, because for the other ones the problem became more complex and it was no longer possible to derive the singular control.

In the second case a fully analytical optimal operation was derived without any needs for numerical optimization. Moreover, this optimal operation is possible to obtain for any fouling model and even if the rejection coefficient R_2 is a function of concentrations $R_2 = R_2(c_1, c_2)$.

We have shown that the optimal operation in both cases is a three step strategy with extremal values for the control variable (α) in the first and the last intervals and singular control in the middle interval. However, the advantage of the second approach lies in the fact that the switching concentration (time) is fully determined by the singular surface equation as compared to the first approach.

We can also conclude that even if the fouling models were different they show similar behavior in terms of the increase of the switching concentration to singular surface with increased fouling rate and in the decrease in the final permeate flux $q(t_f)$.

In Table 7.5 we show the final processing time and the final permeate flow for chosen fouling constants in both proposed approaches (fouling in A or J, respectively). We can observe that by different fouling models and fouling constants we obtained almost the same final permeate flow $q(t_f)$ and final processing time (t_f). Based on this we can conclude that both approaches indicate similar behavior of the overall separation procedure. Moreover, the results from all case

studies indicate that the time-optimal operation compared to traditional opera-
tion (e.g. C-CVD) is more effective in terms of processing time which eventually
translates to reduction of productions costs.

However the last question which rises is which of the two approaches for
obtaining the time-optimal operation in the presence of membrane fouling should
be used. In this case we can conclude that by using the second approach where
the fouling is described by the decrease of the permeate flux is more effective
than the first approach presented in this work. It is because the overall optimal
operation is of fully analytical nature. Moreover, we have no restriction on the
type of the fouling model and we can also consider the case when the rejection
on the second solute is a function of one or both concentrations. Therefore, all
these advantages show the benefits of the second approach compared to the first
one.

Chapter 8

Estimation of Fouling Behavior

Until now we have assumed that the fouling parameters K and n are perfectly known. However, in real process application these parameters can change with time and thus the fouling behavior changes as well. Moreover, several fouling mechanisms can occur in parallel or in series during the run of process. For example Mohsen et al. (2012) have observed experimentally different fouling phenomena during one batch. Salahi et al. (2010) have described experiments where the initial flux decline was attributed to standard pore blocking mechanism and changed to cake formation in the final phase.

Therefore, to achieve better performance of the membrane separation we propose to estimate both the values of the individual fouling constants and the fouling model itself. This can be achieved e.g. by employing an Extended Kalman Filter (Bavdekar et al., 2011; Kalman, 1960) (EKF) for the simultaneous estimation of states and parameters (the fouling constant K and the parameter n). The main idea behind the EKF is that the non-linear system is linearized around the current EKF estimate and the measurements are taken at discrete time instants in order to correct the dynamics of the filter.

The optimal operation is identical to the one discussed in Sec. 7.2.2. A three

step strategy is considered with control on the boundaries in the first and the last mode and the singular control in the middle step. The switching between the individual modes is based on singular surface.

8.1 Problem Definition

In the first step it is necessary to augment the vector of state variables with the estimated parameters n, K that represent new states with no dynamics and unknown initial value. Further, the explicit appearance of time is replaced by a new state x_3, yielding new process description with 5 states

$$\mathcal{J}^* = \min_{\alpha(t)} \int_0^{t_f} 1 \, \mathrm{d}t, \tag{8.1a}$$

s.t.

$$\dot{c}_1 = \frac{c_1^2 A J}{c_{1,0} V_0}(1 - \alpha), \quad c_1(0) = c_{1,0}, \quad c_1(t_f) = c_{1,f}, \tag{8.1b}$$

$$\dot{c}_2 = -\frac{c_1 c_2 A J}{c_{1,0} V_0}\alpha, \qquad c_2(0) = c_{2,0}, \quad c_2(t_f) = c_{2,f}, \tag{8.1c}$$

$$\dot{x}_3 = 1, \qquad\qquad x_3(0) = 0, \tag{8.1d}$$

$$\dot{K} = 0, \qquad\qquad K_0(0) = K_0, \tag{8.1e}$$

$$\dot{n} = 0, \qquad\qquad n(0) = n_0, \tag{8.1f}$$

$$J = J(x_3, J_0(c_1, c_2), K, n), \tag{8.1g}$$

$$\alpha \in [0, \infty). \tag{8.1h}$$

The differential equations can be written of the following form

$$\dot{\boldsymbol{x}} = \boldsymbol{f}(\hat{\boldsymbol{x}}, \boldsymbol{u}). \tag{8.2}$$

Possible candidates for the process outputs are the concentrations c_1, c_2, and the permeate flux J. Observability matrix for such process description has rank equal to 4. This shows that parameters K and n are not simultaneously

observable as they enter the process equations via J only and there are infinitely many combinations of them that can lead to the actual value of J.

A possible remedy is to add some new measured variable that is a different function of unknown parameters. One candidate is derivative $\dot{J}$ of the flux with respect to time. Process observability is then of full rank. It is, however, not possible to measure $\dot{J}$ exactly and we use an approximation of the third order to obtain its value. It has to be noted that the structural identifiability of the parameters K and n was also confirmed by the Taylor series method (Pohjanpalo, 1978). However, this approach assumes idealized conditions (e.g., continuous measurements and the availability of the output signal and all its derivatives).

Process outputs measured in discrete-time samples are then given as

$$\boldsymbol{y}_k = \boldsymbol{h}(\boldsymbol{x}_k) = (c_1, c_2, x_3, J, \dot{J})^T. \tag{8.3}$$

The observer dynamics is given by

$$\dot{\hat{\boldsymbol{x}}} = \boldsymbol{f}(\hat{\boldsymbol{x}}, \boldsymbol{u}), \tag{8.4}$$

$$\dot{\boldsymbol{P}}^- = \boldsymbol{F}\boldsymbol{P}^- + \boldsymbol{P}^-\boldsymbol{F}^T + \boldsymbol{Q}, \tag{8.5}$$

for $t \in (t_{k-1}, t_k]$ with $\boldsymbol{P}^-(t_{k-1}) = \boldsymbol{P}^+_{k-1}$ and with the update of the observer defined as follows

$$\boldsymbol{L}_k = \boldsymbol{P}^-_k \boldsymbol{C}^T_k (\boldsymbol{C}_k \boldsymbol{P}^-_k \boldsymbol{C}^T_k + \boldsymbol{R}_k)^{-1}, \tag{8.6a}$$

$$\hat{\boldsymbol{x}}_k = \hat{\boldsymbol{x}}_{k-1} + \boldsymbol{L}_k(\boldsymbol{y}_k - \boldsymbol{h}(\hat{\boldsymbol{x}}_{k-1})), \tag{8.6b}$$

$$\boldsymbol{P}^+_k = (\boldsymbol{I} - \boldsymbol{L}_k \boldsymbol{C}_k)\boldsymbol{P}^-_k, \tag{8.6c}$$

where the state transition and observation matrices are defined by following Jacobians

$$\boldsymbol{F} = \frac{\partial \boldsymbol{f}}{\partial \boldsymbol{x}}\bigg|_{\hat{\boldsymbol{x}}(t), \boldsymbol{u}(t)}, \qquad \boldsymbol{C}_k = \frac{\partial \boldsymbol{h}}{\partial \boldsymbol{x}}\bigg|_{\hat{\boldsymbol{x}}_k}. \tag{8.7}$$

Matrices $\boldsymbol{R}, \boldsymbol{Q}, \boldsymbol{P}$ denote, respectively, the covariance matrix of the noise affecting the measurements, the covariance matrix of the noise affecting the

state dynamics, and the covariance of the estimation error of states and parameters. These matrices can also be thought of as tuning knobs of the estimation algorithm affecting its estimation performance and convergence.

Based on the measured outputs the Kalman filter provides on-line estimates of parameters K and n. This knowledge is then used to update regions and parameters of the time-optimal controller. However one of the drawbacks of EKF is that we cannot consider constraints for the estimated parameters. This can cause the estimated parameter n can overcome the minimal and maximal considered value for which the fouling models are validated. Further, also the fouling rate cannot be negative. The proposed approach for estimation of fouling parameters will be applied in a case study.

8.2   Case Study

We consider the batch membrane process which operates under limiting flux conditions. The permeate flux of the unfouled membrane is then as follows

$$J_0(c_1) = k \ln \left(\frac{c_{\text{lim}}}{c_1} \right), \tag{8.8}$$

where k is the mass transfer coefficient and c_{lim} is the limiting concentration of the macro-solute. We can observe that the permeate flux depends solely on the macro-solute concentration. The goal is to drive the system from initial concentrations $[c_{1,0}, c_{2,0}] = [10 \, \text{mol/m}^3, 100 \, \text{mol/m}^3]$ to final concentrations $[c_{1,\text{f}}, c_{2,\text{f}}] = [100 \, \text{mol/m}^3, 1 \, \text{mol/m}^3]$ in minimum time. The initial volume of the filtered solution is $V_0 = 0.1 \, \text{m}^3$. We consider the limiting flux model with parameters $k = 4.79 \, \text{m/s}$, $c_{\text{lim}} = 319 \, \text{mol/m}^3$ and the membrane area $1 \, \text{m}^2$.

Three simulation experiments were performed with one constant value of the fouling rate $K = 2$ and different values of n, hence with different fouling models.

A crucial point in the design of an EKF is the choice of the covariance matrices that affect the performance and the convergence of EKF. In this preliminary
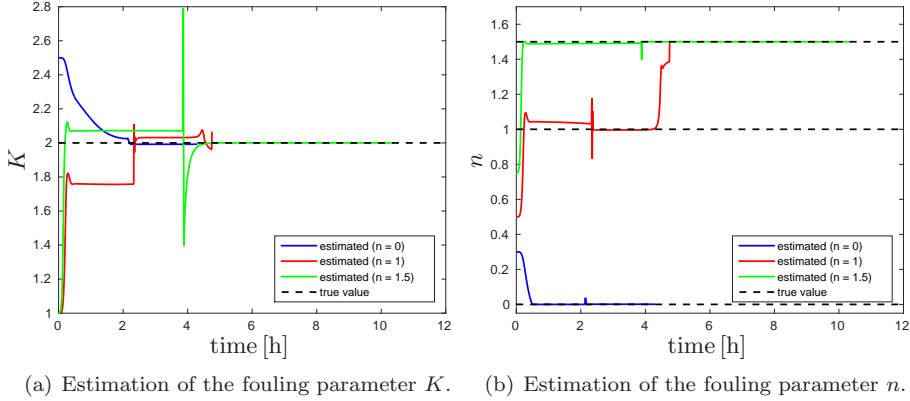
(a) Estimation of the fouling parameter K.   (b) Estimation of the fouling parameter n.

Figure 8.1: Estimation of the fouling parameter n for the three chosen cases.

study we did not consider any measurement noise therefore we chose the matrix $\boldsymbol{R} = 0.001\boldsymbol{I}_5$. The initial estimation error for the states and the estimated parameters represented by matrix $\boldsymbol{P}_0$ is of the following form

$$\boldsymbol{P}_0 = \mathrm{diag}(0.001,\ 0.001,\ 0.001,\ 0.1,\ 0.1), \tag{8.9}$$

where we assume that the initial measurement error for the first three states is small since the concentrations are known. Similarly, the covariance matrix which affects the state dynamics $\boldsymbol{Q}$ is chosen as follows

$$\boldsymbol{Q} = \mathrm{diag}(0.001,\ 0.001,\ 0.001,\ 100,\ 20). \tag{8.10}$$

Time evolutions of the parameter estimates for the individual fouling models are shown in Fig. 8.1. Although the estimated values of the parameters do not converge exactly to the true values, they are, in all cases, reasonably close to them. This is mainly caused by the approximation of the derivative of the flux and by nonlinearity of the process model. The convergence is always achieved within the first control arc (concentration mode) of the operation where the control is constant and does not depend on estimated parameters or the states

(a) Concentration state diagram
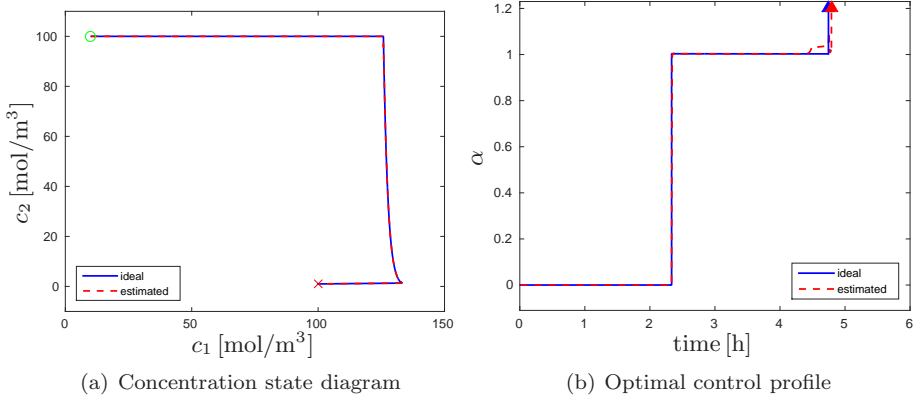
(b) Optimal control profile

Figure 8.2: Concentration state diagram and optimal control profile for ideal and estimated fouling parameters ($K = 2$ and $n = 1.5$).

variables. Fouling parameter estimates are needed to accurately estimate the time of switching to the second control arc and to calculate the singular control. Therefore, as the Kalman filter can converge to the neighborhood of true parameters within the first mode, the proposed procedure yields all considered simulation scenarios having practically the same performance as the optimal control with perfect knowledge of the fouling model and its parameters.

We can observe oscillations of parameter values around the first and the second switching times. In the intermediate fouling model, n actually diverged near the second switch. This is caused by the approximation of $\dot{J}$ as it does not occur when the true value of $\dot{J}$ was used as the measured value.

Parameter estimation can be terminated after the second switch. Control in the third arc is given by $\alpha = \infty$ and this control mode is performed after the separation – we only add water to reach the desired final concentrations.

Fig. 8.2 shows the ideal optimal concentration state diagram and corresponding optimal control profile (blue line) for the case with perfect knowledge of fouling parameters ($K = 2$ and $n = 1$). The dashed red line represents the the

behavior of the concentrations and the control profile with estimated fouling parameters. We note that this was the worst case of the three with parameter convergence issues.

As explained in the theoretical part, the optimal operation is a three step strategy $\alpha = (0, \alpha_2(t), \infty)$ where the second step is the singular control close to one (for this membrane and the fouling model). Difference in optimal switching times and switching concentrations stay below $1\,\%$. The largest difference in the control profile is $4\,\%$ before the second switch. However, as it occurs only during the last few minutes of the separation it has only a minor impact on the state/control profiles and on the operating time.

Chapter 9

Conclusions and Future Research

In this work we investigated time-optimal operation of a batch diafiltration process in the presence of membrane fouling. We have considered several standard fouling models taken from the literature to account for the fouling phenomena during the separation. We outlined development of optimal operation for a membrane separation processes in the presence of fouling based on the Pontryagin's minimum principle. We have discussed two approaches which showed different ways to describe the fouling phenomena. The results showed that the optimal operation consists of three step strategy. The first and the last step use either ultrafiltration or pure dilution and the middle step is characterized by staying on singular surface where singular control is applied. In the first approach the switching conditions need to be obtained by solving a NLP problem.

As an extension to our findings we provided a detailed analysis for the estimation of the membrane fouling. For the on-line estimation of the main fouling parameters we proposed to use extended Kalman filter. The results have shown that EKF was able to converge to the neighborhood of true values of the fouling parameters. The convergence is satisfactory even if the control variable is constant during the first time interval and does not guarantee persistent excitation

conditions. When the parameters converge near their true values, the model approximates the plant well and its operation is close to optimal.

All the findings were critically discussed in this work. Moreover, we provided various types of case studies with different complexity to show the benefits of the derived optimal operation compared to traditional control approaches.

Future work motivation can be summarized in the following items

1. Implementation and verification of the optimal operation on a laboratory scale membrane plant.

   In this case the derived optimal operation in the presence of fouling will be implemented on a real plant to verify the theoretical results presented in this work.

2. Effective estimation of the fouling phenomena.

   In this step of the research more effective techniques of parameter estimation methods will be studied to predict the fouling during the run of the process. By implementation of advanced methods like moving horizon estimation would increase the performance of the optimal operation on real plant, since the singular surface and control depend also on the fouling parameters.

Bibliography

P. Aimar and R. Field. Limiting flux in membrane separations: A model based on the viscosity dependency of the mass transfer coefficient. *Chemical Engineering Science*, 47(3):579–586, 1992. 101

A. Al-Amoudi, W. Robert, and R. W. Lovitt. Fouling strategies and the cleaning system of {NF} membranes and factors affecting cleaning efficiency. *Journal of Membrane Science*, 303(1–2):4 – 28, 2007. ISSN 0376-7388. doi: http://dx.doi.org/10.1016/j.memsci.2007.06.002. 88

A. Arunkumar, M. S. Molitor, and M. R. Etzel. Comparison of flat-sheet and spiral-wound negatively-charged wide-pore ultrafiltration membranes for whey protein concentration. *International Dairy Journal*, 56:129 – 133, 2016. ISSN 0958-6946. 64

H. Attia, M. Bennasar, and B. Tarodo de la Fuente. Study of the fouling of inorganic membranes by acidified milks using scanning electron microscopy and electrophoresis. i. membrane with pore diameter $0 \cdot 2$ μm. *Journal of Dairy Research*, 58:39–50, 1991. 91

R. W. Baker. *Membrane Technology and Applications, Third Edition*. Wiley, 2012. 62, 77

V. A. Bavdekar, A. P. Deshpande, and S. C. Patwardhan. Identification of process and measurement noise covariance for state and parameter estimation using extended Kalman filter. *Journal of Process Control*, 21(4):585 – 601, 2011. ISSN 0959-1524. 123

R. Bellman. *Dynamic Programming*. Princeton University Press, 1957. 38

R. R. Bhave. *Inorganic Membranes Synthesis, Characteristics and Applications ||*, volume 10.1007/978-94-011-6547-1. 1991. 57

L. T. Biegler. Solution of dynamic optimization problems by successive quadratic programming and orthogonal collocation. *Computers and Chemical Engineering*, 8(3/4):243–248, 1984. 44

M. R. Bird and M. Bartlett. Cip optimisation for the food industry: relationships between detergent concentration, temperature and cleaning time. *Transactions of the institution of chemical engineers*, 70:63–70, 1995. 93

W. F. Blatt, A. Dravid, A. S. Michaels, and L. Nelsed. Solute polarization and cake formation in membrane ultrafiltration: Causes, consequences, and control techniques. *Membrane Science and Technology*, pages 47–91, 1970. 89

G. R. Bolton, A. W. Boesch, and M. J. Lazzara. The effects of flow rate on membrane capacity: Development and application of adsortive membrane fouling models. *Journal of Membrane Science*, 279:625–634, 2006. doi: 10. 1016/j.memsci.2005.12.057. 21, 78, 84, 86

K. Boussu, C. Vandecasteele, and B. Van der Bruggen. Relation between membrane characteristics and performance in nanofiltration. *Journal of Membrane Science*, 310(1–2):51 – 65, 2008. ISSN 0376-7388. doi: http: //dx.doi.org/10.1016/j.memsci.2007.10.030. 61

A. E. Bryson, Jr. and Y. C. Ho. *Applied Optimal Control*. Hemisphere Publishing Corporation, 1975. 35, 73

M. Caracotsios and W. E. Stewart. Sensitivity analysis of initial value problems with mixed ODEs and algebraic equations. *Computers and Chemical Engineering*, 9:359–365, 1985. 48

H. Carrére and F. René. Industrial multi-stage continuous filtration process: influence of operating parameters. *Journal of Membrane Science*, 110(2):191 – 202, 1996. ISSN 0376-7388. doi: http://dx.doi.org/10.1016/0376-7388(95)00247-2. 20, 58

B. C. Chachuat. *Nonlinear and Dynamic Optimization: From Theory to Practice*. Polycopiés de l'EPFL. EPFL, 2009. 42

A. Charfi, N. B. Amar, and J. Harmand. Analysis of fouling mechanisms in anaerobic membrane bioreactors. *Water Research*, 46(8):2637 – 2650, 2012. ISSN 0043-1354. doi: http://dx.doi.org/10.1016/j.watres.2012.02.021. 21, 79

J. Chen, L. Wang, and Z. Zhu. Preparation of enzyme immobilized membranes and their self-cleaning and anti-fouling abilities in protein separations. *Desalination*, 86(3):301 – 315, 1992. ISSN 0011-9164. doi: http://dx.doi.org/10.1016/0011-9164(92)80040-G. 93

M. Cheryan. *Ultrafiltration and Microfiltration Handbook*. CRC press, Florida, USA, 1998. 20, 53, 57

H. Choi, H. Kim, I. Yeom, and D. D. Dionysiou. Pilot plant study of an ultrafiltration membrane system fordrinking water treatment operated in the feed-and-bleed mode. *Desalination*, 172(3):281 – 291, 2005. ISSN 0011-9164. doi: http://dx.doi.org/10.1016/j.desal.2004.07.041. 20, 57

M. Čižniar, M. Fikar, and M. A. Latifi. Matlab dynamic optimisation code dynopt. user's guide. Technical report, KIRP FCHPT STU Bratislava, Slovak Republic, 2005. 44

J. G. Crawford and S. R. Stober. Preparation of soluble chymosin or prochymosin from recombinant E. Coli–by solubilizing with urea and renaturing, with removal urea by ultrafiltration for recycle and specific membrane cleaning procedure. 1995. 93

A. G. Fane, C. J. D. Fell, and K. J. Kim. The effect of surfactant pretreatment on the ultrafiltration of proteins. *Desalination*, 53(1–3):37 – 55, 1985. ISSN 0011-9164. doi: http://dx.doi.org/10.1016/0011-9164(85)85051-7. Proceedings of the Symposium on Membrane Technology. 90

M. Fikar, M. A. Latifi, F. Fournier, and Y. Creff. Control vector parametrisation versus iterative dynamic programming in dynamic optimisation of a distillation column. *Computers & Chemical Engineering*, 22, Supplement 1:S625 – S628, 1998. ISSN 0098-1354. doi: http://dx.doi.org/10.1016/S0098-1354(98)00110-0. European Symposium on Computer Aided Process Engineering-8. 46

M. Fikar, Z. Kovács, and P. Czermak. Dynamic optimization of batch diafiltration processes. *Journal of Membrane Science*, 355(1–2):168 – 174, 2010. ISSN 0376-7388. doi: http://dx.doi.org/10.1016/j.memsci.2010.03.019. 20, 116

G. Foley. Minimisation of process time in ultrafiltration and continuous diafiltration: the effect of incomplete macrosolute rejection. *Journal of Membrane Science*, 163(1–2):349–355, 1999. 20

S. M. Forman, E.R. DeBernardez, R. S. Feldberg, and R. W. Swartz. Crossflow filtration for the separation of inclusion bodies from soluble proteins in recombinant escherichia coli cell lysate. *Journal of Membrane Science*, 48(2–3):263 – 279, 1990. ISSN 0376-7388. doi: http://dx.doi.org/10.1016/0376-7388(90)85008-9. 90

S. Galaj, A. Wicker, J. P. Dunas, J. Grillot, and D. Garacera. Microfiltration

tangentielle avec decolmatage sur membranes ceramiques. *Le Lait*, (64):129–140, 1984. 92

P. Gatenholm, C. J. Fell, and A. G. Fane. Influence of the membrane structure on the composition of the deposit-layer during processing of microbial suspensions. *Desalination*, 70(1–3):363 – 378, 1988. ISSN 0011-9164. doi: http://dx.doi.org/10.1016/0011-9164(88)85067-7. International Membrane Technology Conference '88. 89

C. J. Goh and K. L. Teo. Control parameterization: a unified approach to optimal control problems with general constraints. *Automatica*, 24(1):3–18, 1988. 101

J. Hermia. Constant pressure blocking filtration laws-application to power-law non-Newtonian fluids. *Trans. IchemE*, 60(183), 1982. 21, 78

B. H. J Hofstee. Hydrophobie and other non-ionic parameters in protein separation and adsorptive immobi1ization by substituted agaroses. *Polymeric Separation Media*, pages 87–92, 1982. 90

D. G. Hull. *Optimal Control Theory for Applications*. Mechanical Engineering Series. Springer-Verlag New York, 2003. 35

K. J. Hwang and P. Y. Sz. Effect of membrane pore size on the performance of cross-flow microfiltration of bsa/dextran mixtures. *Journal of Membrane Science*, 378:272 – 279, 2011. ISSN 0376-7388. doi: http://dx.doi.org/10.1016/j.memsci.2011.05.018. Membranes for a Sustainable Future Section. 54

E. Iritani and N. Katagiri. Developments of blocking filtration model in membrane filtration. *KONA Powder and Particle Journal*, 33:179–202, 2016. doi: 10.14356/kona.2016024. 84, 86

M. Jelemenský, R. Paulen, M. Fikar, and Z. Kovács. Multi-objective optimal control of ultrafiltration/diafiltration processes. In *Proceedings of the European Control Conference*, pages 3384–3389, Zurich, Switzerland, 2013. 102

M. Jelemenský, R. Paulen, M. Fikar, and Z. Kovacs. Time-optimal diafiltration in the presence of membrane fouling. In *Preprints of the 19th IFAC World Congress Cape Town (South Africa) August 24 - August 29, 2014*, pages 4897–4902, 2014. 21, 79, 97, 98, 113

M. Jelemenský, R. Paulen, M. Fikar, and Z. Kovács. Time-optimal operation of multi-component batch diafiltration. *Computers & Chemical Engineering*, 83:131 – 138, 2015. ISSN 0098-1354. doi: http://dx.doi.org/10.1016/j. compchemeng.2015.05.029. 24th European Symposium on Computer Aided Process Engineering(ESCAPE). 70, 97

M. Jelemenský, M. Klaučo, R. Paulen, J. Lauwers, F. Logist, J. Van Impe, and M. Fikar. Time-optimal control and parameter estimation of diafiltration processes in the presence of membrane fouling. In *11th IFAC Symposium on Dynamics and Control of Process Systems*, Norway, 2016a. (accepted). 22, 79

M. Jelemenský, A. Sharma, R. Paulen, and M. Fikar. Time-optimal control of diafiltration processes in the presence of membrane fouling. *Computers & Chemical Engineering*, 2016b. doi: http://dx.doi.org/10.1016/j. compchemeng.2016.04.018. 21, 98, 104

A. S. Jönsson and G. Trägårdh. Ultrafiltration applications. *Desalination*, 77:135 – 179, 1990. ISSN 0011-9164. doi: 10.1016/0011-9164(90)85024-5. Proceedings of the Symposium on Membrane Technology. 53

R. E. Kalman. A new approach to linear filtering and prediction problems. *Transactions of the ASME–Journal of Basic Engineering*, 82(Series D):35–45, 1960. 123

H. Kim, Ch. Park, J. Yang, B. Lee, S. S. Kim, and S. Kim. Optimization of backflushing conditions for ceramic ultrafiltration membrane of disperse dye solutions. *Desalination*, 202(1–3):150 – 155, 2007. ISSN 0011-9164. doi:

http://dx.doi.org/10.1016/j.desal.2005.12.051. Wastewater Reclamation and Reuse for Sustainability. 92

Z. Kovács, M. Discacciati, and W. Samhaber. Modeling of batch and semi-batch membrane filtration processes. *Journal of Membrane Science*, 327(1–2):164 – 173, 2009. ISSN 0376-7388. doi: http://dx.doi.org/10.1016/j.memsci.2008. 11.024. 116

Z. Kovács, M. Fikar, and P. Czermak. Mathematical modeling of diafiltration. In *Conference of Chemical Engineering*, pages 135–135, Veszprem, 21-23.4.2009 2009. Pannonia University. 69

K. P. Lee, T. C. Arnot, and D. Mattia. A review of reverse osmosis membrane materials for desalination–development to date and future potential. *Journal of Membrane Science*, 370(1–2):1 – 22, 2011. ISSN 0376-7388. doi: http://dx.doi.org/10.1016/j.memsci.2010.12.036. 62

M. J. Luján-Facundo, J. A. Mendoza-Roca, B. Cuartas-Uribe, and S. Álvarez-Blanco. Evaluation of cleaning efficiency of ultrafiltration membranes fouled by BSA using FTIR–ATR as a tool. *Journal of Food Engineering*, 163:1 – 8, 2015. ISSN 0260-8774. doi: http://dx.doi.org/10.1016/j.jfoodeng.2015.04. 015. 21

J. D. Mannapperuma. *Design and performance evaluation of membrane systems*. Taylor & Francis Group, LLC Books, Boca Raton, Florida, USA, 1997. 57

Ch. Mat, N, Y. Lou, and G. G. Lipscomb. Hollow fiber membrane modules. *Current Opinion in Chemical Engineering*, 4:18 – 24, 2014. ISSN 2211-3398. Nanotechnology / Separation engineering. 63

E. J. McAdam and S. J. Judd. Optimisation of dead-end filtration conditions for an immersed anoxic membrane bioreactor. *Journal of Membrane Science*, 325(2):940 – 946, 2008. ISSN 0376-7388. doi: http://dx.doi.org/10.1016/j. memsci.2008.09.032. 53

A. Mohsen, R. S. Mohammad, S. Abdolhamid, and M. Behrooz. Modeling of membrane fouling and flux decline in microfiltration of oily wastewater using ceramic membranes. *Chemical Engineering Communications*, 199(1):78–93, 2012. 123

L. L. Muller, J. F. Hayes, and A. T. Griffin. Studies on whey processing by ultrafiltration. ii. improving permeation rates by preventing fouling. *Australian Journal of Diary Technology*, pages 70–77, 1973. 88

P. Ng, J. Lundblad, and G. Mitra. Optimization of Solute Separation by Diafiltration. *Separation Science and Technology*, 11(5):499–502, 1976. 20

R. Paulen, G. Foley, M. Fikar, Z. Kovács, and P. Czermak. Minimizing the process time for ultrafiltration/diafiltration under gel polarization conditions. *Journal of Membrane Science*, 380(1-2):148–154, 2011. doi: 10.1016/j.memsci. 2011.06.044. 74

R. Paulen, M. Fikar, G. Foley, Z. Kovács, and P. Czermak. Optimal feeding strategy of diafiltration buffer in batch membrane processes. *Journal of Membrane Science*, 411-412:160–172, 2012. ISSN 0376-7388. doi: 10.1016/j.memsci.2012.04.028. 21, 108, 113

R. Paulen, M. Jelemenský, M. Fikar, and Z. Kovács. Optimal balancing of temporal and buffer costs for ultrafiltration/diafiltration processes under limiting flux conditions. *Journal of Membrane Science*, 444(0):87 – 95, 2013. ISSN 0376-7388. doi: http://dx.doi.org/10.1016/j.memsci.2013.05.009. 74, 97

R. Paulen, M. Jelemenský, Z. Kovacs, and M. Fikar. Economically optimal batch diafiltration via analytical multi-objective optimal control. *Journal of Process Control*, 28:73–82, 2015. 72, 74, 97, 116

H. Pohjanpalo. System identifiability based on the power series expansion of the solution. *Mathematical Biosciences*, 41(1–2):21 – 33, 1978. ISSN 0025-5564. 125

L. S. Pontryagin, V. G. Boltyanskii, R. V. Gamkrelidze, and E. F. Mishchenko. *The Mathematical Theory of Optimal Processes*. Wiley (Interscience), New York, New York, 1962. 39

C. Psoch and S. Schiewer. Anti-fouling application of air sparging and back-flushing for {MBR}. *Journal of Membrane Science*, 283(1–2):273 – 280, 2006. ISSN 0376-7388. doi: http://dx.doi.org/10.1016/j.memsci.2006.06.042. 92

N. Rajagopalan and M. Cheryan. Process optimization in ultrafiltration: Flux-time considerations in the purification of macromolecules. *Chemical Engineering Communications*, 106(1):57–69, 1991. 113

S. K. Sayed Razavi, J. L. Harris, and F. Sherkat. Fouling and cleaning of membranes in the ultrafiltration of the aqueous extract of soy flour. *Journal of Membrane Science*, 114(1):93 – 104, 1996. ISSN 0376-7388. doi: http://dx.doi.org/10.1016/0376-7388(95)00311-8. 94

A. Salahi, M. Abbasi, and T. Mohammadi. Permeate flux decline during UF of oily wastewater: Experimental and modeling. *Desalination*, 251(1-3):153–160, 2010. 123

H. J. See, V. S. Vassiliadis, and D. I. Wilson. Optimisation of membrane regeneration scheduling in reverse osmosis networks for seawater desalination. *Desalination*, 125(1–3):37 – 54, 1999. ISSN 0011-9164. doi: http://dx.doi.org/10.1016/S0011-9164(99)00122-8. European Conference on Desalination and the Environment. 91

A. Sharma, M. Jelemenský, R. Paulen, and M. Fikar. Modelling and optimal control of membrane process with partial recirculation. In M. Fikar and M. Kvasnica, editors, *Proceedings of the 20th International Conference on Process Control*, pages 90–95, Štrbské Pleso, Slovakia, June 9-12, 2015 2015. Slovak University of Technology in Bratislava, Slovak Chemical Library. doi: 10.1109/PC.2015.7169944. 56

A. Sharma, M. Jelemenský, R. Paulen, and M. Fikar. Estimation of membrane fouling parameters for concentrating lactose using nanofiltration. In *26th European Symposium on Computer Aided Process Engineering*, Slovenia, 2016. (accepted). 79

B. Shi, P. Marchetti, D. Peshev, S. Zhang, and A. G. Livingston. Performance of spiral-wound membrane modules in organic solvent nanofiltration – fluid dynamics and mass transfer characteristics. *Journal of Membrane Science*, 494:8 – 24, 2015. ISSN 0376-7388. 64

B. Srinivasan, S. Palanki, and D. Bonvin. Dynamic optimization of batch processes: I. Characterization of the nominal solution. *Computers & Chemical Engineering*, 27(1):1–26, 2003. 73

E. Steiner. *The Chemistry Maths Book, Second Edition*. Oxford University Press, USA, 2nd edition, 2008. ISBN 0199205353,9780199205356. 100

A. Takači, T. Žikić-Došenović, and Z. Zavargó. Mathematical model of variable volume diafiltration with time dependent water adding. *Engineering Computations: International Journal for Computer-Aided Engineering and Software*, 26(7):857–867, 2009. 20

S. Takizawa, K. Fujita, and K. Y. Soo. Membrane fouling decrease by microfiltration with ozone scrubbing. *Desalination*, 106:423–426, 1988. 92

K. L. Teo, C. J. Goh, and K. H. Wong. *A Unified Computational Approach to Optimal Control Problems*. John Wiley and Sons, Inc., New York, 1991. 46

S. Van Geluwe, L. Braeken, and B Van der Bruggen. Ozone oxidation for the alleviation of membrane fouling by natural organic matter: A review. *Water Research*, 45(12):3551 – 3570, 2011. ISSN 0043-1354. doi: http://dx.doi.org/10.1016/j.watres.2011.04.016. 92

M. Cinta Vincent Vela, Silvia Álvarez Blanco, Jaime Lora García, and Enrique Bergantinos Rodríguez. Analysis of membrane pore blocking models applied to the ultrafiltration of {PEG}. *Separation and Purification Technology*, 62(3):489 – 498, 2008. ISSN 1383-5866. doi: http://dx.doi.org/10.1016/j.seppur.2008.02.028. 21, 78, 79

Ch. M. Williams, A. Ghobeity, A. J. Pak, and A. Mitsos. Simultaneous optimization of size and short-term operation for an {RO} plant. *Desalination*, 301(0):42 – 52, 2012. ISSN 0011-9164. doi: http://dx.doi.org/10.1016/j.desal.2012.06.009. 91

F. Xiao, P. Xiao, W. J. Zhang, and D. S. Wang. Identification of key factors affecting the organic fouling on low-pressure ultrafiltration membranes. *Journal of Membrane Science*, 447(0):144 – 152, 2013. ISSN 0376-7388. doi: http://dx.doi.org/10.1016/j.memsci.2013.07.040. 61

X. Zhang, L. Fan, and F. A. Roddick. Understanding the fouling of a ceramic microfiltration membrane caused by algal organic matter released from microcystis aeruginosa. *Journal of Membrane Science*, 447(0):362 – 368, 2013. ISSN 0376-7388. doi: http://dx.doi.org/10.1016/j.memsci.2013.07.059. 61

Y. J. Zhao, K.F Wu, Z. J. Wang, L. Zhao, and S. S. Li. Fouling and cleaning of membrane a literature review. *Journal of Enviromental Science*, 12(2):241–251, 2000. 77, 87, 92

A. Ziylan and N. H. Ince. Ozonation-based advanced oxidation for pretreatment of water with residuals of anti-inflammatory medication. *Chemical Engineering Journal*, 220(0):151 – 160, 2013. ISSN 1385-8947. doi: http://dx.doi.org/10.1016/j.cej.2012.12.071. 92

Author's Publications

List of publications of the author in the field of optimal control of membrane processes is as follows:

- Articles in journals indexed in Current Contents Database

    1. R. Paulen, M. Jelemenský, M. Fikar, and Z. Kovacs. Optimal balancing of temporal and buffer costs for ultrafiltration/diafiltration processes under limiting flux conditions. *Journal of Membrane Science*, vol. 444, pp. 87–95, 2013.

    2. R. Paulen, M. Jelemenský, Z. Kovacs, and M. Fikar. Optimal balancing of temporal and buffer costs for ultrafiltration/diafiltration processes under limiting flux conditions. *Journal of Process Control*, vol. 28, pp. 73–82, 2015.

    3. M. Jelemenský, R. Paulen, M. Fikar, and Z. Kovacs. Time-Optimal Operation of Multi-Component Batch Diafiltration. *Computers & Chemical Engineering*, vol. 83, pp. 131–138, 2015.

    4. M. Jelemenský, A. Sharma, R. Paulen, and M. Fikar. Time-optimal control of diafiltration processes in the presence of membrane fouling. *Computers & Chemical Engineering*, 2016, (accepted).

- Chapter or pages in book

    1. M. Jelemenský, L. Petáková, R. Paulen, and M. Fikar. Dynamic optimization of emulsion polymerization reactor, In *Selected Topics in Modelling and Control*, Editor(s): Mikleš, J., Veselý, V., Slovak University of Technology Press, no. 8, pp. 1–6, 2012.

- Articles in international conference proceedings

    1. M. Jelemenský, R. Paulen, M. Fikar, and Z. Kovacs. Economically Optimal Water Utilization in Batch Ultrafiltration/Diafiltration Processes. In *Permea 2013 - Proceedings of the 6th Membrane Conference of the Visegad Countries*, pp. 27–27, 2013.

    2. M. Jelemenský, R. Paulen, M. Fikar, and Z. Kovacs. Economically Optimal Control of Batch Diafiltration Processes. In *IEEE Multi-Conference on Systems and Control*, Hyderabad, India, pp. 734–739, 2013.

    3. M. Jelemenský, R. Paulen, M. Fikar, and Z. Kovacs. Multi-objective optimal control of ultrafiltration/diafiltration processes. In *Proceedings of the 12th European Control Conference*, Zurich, Switzerland, pp. 3384–3389, 2013.

    4. M. Jelemenský, R. Paulen, M. Fikar, and Z. Kovacs. Economically Optimal Batch Ultrafiltration with Diafiltration under Limiting Flux Conditions. In *Desalination using membrane technology*, Elsevier, no. 1, vol. 1, 2013.

    5. M. Jelemenský, R. Paulen, M. Fikar, and Z. Kovacs. Time-Optimal Control of Batch Multi-Component Diafiltration Processes. Editor(s): Jirí Jaromír Klemeš, Petar Sabev Varbanov, Peng Yen Liew, In *24th European Symposium on Computer Aided Process Engineering*, Elsevier B.V, Radarweg 29, PO Box 211, 1000 AE Amsterdam, Netherlands, vol. 2014, pp. 553–558, 2014.

6. M. Jelemenský, R. Paulen, M. Fikar, and Z. Kovacs. Time-optimal Diafiltration in the Presence of Membrane Fouling. In *Preprints of the 19th IFAC World Congress*, Cape Town, South Africa August 24 - August 29, 2014, pp. 4897–4902, 2014.

7. M. Jelemenský, A. Sharma, R. Paulen, and M. Fikar. Time-optimal Operation of Diafiltration Processes in the Presence of Fouling. Editor(s): Krist V. Gernaey and Jakob K. Huusom and Rafiqul Gani, In *12th International Symposium on Process Systems Engineering And 25th European Symposium on Computer Aided Process Engineering*, Elsevier B.V, Copenhagen, Denmark, pp. 1577–1582, 2015.

8. M. Jelemenský, M. Klaučo, R. Paulen, J. Lauwers, F. Logist, J. Van Impe, and M. Fikar. Time-optimal control and parameter estimation of diafiltration processes in the presence of membrane fouling. In *11th IFAC Symposium on Dynamics and Control of Process Systems*, Norway, 2016.

9. A. Sharma, M. Jelemenský, R. Paulen, and M. Fikar. Estimation of membrane fouling parameters for concentrating lactose using nanofiltration. In *26th European Symposium on Computer Aided Process Engineering*, Slovenia, 2016.

- Articles in domestic conference proceedings

    1. M. Jelemenský, R. Paulen, M. Fikar, and Z. Kovacs. Economically Optimal Diluant Addition for Batch Ultrafiltration/Diafiltration Processes. Editor(s): Fikar, M., Kvasnica, M., In *Proceedings of the 19th International Conference on Process Control*, Slovak University of Technology in Bratislava, Štrbské Pleso, Slovakia, pp. 415–420, 2013.

    2. A. Sharma, M. Jelemenský, R. Paulen, and Fikar, M. Modelling and Optimal Control of Membrane Processs with Partial Recirculation.

Editor(s): M. Fikar and M. Kvasnica, In *Proceedings of the 20th International Conference on Process Control*, Slovak Chemical Library, Štrbské Pleso, Slovakia, pp. 90–95, 2015.

3. M. Jelemenský, A. Sharma,R. Paulen and M. Fikar. Multi-Objective Optimization of Batch Dialfiltration Processes in the Presence of Membrane Fouling. Editor(s): M. Fikar and M. Kvasnica, In *Proceedings of the 20th International Conference on Process Control*, Slovak Chemical Library, Štrbské Pleso, Slovakia, pp. 84–89, 2015.

Curriculum Vitae

Martin Jelemenský

Date of Birth: September 16, 1985

Citizenship: Slovakia

Email: martin.jelemensky@gmail.com

Homepage: http://www.kirp.chtf.stuba.sk/∼jelemensky

Education

- B.S. Process Control, Slovak University of Technology, 2010.

    - *Minors*: Optimal Process Control and Chemical Engineering.

- M.S. Process Control, Slovak University of Technology, 2012

    - *Minor*: Dynamic Optimization

    - *Advanced study*: Global Dynamic Optimization at Lorraine Institute of Technology, Nancy, France, Febuary 2012 – April 2012

- Ph.D. Process Control, Slovak University of Technology, *expected* 2016

- *Majors*: Optimal Control of Membrane Processes in the Presence of Membrane Fouling

- *Minors*: Global and Dynamic Optimization of Process

- *Advanced Study*: Optimal control of separation processes at Corvinus University of Budapest, Budapest, Hungary, March 2014 – June 2014

Research Fields

- Global and Dynamic Optimization, Optimization and Control of Membrane Processes, Parameter Estimation Techniques

Miscellaneous

Computer Skills

- C/C++, Fortran, Matlab, Simulink, gPROMS, PHP, HTML, XML

- Windows, Unix/Linux, Solaris, MS Office, LaTeX

- Siemens Simatic, Foxboro

Language Skills

- English, German

- German : Zentrale Mittelstufenprüfung (Intermediate Exam), Goethe-Institute Bratislava, 2007.

Research Projects

Participation on Research Projects Funded by Government of Slovak Republic

- APVV SK-FR-0004-11 : Cooperation Štefánik – Dynamic and Global Optimisation of Processes (2012 – 2013)

- APVV 0551–11 : Advanced and effective methods of optimal process control (2012– 2015)

- APVV SK-FR-2015-0001 : Real Time Optimal Process Control (2016 – 2017)

- VEGA 1/0403/15 : Verifiably Safe Optimal Control (2012 – 2016)

- VEGA 1/0053/13 : Optimal Process Control (2012 – 2016)

- Grant for Young Researchers : Design of Optimal Control for Membrane Processes (2015 – 2016), principal investigator

- Grant for Excellent Teams of Young Researchers : Safe Optimal Control of Technological Processes (2015 – 2016), principal investigator

Resumé

V predkladanej dizertačnej práci sa venujeme optimálnemu riadeniu vsádzkových diafiltračných membránových procesov v prítomnosti zanášania membrány. Membránové procesy našli široké uplatnenie v chemickom, potravinárskom a farmaceutickom priemysle. Hlavným princípom membránovej separácie je separácia dvoch alebo viacerých látok v roztoku na základe molekulárnych veľkosti látok. Diafiltrácia je frakčná metóda, ktorá využíva rozličné techniky membránových separácií (napr. ultrafiltráciu, nanofiltráciu, mikrofiltráciu a reverznú osmózu), pre zníženie obsahu nečistôt (napr. soli) a pre zvýšenie koncentrácie produktu (napr. bielkoviny, enzýmy, alebo farbivá) v roztoku.

V rámci práce skúmame diafiltračný membránový proces znázornený na Obr. 5.1, kde uvažujeme, že celý proces pracuje pri konštantnom tlaku a konštantnej teplote. Počiatočný roztok sa pridá do zásobníka a pomocou čerpadla sa privádza na membránu. Membrána je pritom navrhnutá tak, aby zadržala látky s veľkými molekulami (makro zložka) a nechala látky s malými molekulami (mikro zložky) prejsť cez membránu. Priepustnosť je vyjadrená cez koeficient odporu, ktorý charakterizuje schopnosť membrány odmietnuť danú látku. Koeficient odporu je definovaný ako konštanta alebo ako funkcia koncentrácií. Časť roztoku, ktorá je zachytená membránou (retentát), je privádzaná naspäť

do zásobníka. Časť, ktorá prejde cez membránu a je odvádzaná zo systému, sa nazýva permeát. Celý proces je navrhnutý tak, aby koncentroval látku s veľkou molekulovou hmotnosťou a znížil koncentráciu látky s malou molekulovou hmotnosťou. Koncentrácie jednotlivých zložiek sa dajú ovplyvňovať pomocou riadiacej veličiny (pridávanie rozpúšťadla) α, ktorá je definovaná ako podiel medzi vstupným a výstupným prietokom. Existuje viacero tradičných módov, ktoré sú odlišné v hodnote α. Tieto módy sú napríklad (a) koncentračný mód $\alpha = 0$, (b) diafiltračný mód s konštatným objemom $\alpha = 1$, (c) diafiltrácia s premenlivým objemom $\alpha = (0, 1)$, (d) zrieďovací mód $\alpha = \infty$. Hlavnou podmienkou membránovej separácie je minimalizácia nákladov a maximalizácia vyrobeného množstva produktu. Aby sme splnili tieto požiadavky, potrebujeme použiť metódy dynamickej optimalizácie, ktoré vyžadujú typ účelovej funkcie, model procesu a ohraničenia. V membránových separačných procesoch poznáme viacero druhov účelových funkcii, ale v predkladanej práci sa sústredime primárne na minimalizáciu času. Je to hlavne z toho dôvodu, že vďaka minimálnemu času separácie sme schopní vykonať viacero vsádzok, čo v dnešnej dobe predstavuje jednu z hlavných požiadaviek priemyslu.

Hlavným problémom membránových procesov je zanášanie membrány, ktoré je zapríčinené ukladaním (nanášaním) látok v/na póroch membrány. Tento fenomén zapríčiňuje zníženie výkonu a tiež kvalitu finálneho produktu. Navyše, zanášanie membrány predlžuje celkový čas separácie, a tým pádom aj zvyšuje náklady na produkciu. K ďalším zvyšovaním nákladov dochádza aj pri čistení membrány. Zanášanie membrány môžu ovplyvniť aj rôzne faktory ako sú napríklad: vlastnosti suroviny, materiál, vlastnosti membrány, tlak a teplota. Z týchto dôvodov je modelovanie zanášania veľmi dôležité. V roku 1982 bol odvodený univerzálny model zanášania, z ktorého sa dajú odvodiť štyri štandardné modely znázornené na Obr. 6.1: (a) model kompletného zanášania, (b) model stredného zanášania, (c) model vnútorného zanášania a (d) model koláčovitého zanášania. Tieto modely sa hlavne odlišujú v princípe, ako sa molekuly látok ukladajú v/na membráne.

Hlavným cieľom dizertačnej práci je odvodenie časovo-optimálnej prevádzky membránovej separácie v prítomnosti zanášania. Na definovanie takejto optimálnej prevádzky môžeme použiť numerické metódy dynamickej optimalizácie, ktoré nám definujú optimálnu stratégiu pridávania rozpúšťadla do systému na dosiahnutie koncových koncentrácií za minimálny čas. Avšak, v tomto prípade je možné získať aj úplne analytické riešenie. Na odvodenie analytického riešenia optimálnej prevádzky je použitá metóda Pontryaginovho princípu minima. V práci sú odvodené dva prístupy, ktoré sa odlišujú v použitom modeli zanášania. V prvom prípade sa uvažuje, že zanášanie sa prejavuje znižovaním efektívnej plochy membrány. V druhom prístupe je uvažované, že prietok cez membránu sa znižuje v dôsledku zanášania. V prvom prípade, pri uvažovaní poklesu efektívnej plochy membrány, sme neboli schopní odvodiť predpis pre singulárny povrch, ktorý udáva podmienku prepnutia medzi prvým módom a singulárnym. V tomto prípade je možné odvodiť iba predpis pre singulárne riadenie. Preto na zistenie trvania jednotlivých módov sa použili numerické metódy. V druhom prípade, pri uvažovaní poklesu prietoku cez membránu, optimálna prevádzka je daná plne analyticky s presne definovaným singulárnym povrchom (7.27) a riadením (7.29). Na základe výsledkov sme zistili, že optimálna prevádzka je trojkroková a definovaná nasledovne:

- použitie koncentračného alebo zrieďovacieho módu, pokiaľ nie je dosiahnutý singulárny povrch,

- v druhom kroku sa použije singulárne riadenie, aby koncentrácie zostali na singulárnom povrchu,

- posledný krok je charakterizovaný koncentračným alebo zrieďovacím módom, pokiaľ sa nedosiahnú koncové koncentrácie.

Získané teoretické výsledky boli aplikované na rôznych prípadových štúdiách, ktoré boli prevzaté z literatúry. V rámci každej prípadovej štúdie sme porovnali navrhnutú optimálnu prevádzku s tradičnými prístupmi riadenia pre rôzne

stupne zanášania. Na základe výsledkov môžeme povedať, že v každom prípade časovo-optimálna prevádzka dosiahla koncové koncentrácie rýchlejšie ako pomocou tradičnej prevádzky. Taktiež sme porovnali použité modely zanášania a prišli sme k záveru, že hoci sú tieto modely odlišné, ich výsledky poukazujú na veľmi podobné správanie celkovej separácie.

V poslednej prípadovej štúdii sme uvažovali, že nepoznáme mieru a ani samotný model (predpis) zanášania. V tomto prípade sme navrhli použitie rozšíreného Kalmanovho filtra na odhadovanie koeficientov zanášania v reálnom čase, pričom sme uvažovali meranie koncentrácií, prietoku a derivácie prietoku. Výsledky ukazujú, že parametre zanášania sa podarilo odhadnúť počas prvého kroku, kde riadenie nezávisí od koncentrácií a ani od parametrov zanášania. Keďže tieto parametre boli správne odhadnuté už počas prvého kroku, prepnutie na singulárny povrch bolo vykonané už so správnymi parametrami. Avšak použitie rozšíreného Kalmanovo filtra prinieslo aj nevýhody v zmysle, že neuvažuje ohraničenia na odhadované parametre, čo by mohlo spôsobiť problémy pri implementácii na reálnom zariadení.

Na záver je možné zhrnúť, že predkladaná práca sa zaoberala návrhom časovo-optimálnej prevádzky pre diafiltračný membránový proces. Na základe výsledkov sme zistili, že celková prevádzka je trojkroková so singulárnym riadením v strede. Ďalej, sme poukázali na fakt, že ak nepoznáme parametre zanášania, je možné ich odhadovať v reálnom čase použitím rozšíreného Kalmanovho filtra. Budúce rozšírenia tejto práce môžu spočívať v nasledovných bodoch:

- implementácia optimálnej prevádzky na laboratórnom membránovom procese,

- návrh a implementácia pokročilých metód odhadu parametrov metódou posuvného horizontu.